

2000

Factors influencing precision and accuracy of a carbon-in ash monitor

Maohong Fan
Iowa State University

Follow this and additional works at: <https://lib.dr.iastate.edu/rtd>

 Part of the [Mechanical Engineering Commons](#)

Recommended Citation

Fan, Maohong, "Factors influencing precision and accuracy of a carbon-in ash monitor " (2000). *Retrospective Theses and Dissertations*. 13898.
<https://lib.dr.iastate.edu/rtd/13898>

This Dissertation is brought to you for free and open access by the Iowa State University Capstones, Theses and Dissertations at Iowa State University Digital Repository. It has been accepted for inclusion in Retrospective Theses and Dissertations by an authorized administrator of Iowa State University Digital Repository. For more information, please contact digirep@iastate.edu.

INFORMATION TO USERS

This manuscript has been reproduced from the microfilm master. UMI films the text directly from the original or copy submitted. Thus, some thesis and dissertation copies are in typewriter face, while others may be from any type of computer printer.

The quality of this reproduction is dependent upon the quality of the copy submitted. Broken or indistinct print, colored or poor quality illustrations and photographs, print bleedthrough, substandard margins, and improper alignment can adversely affect reproduction.

In the unlikely event that the author did not send UMI a complete manuscript and there are missing pages, these will be noted. Also, if unauthorized copyright material had to be removed, a note will indicate the deletion.

Oversize materials (e.g., maps, drawings, charts) are reproduced by sectioning the original, beginning at the upper left-hand corner and continuing from left to right in equal sections with small overlaps.

Photographs included in the original manuscript have been reproduced xerographically in this copy. Higher quality 6" x 9" black and white photographic prints are available for any photographs or illustrations appearing in this copy for an additional charge. Contact UMI directly to order.

**Bell & Howell Information and Learning
300 North Zeeb Road, Ann Arbor, MI 48106-1346 USA
800-521-0600**

UMI[®]

Factors influencing precision and accuracy of a carbon-in ash monitor

by

Maohong Fan

A dissertation submitted to the graduate faculty
in partial fulfillment of the requirements for the degree of

DOCTOR OF PHILOSOPHY

Major: Mechanical Engineering

Major Professor: Robert C. Brown

Iowa State University

Ames, Iowa

2000

UMI Number: 9962814

UMI[®]

UMI Microform 9962814

Copyright 2000 by Bell & Howell Information and Learning Company.

All rights reserved. This microform edition is protected against
unauthorized copying under Title 17, United States Code.

Bell & Howell Information and Learning Company
300 North Zeeb Road
P.O. Box 1346
Ann Arbor, MI 48106-1346

**Graduate College
Iowa State University**

**This is to certify that the Doctoral dissertation of
Maohong Fan
has meet the dissertation requirements of Iowa State University**

Signature was redacted for privacy.

Committee Member

Signature was redacted for privacy.

Major Professor

Signature was redacted for privacy.

For the Major Program

Signature was redacted for privacy.

For the Graduate College

TABLE OF CONTENTS

LIST OF TABLES	vi
LIST OF FIGURES	vii
NOMENCLATURES	x
ACKNOWLEDGEMENTS	xiii
1. INTRODUCTION	1
2. BACKGROUND	4
2.1 Fly Ash Characteristics	4
2.1.1 Physical characterization of fly ash	6
2.1.2 Chemical characterization of fly ash.....	11
2.2 Photoacoustic Effect and Its Application.....	12
2.2.1 Selection of radiation source.....	14
2.2.2 Photoacoustic theory.....	14
2.2.3 Practical consideration in design of photoacoustic chambers.....	18
2.2.4 Volumetric effects in photoacoustic chamber.....	18
2.2.5 Modulation of excitation source.	19
2.2.6 Photoacoustic signal saturation.....	20
2.2.7 Models of the photoacoustic effect in solid.	21
2.2.8 Photoacoustic saturation.	27
2.3 Photoacoustic Effect Application in Testing Unburned Carbon in Fly Ash...	28
3. EXPERIMENTS	31
3.1 Fly Ash Characterization	31

3.1.1	Determination of TL and TOC using TGA.....	31
3.1.2	Scanning electron micrographs.....	34
3.2	Photoacoustic Apparatus.....	36
3.2.1	Design of new head.....	36
3.2.2	Design of new LED holder	40
3.2.3	Excitation source.....	42
3.2.4	Signal detection and processing	43
3.3	Establishment of a Standard Sample Preparation Procedure.....	44
3.4	Choice of Modulation Frequency	46
3.5	Sample Homogeneity.....	46
3.6	Photoacoustic Signal Saturation	47
3.7	Precision of Carbon-in-Ash Monitor	48
4.	RESULTS AND DISSCUSSIONS.....	50
4.1	Comparison of LOI and TOC As Carbon Indicators of Fly Ash.....	50
4.2.	Effect of Fly Ash Sampling on Precision and Accuracy	56
4.2.1	Heterogeneity of as-received fly ash.....	56
4.2.2	Effect of grinding on sample homogeneity.....	62
4.2.3	Selection of machine-grinding time for as-received fly ash Samples.....	64
4.2.4	Effect of sample density on photoacoustic signal.....	66
4.2.5	Effect of homogeneity on the calibration of photoacoustic set-up.....	69
4.2.6	Addition of diluent to fly ash samples	72
4.3	Effect of Instrument Design and Operation on Precision and Accuracy	74

4.3.1 Investigation of modulation frequency	74
4.3.2 Universal calibration of photoacoustic instruments with various samples.....	76
4.3.3 Saturation of photoacoustic signal and dilution of fly ash.....	78
4.3.4 Improvement of photoacoustic signal responsivity	81
4.3.4.1 Effect of new head and LED holder	82
4.3.4.2 Effect of the increase of the excitation power output	82
4.3.5 Effect of raw coal on instrument accuracy	85
4.3.6 Effect of ambient environment on photoacoustic signal	86
5. CONCLUSIONS	90
5.1 Accuracy of Carbon-in-Ash Monitor.....	90
5.2 Precision of Carbon-in-Ash Monitor	92
APPENDIX 1. LOSS ON IGNITION (LOI)	94
APPENDIX 2. TGA-7 OPERATION PROCEDURE	95
APPENDIX 3. SERIES 2000 CONTROLLER OPERATION PROCEDURE.....	104
APPENDIX 4. STANDARD SAMPLE PREPARATION PROCEDURE	105
APPENDIX 5. SAS PROGRAM AND OUTPUT OF THE REGRESSION MODEL FOR THE EFFECT OF TEMPERATURE AND HUMIDITY ON PHOTOACOUSTIC SIGNAL OF CA200	108
APPENDIX 6. DATA ACQUISITION PROGRAM.....	111
REFERENCES.....	136

LIST OF TABLES

Table 2.1.	Chemical analysis of mechanically and ESP collected fly ashes	10
Table 2.2.	Typical chemical components of fly ash	12
Table 3.1.	Triple TOC measurements of several as-received fly ashes.....	47
Table 4.1.	Results of “unburned carbon” determination by various measures.....	51
Table 4.2.	Relative errors of LOI for samples in Table 4.1.....	55
Table 4.3.	Evaluation of heterogeneity of as-received fly ash.....	60
Table 4.4.	TOC obtained for five fly ashes ground four times through machine Grinder	62
Table 4.5.	Absolute errors of the ground 2A boiler sample calibration shown in Figure 4.13 (b)	72
Table 4.6.	Absolute errors of the ground 3B boiler sample calibration shown in Figure 4.14.	72
Table 4.7.	Absolute errors of the ground 2A boiler sample calibration shown in Figure 4.15.	74
Table 4.8.	Photoacoustic signals of selected diluents for IR LED excitation source	81
Table 4.9.	Effect of IR LED output on accuracy of calibration.....	85
Table 4.10.	Comparison of volatile content to CA200 measurements in Figure 4.2.....	86
Table 4.11.	Effect of ambient temperature (°C) and humidity (%) on photoacoustic signal (microvolt) (sample 22473AT, m=0.1144 g, IR LED, f=15 H).....	87
Table 4.12.	Effect of ambient temperature control on photoacoustic signal (microvolt) (sample 22473AT, m=0.1144 g, IR LED, f=15 Hz).....	89

LIST OF FIGURES

Figure 2.1. Mechanisms of fly ash formation.....	5
Figure 2.2. Example of complex inhomogeneous spherical particle types.....	7
Figure 2.3. Particle size distribution of fly ash... ..	8
Figure 2.4. Sketch of typical photoacoustic system.....	13
Figure 2.5. Cross-section view of a simple cylinder photoacoustic chamber.....	22
Figure 2.6. Spectral photoacoustic absorption for a typical fly ash as measured by FTIR.....	30
Figure 3.1. Photograph of the Perkin Elmer TGA-7.....	33
Figure 3.2. Example of TGA result (fly ash sample AM36)	34
Figure 3.3. SEM micrographs of as-received fly ashes (a) 22356AT (b) 32AT	35
Figure 3.4. Photographs of photoacoustic system set-up.....	37
Figure 3.5. Drawing of photoacoustic chamber of CA200.....	38
Figure 3.6. Drawing of new head.....	39
Figure 3.7. Drawing of IR LED holder designed by Ametek.....	41
Figure 3.8. Drawing of new IR LED holder designed by ISU	41
Figure 3.9. Sample preparation jig.....	45
Figure 4.1 Comparison of TL based on TGA methodology and LOI based on ASTM Methodology	53
Figure 4.2. Comparison of TOC based on TGA methodology and LOI based on ASTM methodology	54
Figure 4.3. The triple trial results of the as-received parent fly ash 22473AT	58

Figure 4.4. SEM micrograph of the as-received fly ash 22336A (a) first trial (b) second trial (c) third trial	59
Figure 4.5. As-received 2A boiler sample calibration with IR LED excitation (m=0.1144g, f=15Hz, diluent; CaCO ₃).....	61
Figure 4.6. As-received 3B boiler sample calibration with IR LED excitation (m=0.1144g, f=15Hz, diluent; CaCO ₃).....	61
Figure 4.7. The triple trial results of the ground parent fly ash 22372AT (a) first trial (b) second trial (c) third trial.....	63
Figure 4.8. SEM micrograph of the ground fly ash 22336AT	65
Figure 4.9. Effect of sample grinding time on photoacoustic signal for IR LED excitation source (AM36, m=0.1144g, f=15Hz, diluent; CaCO ₃).....	66
Figure 4.10. Effect of sample density on photoacoustic signal for laser excitation source (AM36, f=15Hz, diluent; CaCO ₃)	68
Figure 4.11. Effect of sample density on photoacoustic signal for visible LED excitation source (AM36, f=15Hz, diluent; CaCO ₃)	68
Figure 4.12. As-received 2A boiler sample calibration with IR LED excitation source (m=0.1144g, f=15Hz, diluent; CaCO ₃)	70
Figure 4.13. (a) As-received 2A boiler sample calibration with IR LED excitation source (m=0.1144g, f=15Hz, diluent; CaCO ₃)	70
(b) Ground 2A boiler sample calibration with IR LED excitation source (m=0.1144g, f=15Hz, diluent; CaCO ₃).....	70
Figure 4.14. (a) As-received 3B boiler sample calibration with IR LED excitation source (m=0.1144g, f=15Hz, diluent; CaCO ₃)	71
(b) Ground 3B boiler sample calibration with IR LED excitation source (m=0.1144g, f=15Hz, diluent; CaCO ₃).....	71
Figure 4.15. Calibration of 2A boiler samples prepared by diluting and grinding (four minutes) IR LED excitation source (m=0.1144g, f=15Hz, diluent; CaCO ₃).....	73
Figure 4.16. Photoacoustic signal vs. modulation frequency for laser excitation source (as-received AM36, m=0.1144g, diluent; CaCO ₃)	75
Figure 4.17. Photoacoustic signal vs. modulation frequency for IR LED excitation source (as-received AM36, m=0.1144g, diluent; CaCO ₃).....	75

Figure 4.18. Universal calibration on various samples for laser excitation source (as-received AM36, m=0.1144g, diluent; CaCO ₃)	77
Figure 4.19. Universal calibration on various samples for visible LED excitation source (as-received AM36, m=0.1144g, diluent; CaCO ₃)	77
Figure 4.20. Universal calibration on various samples for IR LED excitation source (as-received AM36, m=0.1144g, diluent; CaCO ₃)	78
Figure 4.21. Saturation of photoacoustic signal for visible LED excitation source (21996AT, m=0.1144g, f=15Hz, diluent; fired 21996AT sample).....	79
Figure 4.22. Saturation of photoacoustic signal for IR LED excitation source (21996AT, m=0.1144g, f=15Hz, diluent; fired 21996AT sample)	80
Figure 4.23. Sensitivity increase with IR LED current (sample 22462AT and 22343AT, m=0.1144g, f=15Hz, diluent; CaCO ₃).....	83
Figure 4.24. Ground 2A boiler sample calibration with IR LED excitation source (m= 0.1144g, f=15Hz, diluent; CaCO ₃) (a) current=39% (b) current=80%	84

NOMENCLATURES

a	=	characteristic width of light beam
a_j	=	thermal diffusion coefficient of material j
A_c	=	photoacoustic chamber cross-sectional area
A_j	=	j^{th} mode amplitude
b	=	length of back material
B	=	Einstein coefficient
c	=	speed of sound (m/s)
C_p	=	specific heat at constant pressure (J/mole-K)
C_v	=	specific heat at constant volume (J/mole-K)
E	=	energy of the excited level (J)
f	=	excitation frequency (Hz)
$H(\mathbf{r}, t)$	=	heat produced by the absorption of light (J)
I	=	incident light intensity (J/m ²)
I_0	=	incident monochromatic light flux (J/m ²)
j	=	j^{th} order mode
k	=	Boltzmann constant (1.381×10^{-23} J/K)
k_j	=	thermal conductivity of material j (J/m-sec-°C)
l	=	length of sample (m)
N	=	number of gas molecules

p	=	acoustic pressure, difference between total pressure P and average pressure P_0 (Pa)
P	=	total pressure (Pa)
P_0	=	average pressure value (Pa)
P_{abs}	=	one half the peak power absorbed by gas (W)
p_j^*	=	complex conjugate of p_j (W)
P_j	=	power absorbed in j^{th} order mode (W)
Q_j	=	the acoustic resonant enhancement of the j^{th} mode at frequency ω_j
Q	=	complex envelope of the sinusoidal pressure variation
r	=	chamber radius (m)
t	=	time (sec)
$T(x, t)$	=	temperature distribution in photoacoustic chamber
$\mathbf{u}(\mathbf{r}, t)$	=	acoustic velocity (m/sec)
V_c	=	volume of photoacoustic chamber (m^3)
W	=	complex amplitudes of the periodic temperature at the sample-backing Boundary
\bar{x}	=	average
$\alpha_{o,j}$	=	absorption coefficient of gas at $r=0$ and j^{th} order mode (m^{-1})
α_g	=	gas absorption coefficient (m^{-1})
α_s	=	solid absorption coefficient (m^{-1})
β_j	=	the thermal diffusivity of material ($\text{m}^2 \text{sec}^{-1}$)
γ	=	ratio of the specific heat of the gas in chamber at constant pressure C_p to that at constant volume C_v
δ	=	standard deviation

Φ	=	ambient temperature (K)
μ_g	=	thermal diffusion length of gas (m)
μ_j	=	thermal diffusion length of material j (m)
θ	=	complex amplitudes of the periodic temperatures at the sample-gas boundary
ρ_g	=	density of gas (kg/m^3)
ρ_j	=	density of material j (kg/m^3)
τ	=	collision lifetime (sec)
ω_j	=	resonant frequency of the normal mode (Hz)
ω	=	excitation frequency (Hz)
$\Theta(\mathbf{r}, t)$	=	acoustic temperature distribution

ACKNOWLEDGMENTS

Special thanks go to Professor Robert C. Brown for his support and guidance throughout the process of this research and for providing me with great opportunities to pursue challenging research in photoacoustic affect. I would also like to give thanks to Dr. Gerald M. Colver, Dr. Kenneth Bryden, Dr. Thomas D. Wheelock and Dr. Steven Hoff for serving on my graduate committee. Dr. Mark Coppler, Dr. Bob Novack, Mr. Jeff Winter and Mr. Dennis Hungerman at Ametek Corporation deserve special recognition for their invaluable assistance throughout this project. Thanks also goes to Lee Girard for his talent and time in helping this research, Glenn Norton for his help in making analytical equipment operate properly, and Diane Love and McCarley Tonia for their administrative support of this project.

My wife Haiyan's support and my son Bo's patience were also greatly appreciated during my graduate study.

This work was funded by the Iowa State University Research Foundation. Without its financial support this project could not have been completed.

1. INTRODUCTION

The improvement of coal combustion in coal-fired power industry is increasingly important due to energy conservation and environmental concerns. Unburned carbon in fly ash is a major index of coal combustion efficiency. Therefore, finding a convenient and accurate method to measure unburned carbon in fly ash is very important. Currently, the loss-on-ignition (LOI) test is the standard method for determination of carbon in fly ash from coal-fired boilers [1]. However, it has been found that LOI is not an accurate indicator of unburned carbon in fly ash [2]. The assumption that oxidation of unburned carbon in fly ash is the only source of weight loss when heating a sample in a furnace for several hours at 725 °C is incorrect. In fact, mineral matter in fly ash can decompose and release gas upon heating with the result that LOI can be greater than the actual carbon content.

Thermogravimetric analysis (TGA) is a very accurate instrument to measure unburned carbon in the fly ash, but it is a very expensive instrument. Consequently, a cheap and accurate instrument to test unburned carbon in the fly ash is sought by the power industry.

Even though Alexander Graham Bell discovered the photoacoustic effect in 1880, photoacoustic spectroscopy did not become widespread until 1973 [3]. The photoacoustic effect results from the absorption of modulated light energy. The photoacoustic effect is different from other optical techniques in the way absorbed radiation is detected [4-10]. When the modulated light irradiates the fly ash, fly ash will absorb irradiated energy. The energy absorbed by fly ash is transferred as heat to the surrounding gas, where it results in a minute temperature change. Subsequent expansion of heated gas causes a periodic pressure oscillation at the modulation frequency of the excitation, which propagates through the gas

acoustic waves or signals. The acoustic signals can be detected by a sensitive microphone combined with a lock-in amplifier. The strength of the acoustic signals is measured in microvolts. The amplitude of the photoacoustic signal is proportional to the carbon content of the fly ash at low carbon concentration.

Photoacoustic techniques have some advantages over other optical methods, which leads to its more and more application in environmental research and pollution control industries [11-15]. Photoacoustic effects can be used as a spectroscopy method to measure the amount of the electromagnetic radiation absorbed by a sample and converted to heat.

However, the photoacoustic effect may also be used as a means to measure thermal and elastic properties of materials, to study chemical reactions and to measure thickness of layers and thin films. Photoacoustics has been utilized in many research areas including mechanical, chemical and environmental studies [3].

Brown and Waller [16-17] investigated the photoacoustic effect as an alternative method to measure carbon in fly ash. An off-line carbon-in-ash monitor prototype with an infrared diode laser as an excitation source was successfully developed in 1995. Based on this prototype, Ametek Corporation designed a commercial version of the instrument called the Carbon Analyzer 200 (CA200). Ametek developed three versions of the CA200 using different excitation sources: infrared (IR) diode laser, visible light-emitting-diode (LED) and IR LED.

During market acceptance evaluations of these instruments, Ametek encountered problems with precision and accuracy of carbon in ash measurements. Iowa State University (ISU) was asked to investigate these problems and recommend improvements in its construction, calibration, and operation. This study, commissioned as a result of problems

encountered by Ametek, is a comprehensive evaluation of the photoacoustic effect as it applies to the detection of carbon in fly ash.

2. BACKGROUND

Fly ash is the byproduct of coal combustion. Differences in fuel composition and boiler operation conditions lead to various and complicated compositions of fly ash. Most fly ash consists of inorganic mineral material and elemental carbon. Occasionally fly ash will contain small quantities of raw coal or volatile organic compounds.

2.1 Fly Ash Characteristics

During the combustion of coal, the products formed are divided into three parts: flue gases, bottom ash and fly ash. Fly ash is that part of the ash that is entrained in the combustion gas leaving the boiler and collected in either mechanical collectors and/or electrostatic precipitators. Figure 2.1 shows the formation processes of fly ash proposed by Sahu and Flagan [18]. Sahu and Flagan described the mechanism as follows:

The bulk of the mineral matter in coal remains as an ash residue when the carbon burns. Minerals may melt under high-temperature pulverized coal combustion condition. As the carbon surface recedes due to oxidation, ash droplets adhering to the carbon surface come into contact with one another and may coalesce to form larger droplets. At the same time, oxidation of the porous microstructure leads to loss of the physical integrity of the char structure, and ultimately the formation of a number of fragment of from each char particle. Since each of these fragments contains some ash, as they burn out they generate a number of residual ash particles from each parent coal particle. (p. 461-462)

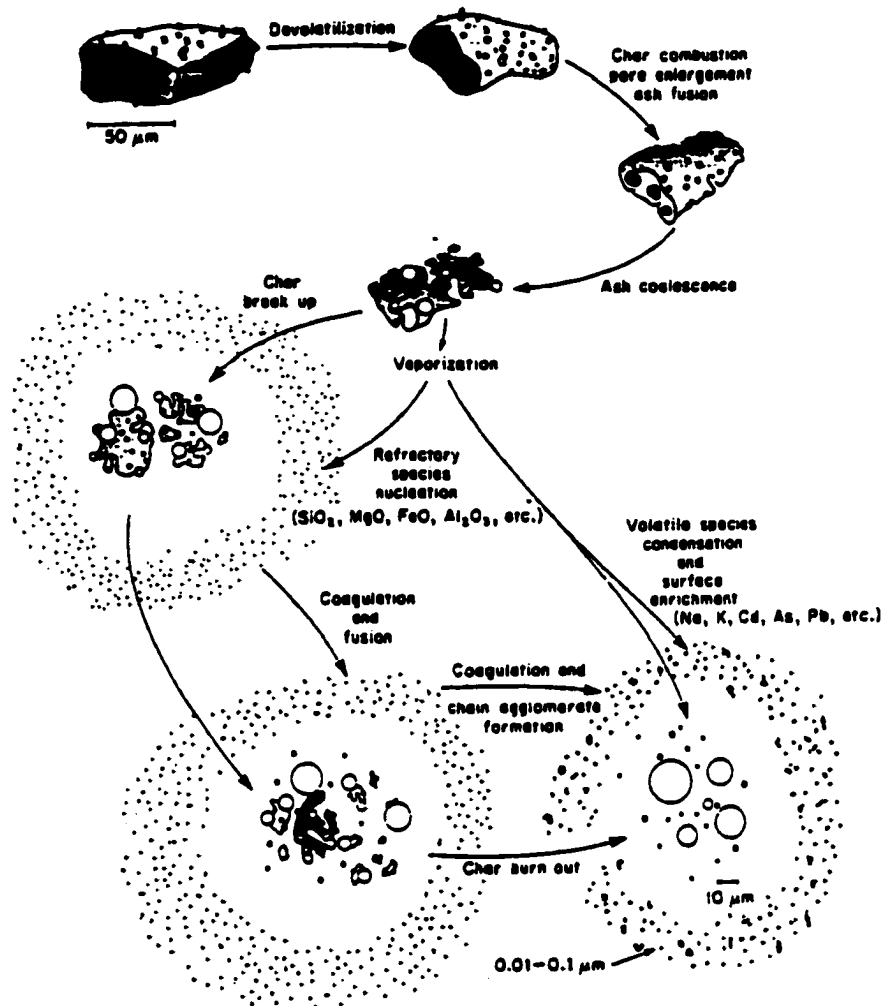


Figure 2.1. Mechanisms of fly ash formation [18, p. 462]

The distribution of ash between bottom ash and fly ash fractions is a function of burner type, the type of coal, and the type of boiler bottom (wet or dry). The flue gas is that part of the coal material which is volatilized or oxidized during combustion. Parts of gases condense onto the surface of fly ash and may be collected through fly ash collectors. The complexity of coal composition [19-21] results in the diversity of fly ash characteristics. However, fly ash still can be generally characterized from physical and chemical viewpoints.

2.1.1 Physical characterization of fly ash

Fly ash generally consists of fine spherical particulate usually ranging in diameter from 0.5 μm to 100 μm [22-23]. Fly ash particles are inhomogeneous, which is evident in Figure 2.2 [24-25]. The color of fly ash spans the spectrum from light tan to gray to black. Increased carbon content causes a darker gray-black tone, while increased iron content tends to produce a tan-colored or reddish fly ash. The pH of fly ash contacted with water may vary widely, with pH for the majority of pulverized coal-burned fly ash with ranging from 8-12 [26].

Particle size distribution and total surface area of fly ash varies depending on the types of collection equipment. A comparison of the particle size distribution of fly ash collected in an electrostatic precipitator and that collected in a mechanical collector is shown in Figure 2.3 [27]. The ash collected by electrostatic precipitators contains a much greater percentage of the very small particles ($<1.5\mu\text{m}$).

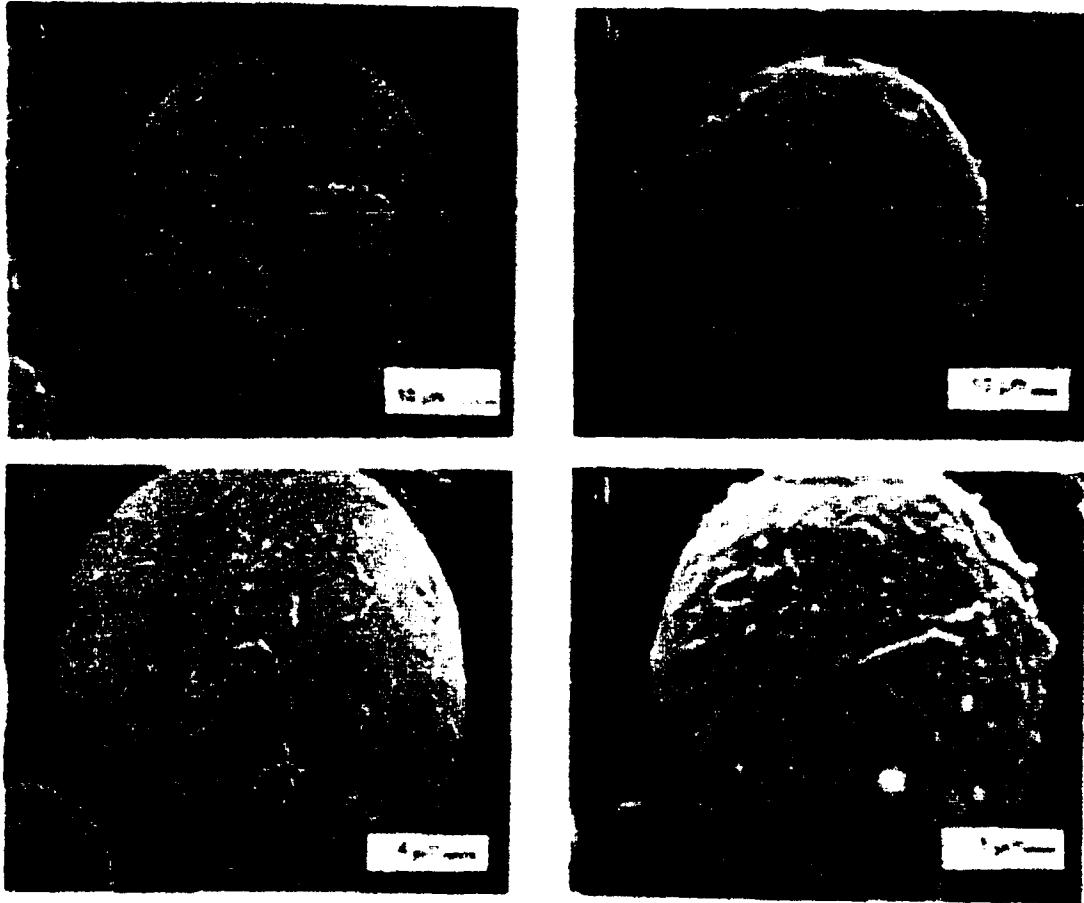


Figure 2.2 Example of complex inhomogeneous spherical particle types

(a) plerosphere

(b) clathrosphere

(c) cenosphere (density $<0.8 \text{ g.cm}^{-3}$) with mullite crystallization [24, p. 87]

(d) high-Fe, magnetic particle with surface crystallization [24, p. 87]

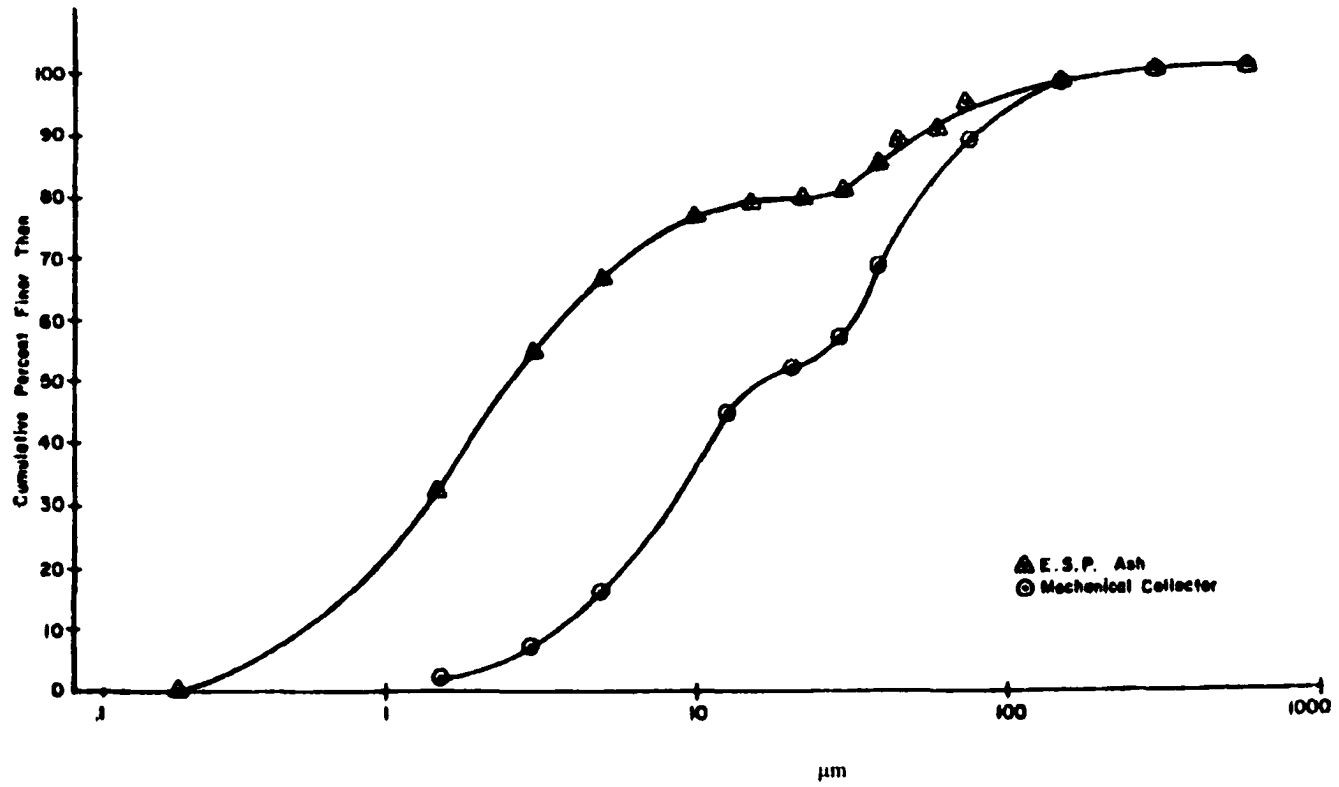


Figure 2.3. Particle size distribution of fly ash [27, p. 33]

However, as the diameter of the particles approach the 150 μm , the percentages of ash collected by the two methods are approximately equal [28]. It is recognized that fly ash varies to some degree in their physical properties. Mather [27] conducted analysis of two ashes collected with a mechanical collector and an electrostatic precipitator. He divided each fly ash sample into three fractions: coarse, medium, and fine. He found that fineness and the specific gravity of fly ash are correlated. Coarse materials have higher specific gravity for both types of collection devices. Table 2.1 shows the results of chemical analysis for the physically size-differentiated fractions. The obvious difference clearly shown in this analysis can be summarized as follows [27]. The lithophile materials (alumino-silicates) were more concentrated in the finer fractions. The magnetite-hematite materials (iron-bearing) were more concentrated in the coarser fractions. The alkalis (Na and K) were generally more concentrated in the finer fractions. This occurrence is probably because of their association with the lithophiles.

The highest loss-on-ignition occurred in the finer fraction. The most abundant component in fly ash, glassy compounds, is concentrated in the electrostatic precipitator fly ash. As shown in Table 2.1, the percentage of glass, with the material passing 500-mesh sieve containing the highest percentage of glass.

More magnetite-hematite substance is concentrated in the fly ash collected from the mechanical collector than is collected in the electrostatic precipitator. Magnetite-hematite is the second most abundant constituent in fly ash. Magnetite-hematite particles may also be found as small opaque inclusions in the glass particles.

Table 2.1. Chemical analysis of mechanically and ESP collected fly ashes [27, p. 39]

Chemical (%)	Mechanically Collected Fly Ash				ESP Collected Fly Ash			
	As Received	Fine	Medium	Coarse	As Received	Fine	Medium	Coarse
SiO ₂	41.57	44.65	37.57	33.08	44.29	46.38	36.40	26.72
AlO ₃	18.53	18.53	18.19	14.19	13.05	17.94	18.36	15.48
Fe ₂ O ₃	24.33	19.87	38.23	43.46	19.64	16.46	37.28	53.35
CaO	4.83	5.07	4.00	5.56	6.67	6.61	5.08	4.92
MgO	0.96	0.78	0.86	0.71	1.03	0.91	0.72	0.59
Sulfide Sulfur	0.05	0.00	0.01	0.07	0.00	0.00	0.005	0.02
SO ₃	0.64	0.70	0.42	0.76	2.40	2.60	0.87	0.74
LOI	4.34	5.61	0.80	0.20	2.64	2.87	2.44	1.49
Na ₂ O	0.23	0.24	0.17	0.20	0.94	1.2	0.51	0.36
K ₂ O	1.96	2.10	1.54	1.23	1.90	2.03	1.20	0.86
Total Alkali As Na ₂ O	1.52	1.62	1.18	1.01	2.19	2.54	1.30	0.93
Total Carbon	3.68	4.75	0.72	0.36	1.53	1.40	2.04	1.19
Moisture Loss	0.28	0.26	0.08	0.11	0.43	0.65	0.24	0.18
Insoluble Residue	84.40	82.92	89.26	73.82	75.68	75.72	87.13	83.99

Carbon particles in fly ash have various shapes with the predominant shape being highly irregular cellular particles. These particles increase in abundance as the particle size increases. Carbon particles in the coarser fly ash has a cinder-like appearance and are magnetic because of the presence of particles of magnetite and hematite lodged in the cellular structure of their walls. It has been reported that wood structure was seen in some particles [29].

The aggregates of glass, magnetite, hematite, and carbon particles are present in all size ranges in fly ash. Some of these particles are fused; however, most of them are very loosely held together. X-ray diffraction studies showed that crystalline constituents were hematite, quartz, mullite and anhydrite.

2.1.2 Chemical characterization of fly ash

Chemical composition of fly ash is determined by the geologic and geographic factors related to the coal deposit, boiler operation conditions, as well as flue gas pollution control technologies applied. The main inorganic fractions of fly ash are the oxides and salts of Si, Al, Fe, and Ca, which consist of 90 to 99 percent of total inorganic part of fly ash. The remaining inorganic substances in fly ash includes the compounds of Mg, Ti, S, Na, and S as well as the very small quantities (parts per million) of twenty to fifty other elements. Compared with bottom ash, fly ash is richer in the following S, Hg, Cl, Sb, F, Se, V, Pb, Mo, Ni, B, Zn, Cd, Cr, Cu, Co, U, As, and Ag. Elements which are approximately equally distributed in the bottom ash and fly ash include Ba, Be, Fe, Al, Ca, Ti, Mn and Mg. The volatilization-condensation theory of enrichment of certain elements in the fly ash [30] can be used to explain why some elements such as S, Hg and Cl in fly ash are more concentrated than bottom ash. Typical chemical species in fly ash sample are shown in Table 2.2.

The most organic compounds in typical fly ash is expected to be elemental carbon (char), not raw coal under modern boiler operating conditions. However, Ametek reported some fly ash samples contained significant quantities of raw coal and /or distilled coal that reached the softening points but did not burn. It was suspected that the presence of raw coal would adversely affect instrument performance. As mentioned above, carbon in fly ash is

Table 2.2. Typical chemical species in fly ash [31-34]

Chemical Formula	Molecular Weight	Chemical Formula	Molecular Weight
Li ₂ O	29.88	Na ₂ O	61.98
K ₂ O	94.20	SrO	103.62
CaO	56.08	Rb ₂ O	186.94
BaO	153.3	MgO	40.31
Al ₂ O ₃	101.96	SiO ₂	60.08
TiO ₂	79.90	Fe ₂ O ₃	103.85
As ₂ O ₃	197.84	Ag ₂ O	123.87
BeO	25.01	B ₂ O ₃	69.62
CoO	74.93	Bi ₂ O ₃	465.96
CuO	79.55	Cr ₂ O ₃	68.00
GeO ₂	88.59	GaO	85.72
La ₂ O ₃	325.82	HgO	216.59
MoO ₃	143.94	MnO	70.94
P ₂ O ₅	141.94	NiO	74.71
Sb ₂ O ₃	291.50	PbO	223.20
V ₂ O ₅	181.88	SnO ₂	150.69
ZnO	81.37	WO ₃	231.85
C	12.011	ZrO ₂	107.22

mainly distributed in larger particles. It is worthwhile noting that fly ash contains small quantities of hazardous polychlorinated biphenyls (PCB), which is formed during coal combustion.

2.2 Photoacoustic Effect and Its Application

Since the photoacoustic effect was discovered by Graham Bell, Rontgen, and Tyndall [35-37] in 1880, its theory has been developed gradually.

Figure 2.4 illustrates the typical modern photoacoustic system [38]. Radiation penetrates the sample to a depth dependent on the sample's optical absorption coefficient. The material within this depth is accordingly heated and cooled at the modulation frequency of the radiation. The energy absorbed within a characteristic thermal sampling depth is

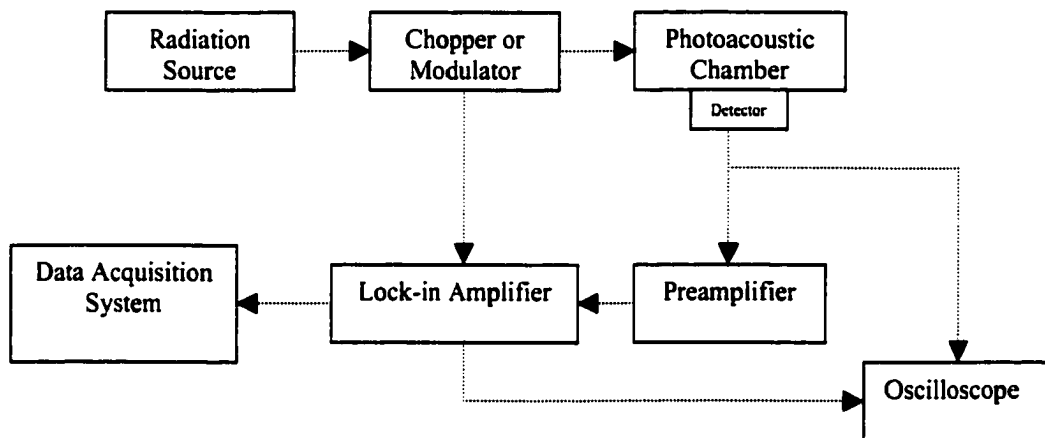


Figure 2.4. Sketch of typical photoacoustic system [38, p. 60]

then conducted out of the sample to a thin layer of gas above the sample surface. This heat transfer is dependent on the thermophysical properties of both the sample and gas. The heated gas layer acts as an acoustic piston as it expands and contracts against the remaining gas in the enclosed cell. This causes a periodic pressure oscillation, or acoustic wave to propagate through the photoacoustic chamber. A microphone detects this signal and relays it to a lock-in amplifier. The lock-in amplifier accepts the noisy microphone signal and processes it to reject frequencies other than the modulation frequency. A data acquisition system collects and records the output signal from the lock-in amplifier.

2.2.1 Selection of radiation source

Radiation sources to excite the photoacoustic response can be of many types including lasers and light emitting diodes (LED). The high sensitivity and linearity of response of laser-excited photoacoustic systems make them useful tools for detecting and monitoring atmospheric pollutants. But they require cooling. Light emitting diodes [39] are semiconductor devices that emit light under positive voltage. Light emitting diodes do not have filaments or other parts that can burn out; as a consequence, they have very long life cycles.

2.2.2 Photoacoustic theory

Part of the modulated light energy incident on the gas sample being analyzed is absorbed, which produces a modulated pressure wave within the sample chamber. A microphone at the chamber wall detects this pressure wave.

The sound generated in the gas within a closed chamber can be described by the acoustic pressure $p(\mathbf{r}, t)$, which is the difference between the total pressure P and its average value P_0 .

$$p = P - P_0 \quad (1)$$

Associated with acoustic pressure is an acoustic velocity $\mathbf{u}(\mathbf{r}, t)$ and an acoustic temperature $\Theta(\mathbf{r}, t)$. The acoustic velocity is the fluid velocity of gas at position \mathbf{r} and time t caused by the sound. The acoustic temperature is the departure from the average temperature T caused by the sound [40].

The heat $H(\mathbf{r}, t)$ produced by the absorption of light acts as a source for the generation of sound is related to $p(\mathbf{r}, t)$. The relationship between $H(\mathbf{r}, t)$ and $p(\mathbf{r}, t)$ can be described as the following [40].

$$(\nabla^2 p - c^{-2} \partial^2 p / \partial t^2 = -[(\gamma - 1) / c^2] \partial H / \partial t \quad (2)$$

After Fourier transform, Equation (2) becomes

$$(\nabla^2 + \omega^2 / c^2) p(\mathbf{r}, \omega) = [(\gamma - 1) / c^2] i \omega H(\mathbf{r}, \omega). \quad (3)$$

where

c : the speed of sound, m.s^{-1}

γ : the ratio of the specific heat of the gas in chamber at constant pressure C_p to that at constant volume C_v

$$p(\mathbf{r}, t) = \int p(\mathbf{r}, \omega) e^{-i\omega t} d\omega \quad (4)$$

$$H(\mathbf{r}, t) = \int H(\mathbf{r}, \omega) e^{-i\omega t} d\omega \quad (5)$$

The acoustic pressure $p(\mathbf{r}, \omega)$ within photoacoustic chamber is simply the sum over all the normal modes.

$$p(\mathbf{r}, \omega) = \sum_j A_j(\omega) p_j(\mathbf{r}) \quad (6)$$

where

$A_j(\omega)$: mode amplitude, m

Pao [40] shows that $A_j(\omega)$ can be calculated from

$$A_j(\omega) = -\frac{i\omega [(\gamma - 1) / V_c] \int p_j^*(\mathbf{r}, \omega_j) H(\mathbf{r}, \omega) dV}{\omega^2 [1 - (\omega / \omega_j)^2 - i(\omega / \omega_j) Q_j]} \quad (7)$$

where

V_c : the volume of photoacoustic chamber, m^3

p_j^* : the complex conjugate of p_j

Q_j : the acoustic resonant enhancement of the j^{th} mode at frequency ω_j , and the volume.

From Equation (7), Pao [40] determined that if the fractional absorption by the gas is small relative to the incident light intensity, then the pressure modulation amplitude is linearly proportional to the gas absorption coefficient, α (m^{-1}),

where

$$\alpha = \frac{H}{I}, \quad (8)$$

and the incident light intensity, I ($N \cdot m^{-2} \text{ sec}^{-1}$), but inversely proportional to sample chamber cross-sectional area, A_c (m^2).

The most common geometrical configuration for photoacoustic cells is a cylinder, with the excitation beam traveling parallel to the tube axis and being radially symmetric about it. In addition, if the excitation beam suffers negligible attenuation along the chamber axis, the spatial distribution of induced pressure is given by Pao [41]:

$$p(r, t) = \sum_j \left(\frac{-i\omega}{\omega_j^2} \right) \frac{\gamma - 1}{(1 - \omega^2 / \omega_j^2 - i\omega / \omega_j Q_j)} \frac{P_{\text{abs}} \exp(-\mu_j)}{V_c J_0^2(\pi\alpha_{0,j})} \times J_0(\pi\alpha_{0,j} r/R) \exp(-i\omega_j t) \quad (9)$$

where

r : radial distance in photoacoustic chamber, m

t: time, sec

$p(\mathbf{r}, t)$: the spatial distribution of induced pressure of position \mathbf{r} and time t , Pa

j : the value of j^{th} order mode

P_{abs} : one half the peak power absorbed by gas

μ_j and $J_0(\pi\alpha_{0,j})$ in Equation (9) are expressed in the following:

$$\mu_j = (a/R)^2 (2\pi\alpha_{0,j})^{-2} \quad (10)$$

$$J_0(\pi\alpha_{0,j}) = P_j^{-1} \quad (11)$$

where

$\alpha_{0,j}$: absorption coefficient of gas at $r=0$ and j^{th} order mode, m^{-1}

a : characteristic width of light beam, m

R : chamber radius, m

P_j : power absorbed in j^{th} order mode, J

ω_j : the resonant frequency of the normal mode $p_j(\mathbf{r})$.

Equation (9) shows that two factors affect the amplitude of the pressure responses coexist at same time. One of them is the excitation frequency ω . When ω is close to one of the resonant frequencies, ω_j , Equation (7) can be simplified to:

$$A_j(\omega) = -\frac{Q_j}{\omega_j} [(\gamma - 1) / V_c] \int p_j^*(\mathbf{r}, \omega_j) H(\mathbf{r}, \omega) dV. \quad (12)$$

The Equation (12) shows that operation at a low-frequency resonance is beneficial to getting higher A_j . The largest pressure in a photoacoustic chamber is obtained for the smallest practicable chamber volume. Considering that commercially available microphones for

detecting signal vary from 8-25 mm in diameter, the practical minimum chamber diameters are on the order of 25-50 mm.

2.2.3 Practical considerations in design of photoacoustic chambers

The photoacoustic chamber is the heart of the photoacoustic instrument. Its high sensitivity, large dynamic range and accuracy are very important. The best way to improve sensitivity of the instrument is to decrease background signals, which come from absorption of excitation radiation on the sample chamber windows and chamber walls. Kreuzer et al. [42] reported a background signal 125 times larger than noise signal from the microphone and amplifier. Increasing the length of chamber is one way to decrease the background signals from chamber windows. Background signals are expected to be inversely proportional to the length of chamber when the total volume of chamber is fixed. An alternative method to eliminate background noise is to use a wavelength-tunable laser and modulate the wavelength of excitation, which was demonstrated by Patel [43-44].

A variety of other noise signals will also affect sensitivity of photoacoustic system including external vibration and ambient noise. A phase-sensitive lock-in amplifier employing long integration times can help eliminate these effects.

2.2.4 Volumetric effects in photoacoustic chamber

The ideal geometry for resonant spectrophones is a cylinder with an excitation source propagating along the axis; however, for solid samples, a spherical chamber geometry should be chosen [45]. To optimize the coupling between the excitation and the standing

wave or the volumetric effects of the chamber, the light beam intensity should be limited to the vicinity of the axis.

Volumetric effects lead to wave dissipation in the photoacoustic chamber. The major energy losses take place in the following ways [45]:

1. Wave reflection due to the compliance of chamber walls.
2. Dissipation at the microphone diaphragm.
3. Viscous and thermal loss occurring in the gas boundary layer near the chamber surface.
4. Losses from wave scattering at surface obstructions, such as microphone mounts.

2.2.5 Modulation of excitation source

Modulation of the excitation beam is necessary to produce acoustic signals in a spectrophone. There are three methods to modulate the excitation radiation: amplitude modulation, frequency modulation, and a combination of these. The frequency with which the modulation is accomplished changes the pressure amplitude as well as the magnitude of background signals that are present [46].

From an operational viewpoint, the method of modulation can be further classified [46]:

1. Low-frequency, nonresonant amplitude modulation at fixed frequency. This mode of operation is simple and widely applied in continuous wave fixed-frequency infrared laser. However a background signal exists with this method.
2. High-frequency, resonant amplitude modulation at a fixed frequency. The diameter of chamber necessary for this mode should be at least two times the light beam

diameter. This method is useful for the photoacoustic operation environment where low-frequency noises appear. Moreover, this method is sensitive to change in ambient temperature and pressure.

3. Low-frequency amplitude modulation of the source frequency.
4. Continuous source with small modulation of the source frequency.
5. Light source amplitude held constant, but frequency of the excitation radiation is modulated.

2.2.6 Photoacoustic signal saturation

It is expected that photoacoustic signal will increase proportionally with excitation power of excitation source increases. Therefore, it would appear that the sensitivity of a photoacoustic system could be increased without limitation by applying more powerful excitation sources.

In fact, this is not true because too high light intensities will lead to optical saturation. Rosencwaig derived the following equation to calculate the photoacoustic signal, q [47]:

$$q = \frac{kE_1 N^2}{C_v \omega} \left\{ \frac{2\tau_c^{-2} B I_0 \delta}{[2B I_0 + \tau^{-1}] [(2B I_0 + \tau^{-1})^2 + \omega^2]^{1/2}} \right\} e^{i(\alpha t - \gamma + \pi/2)} \quad (13)$$

where k is the Boltzmann constant, N is the number of gas molecules per m^3 , E_1 is the energy of the excited level, C_v is the specific heat at constant volume, ω is the modulation frequency, τ is the collision lifetime, B is the Einstein coefficient, I_0 is the beam intensity, δ is the

modulation function, τ is the total lifetime of upper level, and γ is the phase delay due to the deexcitation processes($\gamma=\omega\tau$).

For low intensities ($I_0 < 1/B\tau$), Equation (13) can be simplified to

$$q \approx \frac{kE_1 N^2}{C_v \omega} \left(\frac{\tau}{\tau_c}\right)^2 \frac{2BI_0 \delta}{(1 + \omega^2 \tau^2)^{1/2}} e^{i(a\pi - \gamma + \pi/2)} \quad (14)$$

In this case q is linearly proportional to I_0 . For high intensities ($I_0 > 1/B\tau$), Equation (13) can be simplified to

$$q \approx \frac{kE_1 N^2}{C_v \omega} \tau_c^{-2} \frac{\delta}{BI_0} e^{i(a\pi - \gamma + \pi/2)} \quad (15)$$

In this case, as I_0 increases q actually begins to decrease.

The above discussion illustrates that higher detectability or responsive ability of a photoacoustic instrument must be realized by decreasing noise level instead of increasing the power of excitation sources indefinitely.

2.2.7 Models of the photoacoustic effect in solid

Based on the drawing in Figure 2.5, a general photoacoustic effect model was developed by Pao [48].

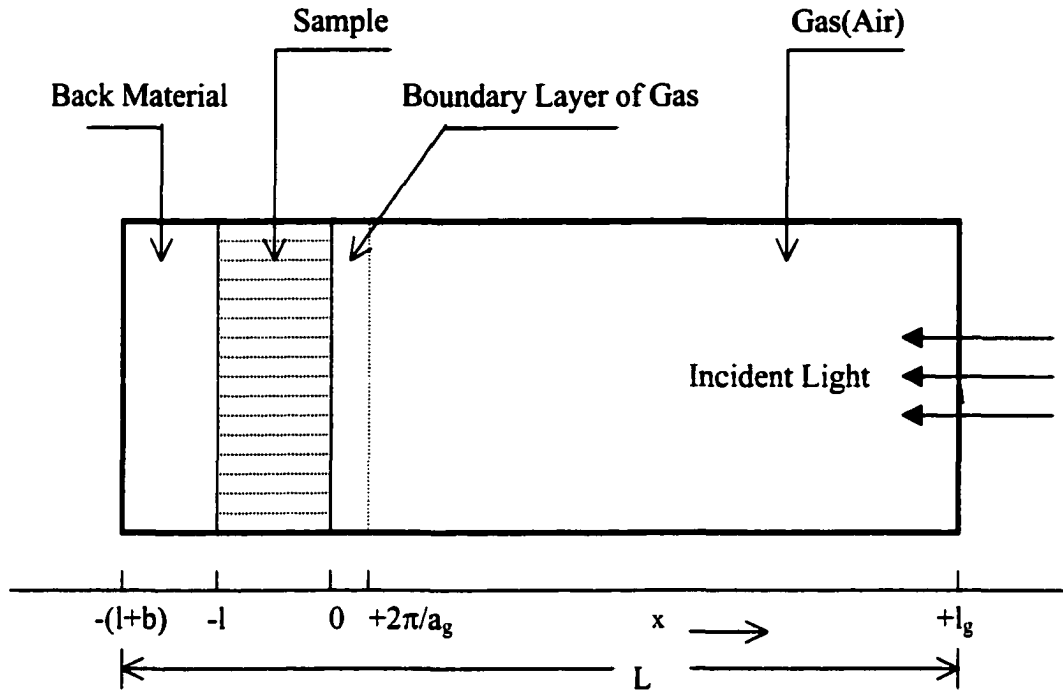


Figure 2.5. Cross-section view of a simple cylinder photoacoustic chamber [48, p. 198]

1. The Temperature Distribution in the Chamber

The temperature distribution in chamber $T(x, t)$ is expressed as

$$T(x, t) = \text{Re}\{\phi(x, t)\} \quad (16)$$

where Φ is the ambient (room) temperature and Re denotes the "real part of" $\{\phi(x, t)\}$.

$\phi(x, t)$ can be described in the following forms according to differences of x positions

$$\phi(x, t) = l_b^{-1}(x+l+l_b)W_0 + W \exp[\sigma_b(x+l) + i\omega t] \quad -l-l_b \leq x < -l \quad (17)$$

$$\phi(x, t) = e_1 + e_2 x + d e^{\alpha x} + (U e^{\delta_1 x} + V e^{-\delta_2 x} - E e^{\alpha x}) e^{i\omega t} \quad -l \leq x \leq 0 \quad (18)$$

$$\phi(x, t) = (1 - x/l_g)\theta_0 + \theta \exp(-\sigma_g x + i\omega t) \quad 0 \leq x \leq l_g \quad (19)$$

where

$$d = -A/\alpha^2 \quad (20)$$

$$E = A/(\alpha^2 - \sigma_s^2) = \alpha I_0 / 2k_s(\alpha^2 - \sigma_s^2) \quad (21)$$

W, U, V, E and θ are complex-valued constants, e_1, e_2, d and W_0 and θ_0 are real-valued constants, and $\sigma_j = (1+i)a_j$ with $a_j = (\omega/2\beta_j)^{1/2}$ and $\beta_j = k_j/\rho_j C_{p,j}$ as well as $\mu_j = a_j^{-1}$. The subscript j denotes materials in the chamber, solid sample, gas (air) and backing material.

Other variables are defined as follows:

k_j : the thermal conductivity of material j, $J(m \text{ sec } ^\circ C)^{-1}$

ρ_j : the density of material j ($kg \text{ m}^{-3}$)

$C_{p,j}$: the specific heat of material j at constant pressure, $J(kg \text{ } ^\circ C)^{-1}$

β_j : the thermal diffusivity of material j, $m^2 \text{ sec}^{-1}$

a_j : the thermal diffusion coefficient of material j, m^{-1}

μ_j : the thermal diffusion length of material j, m

ω : the modulation frequency of the incident light beam, radians/second

α : the optical absorption coefficient of the solid sample for wavelength λ

I_0 : the incident monochromatic light flux, $W \text{ m}^{-1}$

θ and W represent the complex amplitudes of the periodic temperatures at the sample-gas boundary ($x=0$) and the sample-backing boundary ($x=-l$) respectively. The explicit solution for θ , the complex amplitude of the periodic temperature at the solid-gas boundary ($x=0$), is given as

$$\theta = \frac{\alpha I_0}{2k_s(\alpha^2 - \sigma_s^2)} \left\{ \frac{(r-1)(b+1)e^{\sigma_s t} - (r+1)(b-1)e^{-\sigma_s t} + 2(b-r)e^{-\alpha t}}{(g+1)(b+1)e^{\sigma_s t} - (g-1)(b-1)e^{-\sigma_s t}} \right\} \quad (22)$$

where

$$b = k_b a_b / k_s a_s \quad (23)$$

$$g = k_g a_g / k_s a_s \quad (24)$$

$$r = (1-i)\alpha / 2a_s \quad (25)$$

Then the solid-gas boundary temperature $T(x=0,t)$ is described by

$$T(0,t) = \Phi + \theta_0 + \theta_1 \cos \omega t - \theta_2 \sin \omega t \quad (26)$$

where Φ is the ambient temperature at the cell walls and θ_0 is the increase in temperature owing to the steady-state component of the absorbed heat. θ_1 and θ_2 are real and imaginary parts of Equation (26).

2. Generation of the Photoacoustic Signal

Figure 2.5 shows that there is a boundary layer and its depth is $2\pi/a_g$

where

$$a_g = \sqrt{\omega / 2\beta_g} \quad (27)$$

and

a_g : the thermal diffusion coefficient of gas, m^{-1}

ω : modulation frequency of the incident light beams, $rad\ s^{-1}$

β_g is the thermal diffusivity of gas, $m^2\ sec^{-1}$.

Further, in Equation (27), a_g is expressed as

$$a_g = \mu_g^{-1} \quad (28)$$

where μ_g is defined as the thermal diffusion length of gas in m, and β_g is

$$\beta_g = \frac{k_g}{\rho_g C_{p,g}} \quad (29)$$

where

k_g : thermal conductivity of gas, $\text{J m}^{-1} \text{s}^{-1} \text{°C}^{-1}$

ρ_g : density of gas, kg m^{-3}

$C_{p,g}$: specific heat of gas at constant pressure, $\text{J kg}^{-1} \text{°C}^{-1}$.

Pao estimated the boundary layer $2\pi/a_g$ or $2\pi\mu_g$ in Figure 2.5 is close to 0.1 cm for $\omega/2\pi$ equal to 100Hz. He assumes that only this thickness of gas is capable of responding thermally to the periodic temperature at the surface of the sample. In this layer, gas expands and contracts periodically and thus can be thought of as an acoustic piston on the rest of the gas column, producing an acoustic pressure signal that travels through the entire gas column. Therefore, the periodic heat flow from the solid to the surrounding gas produces the acoustic signals.

Pao derived the following explicit formula:

$$Q = \frac{\alpha l_0 \mathcal{P}_0}{2\sqrt{2}k_g l_g a_g T_0 (\alpha^2 - \sigma_s^2)} \times \left\{ \frac{(r-1)(b+1)e^{\sigma_s l} - (r+1)(b-1)e^{-\sigma_s l} + 2(b-r)e^{-\alpha l}}{(g+1)(b+1)e^{\sigma_s l} - (g-1)(b-1)e^{-\sigma_s l}} \right\} \quad (30)$$

$$\Delta P(t) = Q_1 \cos(\omega t - \pi/4) - Q_2 \sin(\omega t - \pi/4) \quad (31)$$

where b, g and r were mentioned in Equation (23-25), Q (signal) specifies the complex envelope of the sinusoidal pressure variation. P_0 is the ambient pressure variation and γ is the ratio of the specific heats. ΔP is the actual physical pressure variation. Q_1 and Q_2 are the real and imaginary parts of Q.

3. The Photoacoustic Signal of Optically Opaque Solids

Equation (30) is difficult to interpret due to its complicated form. However, for special cases Equation (30) can be simplified to give physical insight. For example, in the case of optically opaque solids, most of light is absorbed within a distance small compared to l . Pao classified optically opaque solids into three categories.

1) Thermally thin solids ($\mu_s \gg l$, $\mu_s \gg \mu_\alpha$)

Equation (30) can be simplified as

$$Q \cong [(1-i)/2a_g](\mu_b/k_b)Y \quad (32)$$

$$Y = \gamma P_0 I_0 / 2\sqrt{2}l_g T_0 \quad (33)$$

In this case, the signal is independent of α and varies with ω^{-1} . High concentrations of optically opaque carbon fall into this situation.

2) Thermally thick solid ($\mu_s < l$, $\mu_s > \mu_\alpha$)

The following equation is obtained from Equation (30)

$$Q \approx \frac{Y}{2a_g a_s k_s \alpha} (\alpha - 2a_s - i\alpha) \cong \frac{(1-i)}{2a_g} \left(\frac{\mu_s}{k_s}\right) Y \quad (34)$$

Hence, the acoustic signal is independent of α and varies as ω^{-1} . However, the thermal properties of the solid sample now replace those of the backing material, as occurred for Equation (32).

3) Thermally thick solid ($\mu_s \ll l$, $\mu_s < \mu_\alpha$)

In this very interesting and important case,

$$Q = \frac{\alpha Y}{4a_g a_s^3 k_s} (\alpha - 2a_s - i\alpha) = \frac{-i\alpha\mu_s}{2a_g} \left(\frac{\mu_s}{k_s}\right) Y \quad (35)$$

which represents an optically opaque ($\alpha l \gg 1$) system. However as long as $\alpha\mu_s < 1$, the solid sample is not photoacoustically opaque. Only the light absorbed within the first thermal diffusion length μ_s will contribute to the acoustic signal of the system. The photoacoustic signal will be proportional to $\alpha\mu_s$ and depend on the thermal properties of solid sample and vary as $\omega^{-3/2}$.

2.2.8 Photoacoustic saturation for solid samples

When the optical absorption coefficient, β , of solid sample is 10^4 cm^{-1} or greater, photoacoustic saturation becomes a problem. Sample grinding can make particles of thermally thin and make them more efficient absorbers. Compounds will also be photoacoustically opaque or saturated unless the thermal diffusion length μ is less than the optical absorption length β^{-1} . A modulation frequency in excess of 10^4 Hz is needed to bring these particles out of saturation ($\mu < 1/\beta$). Lin and Dudek [49] have shown that proper sample preparation techniques may bring even these materials out of saturation. Lin and Dudek have used the following methods:

1. A thin layer of a sample is deposited onto a quartz plate. The sample deposition can be made either by vacuum deposition or by smearing with a suitable applicator.
2. The sample can be molecularly disposed over the surface of a nonabsorbing medium such as barium sulfate, magnesium oxide, neutral alumina, and silica gel. The sample is first dissolved in a suitable solvent such as chloroform. The solution is then thoroughly mixed to form slurry, and then the solvent is evaporated with a rotary evaporator.
3. A mechanical dispersion technique can be used wherein the sample is co-ground with a non-absorbing substrate in a vibrating mill.

2.3. Photoacoustic Effect Application in Testing Unburned Carbon in Fly Ash

As mentioned earlier, fly ash is a complicated compound consisting of different kinds of chemical substance. However, the unburned carbon in fly ash can be thought of as a blackbody that has strong absorption ability. Brown and Waller [50] examined the infrared absorption properties of fly ash using Fourier-transform infrared photoacoustic spectroscopy (FTIR-PAS). Figure 2.6 shows the infrared spectrum for a typical fly ash. The irregular and large signals between 400 and 1500 cm^{-1} come from mineral matter. CO_2 in the air produces a large signal around 2350 cm^{-1} and the signals around 3000 to 3700 cm^{-1} wavenumber are mainly caused by the absorption of hydroxyl radical OH^- on fly ash.

Brown and Waller think that unburned carbon, as a blackbody absorber, can generate a photoacoustic signal at virtually any wavelength. On the other hand, mineral matter absorbs only in limited wavelength bands. They claimed that at approximately

2600 cm^{-1} only unburned carbon strongly absorbs. A plot photoacoustic signal vs. carbon concentration showed a strong correlation for measurements around 2600 cm^{-1} . Based on these results, they designed a carbon-in-ash monitor based on the photoacoustic effect.

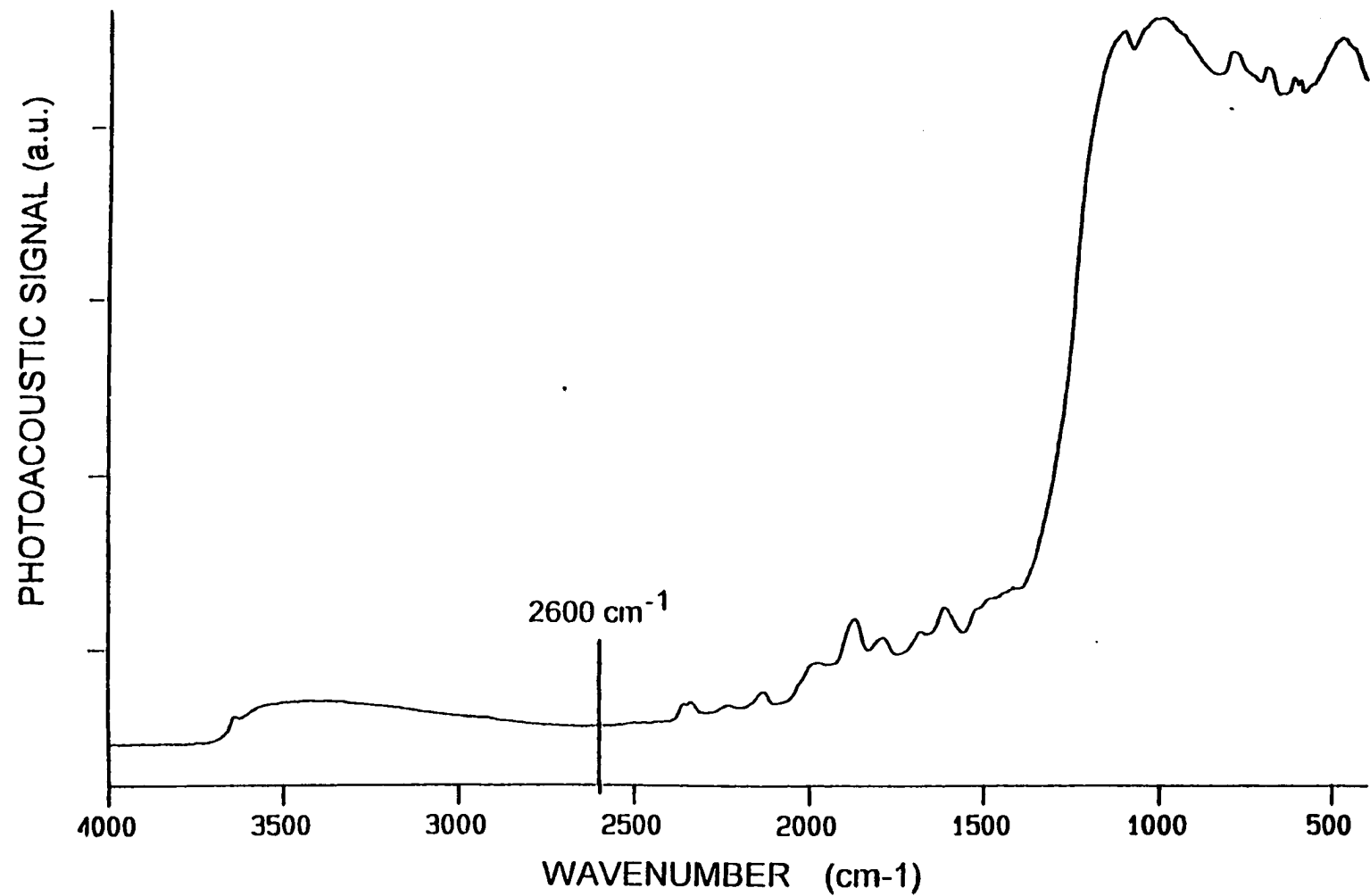


Figure 2.6. Spectral photoacoustic absorption for a typical fly ash as measured by FTIR [50, p.26]

3. EXPERIMENTS

A research program was designed to understand problems in accuracy and precision of the CA200 reported by Ametek. This program investigated the role of fly ash characteristics, sampling procedure and fly ash preparation, and instrument design and operation on instrument performance.

3.1 Fly Ash Characterization

Accordingly, the first task was to collect a wide variety of fly ashes from various sources. Seventy fly ashes were collected from boilers in the U.S., China, Canada and Australia. Types of coal and boilers and boiler operation conditions vary considerably from one sample to another. Ametek conducted LOI tests on some samples. Iowa State University (ISU) independently ran LOI tests on all samples as well as analysis of total loss (TL) and total organic carbon (TOC) of fly ashes using a Perkin Elmer thermogravimetric analyzer: Model TGA-7.

The LOI measurements were performed in an ashing oven using the prescribed ASTM method [1] described in Appendix 1. The experimental method was validated by comparing results for selected samples against LOI measurements performed by an independent laboratory (Materials Analysis Research Laboratory in the ISU Engineering College). The maximum difference between these two sets of LOI measurements was 0.5%.

3.1.1 Detection of TL and TOC using TGA

Total loss (TL) and TOC of fly ash were measured using TGA. A photograph of the Perkin Elmer TGA-7 is shown in Figure 3.1. Before the TL and TOC measurements, the

Perkin Elmer TGA-7 was calibrated. Temperature, weight and furnace were calibrated separately. The Curie points of alumel, nickel, perkalloy and iron were used to conduct temperature calibration described in Appendix 2.

Typical TGA procedure for TL and TOC determinations is first to stabilize fly ash samples of approximately 25 mg with only nitrogen flowing through the furnace at room temperature for about 30 minutes until the sample weight reading on TGA is very stable. At this point a thermal equilibrium between the fly ash sample and environment within furnace of TGA is reached. The sample is then heated from room temperature to 750 °C and held at that temperature until no weight loss is observed, which usually takes about 30 minutes. During these heating and isothermal periods, all the moisture and volatile materials are expected to leave the fly ash sample. After that, the flow of nitrogen is replaced by air, which allows “organic” carbon (that is, unburned carbon) to be oxidized and removed as carbon dioxide. TGA operation is terminated when the TGA weight loss curve becomes level. TL is defined as the total weight loss during a TGA test. Total organic carbon is the weight loss after introduction of air to the sample. A typical TGA weight loss curve, obtained for fly ash sample AM 36, is shown in Figure 3.2. Volatile loss during the time interval 25-45 minutes followed by oxidative loss after 45 minutes is evident in this plot. If the sample showed appreciable weight change during the 10-minute interval at 750 °C in nitrogen, then the test was repeated with a longer time interval to make sure that non-oxidative reactions were complete before air was admitted to the sample. For all the tests, the nitrogen flow rate in the TGA balance was 70 ml/min and nitrogen or air flowing rate was 30 ml/min.

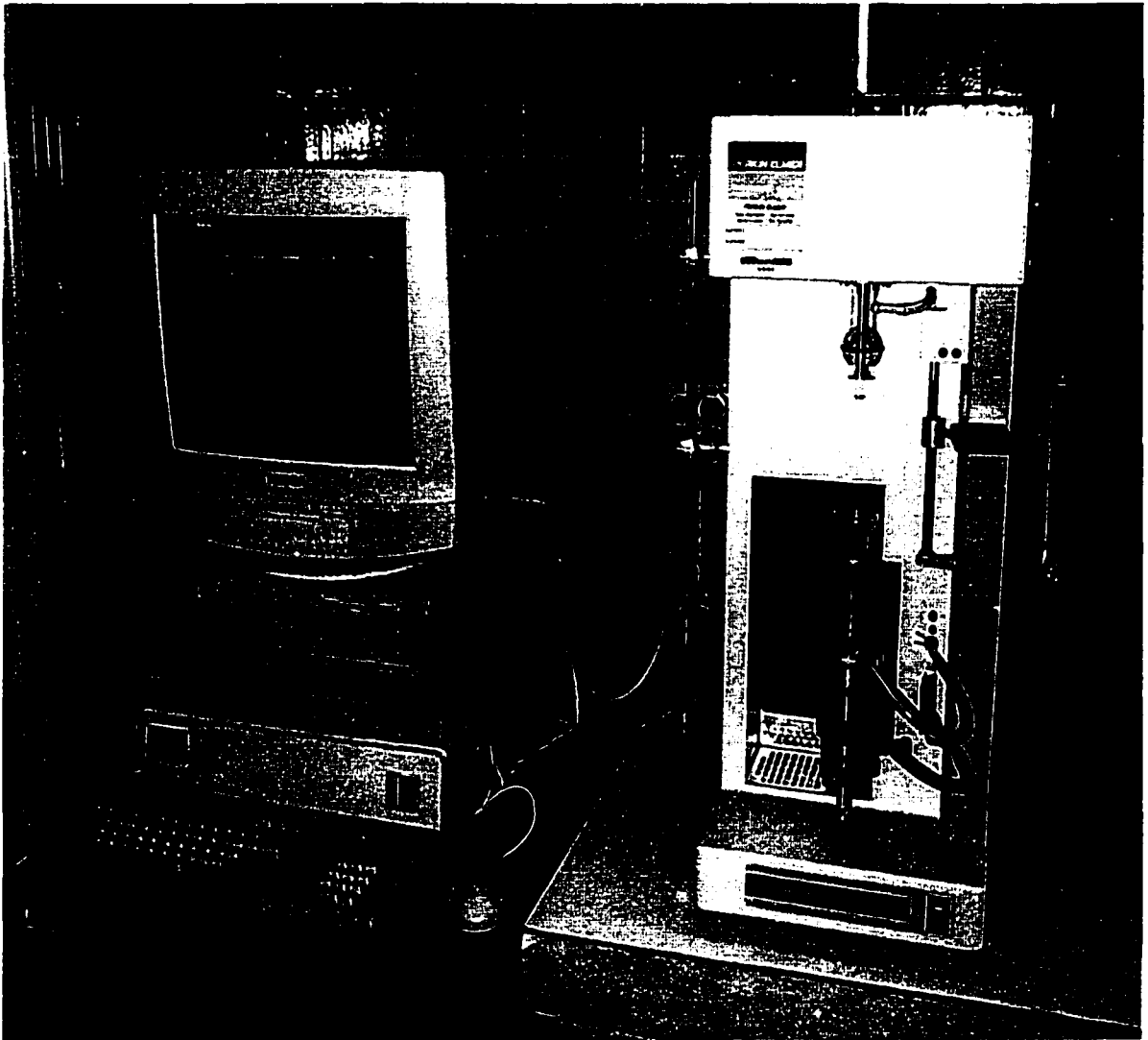


Figure 3.1. Photograph of the Perkin Elmer TGA-7

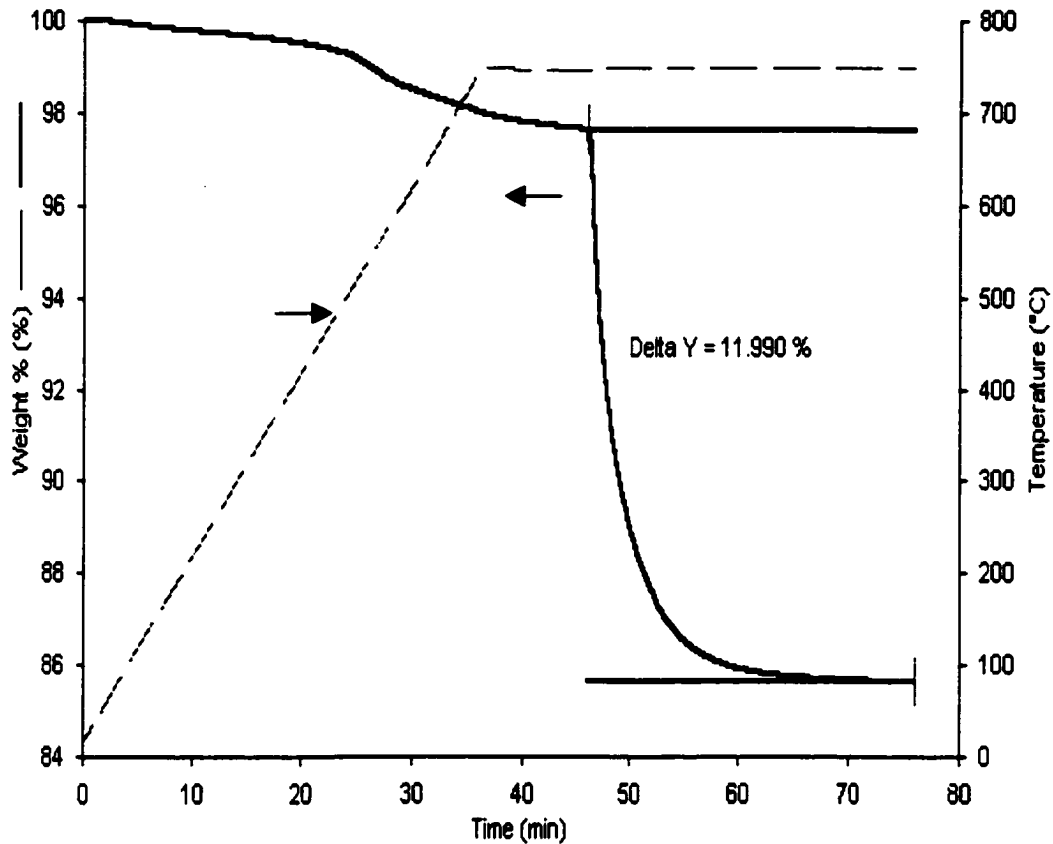
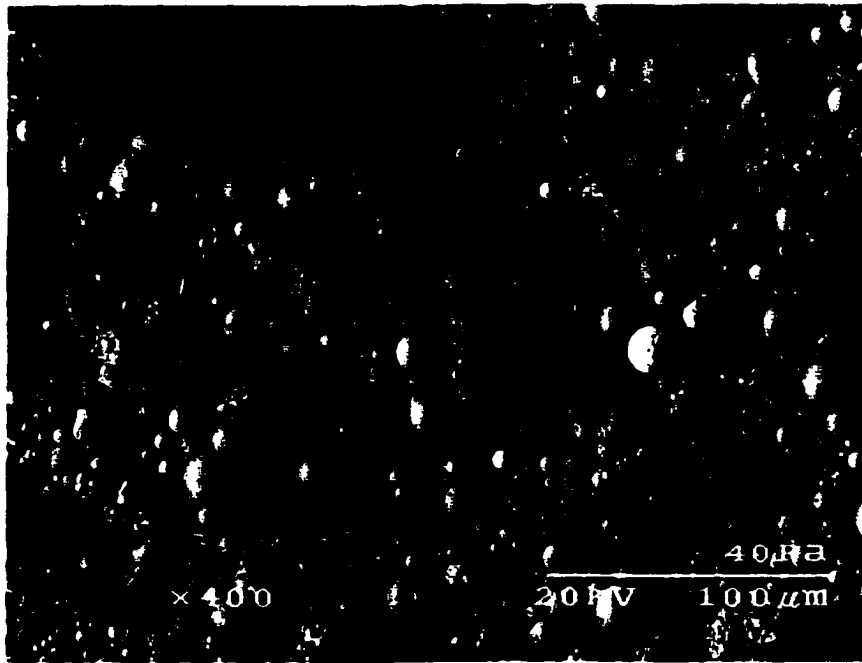


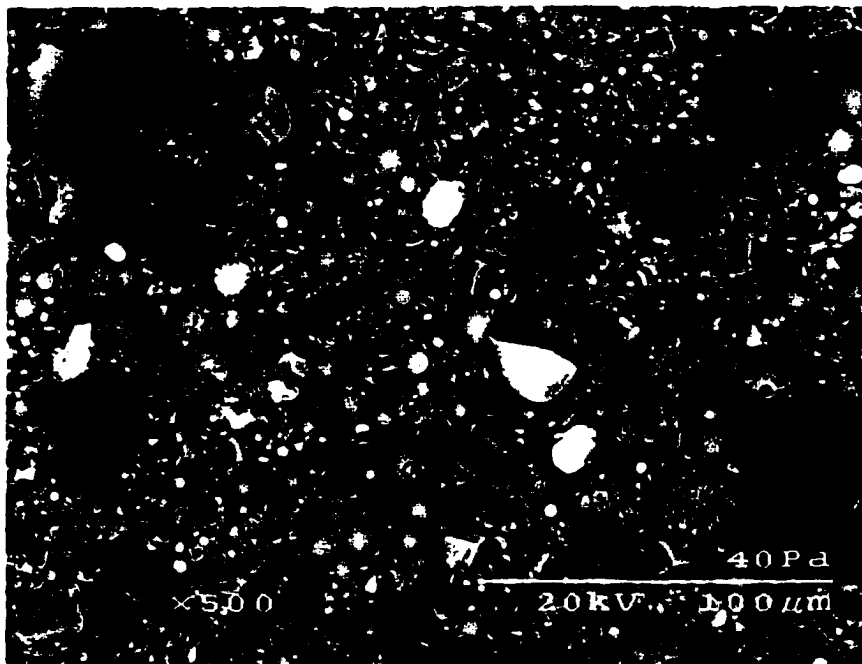
Figure 3.2. Example of TGA result (fly ash sample AM36)

3.1.2 Scanning electron micrographs

Some as-received fly ash samples were analyzed with a Hitachi Model S-2460N Scanning Electron Microscope (SEM) at the Material Analysis and Research Laboratory of ISU. Sample preparation for SEM consisted of spreading a thin layer of fly ash on a carbon SEM stub using double-sided carbon adhesive tape. Figure 3.3 shows typical SEM micrographs of two fly ash samples. Figure 3.3 demonstrates that unburned carbon particles in fly ash from a pulverized coal (pc) boiler are irregular, fragmented and porous relative to the smooth, spherical and glassy inorganic compounds. It is also easy to see that particle size distribution of fly ash is bimodal.



(a)



(b)

Figure 3.3. SEM micrographs of as-received fly ashes (a) 22356AT, (b) 32AT

3.2 Photoacoustic Apparatus

The experiment apparatus consisted of the mechanical assemblies from Ametek Corporation's CA200 instrument and appropriate signal detection circuits assembled in the laboratory. As mentioned earlier, this research employed three versions of the CA200 instrument. Each is based on a different excitation source: an IR diode laser, an IR LED, and a visible LED. These three versions had identical photoacoustic chambers and sample holders, and identical PANASONIC model WM-034B microphones. They shared several common components. A BK PRECISION model 4011 function generator modulated excitation sources. A lock-in amplifier picked up the signal with the frequency of excitation source from microphone. A BK PRECISION model 2120B oscilloscope was used to monitor the output signal from lock-in amplifier. AWM-034CBNC switch was used to supply power to the operating microphone. A data acquisition unit was used to record the photoacoustic signal from each carbon monitor. The data collection program is listed in Appendix 6. Photo of photoacoustic system is shown in Figure 3.4.

3.2.1 Design of new head

The physical arrangement of photoacoustic chamber of Ametek CA200 is shown in Figure 3.5. The microphone in the head of CA200 in Figure 3.5 is not ideally located to detect photoacoustic signals. From Figure 3.5, it is clear that the microphone is not very close to the sample holder nor is there a direct "line of sight" between the sample and the microphone. The tortuous path of the sound wave might dampen the acoustical signal at the face of the microphone. Part of this study was to investigate the effect of alternative head

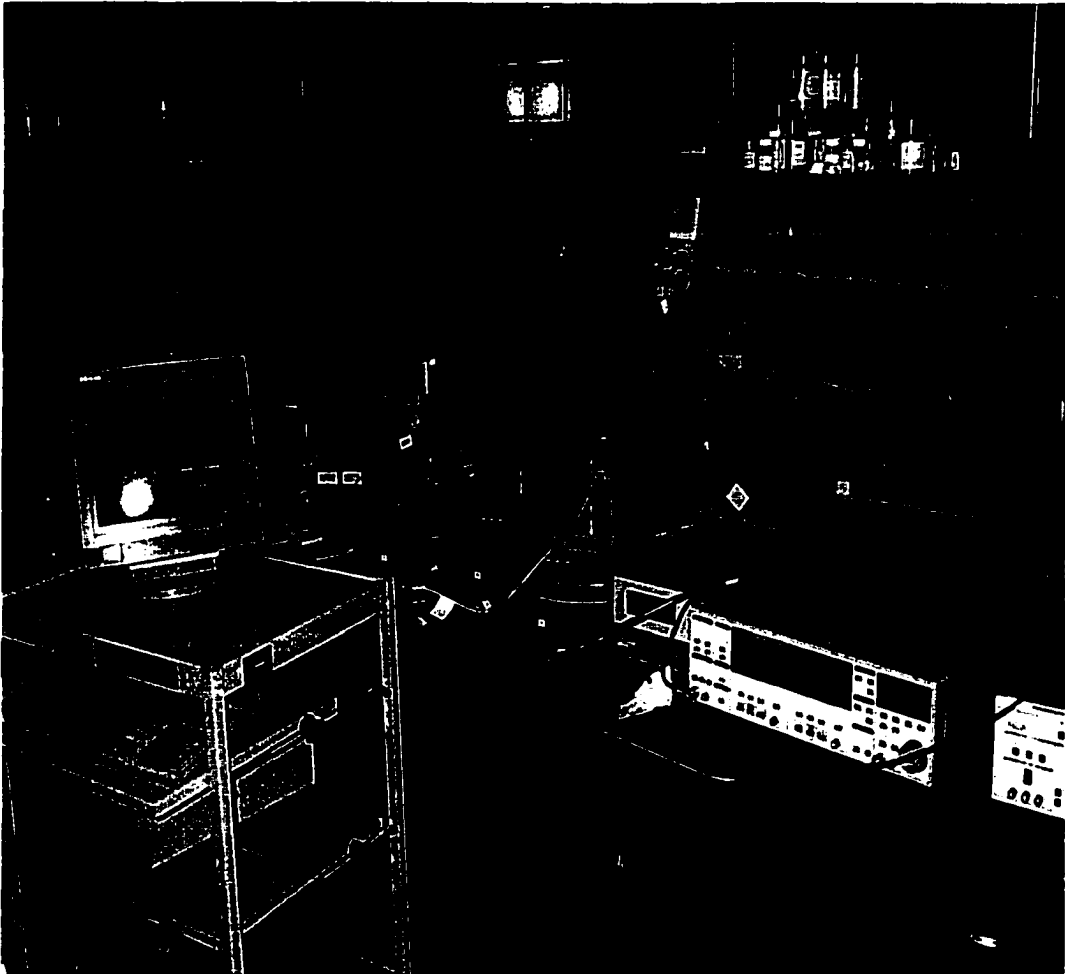


Figure 3.4. Photographs of photoacoustic system set-up

designs for the CA200. The alternative design explored in this study is shown in Figure 3.6. The alternative head brings the microphone closer to the sample holder by drilling the microphone access hole at an angle to the plane of the sample holder. The purpose of this head design was to increase the signal.

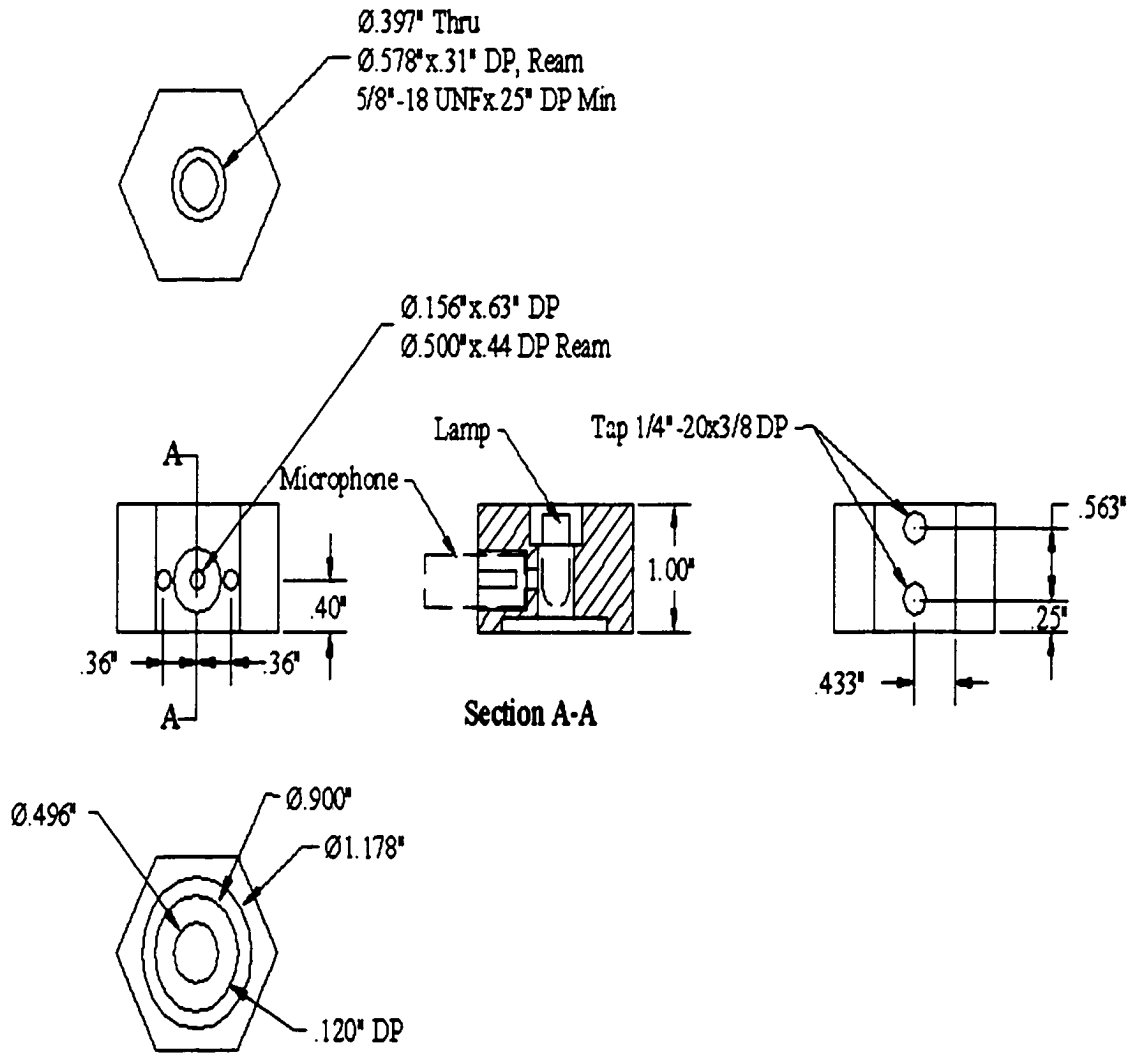


Figure 3.5. Drawing of photoacoustic chamber of CA200

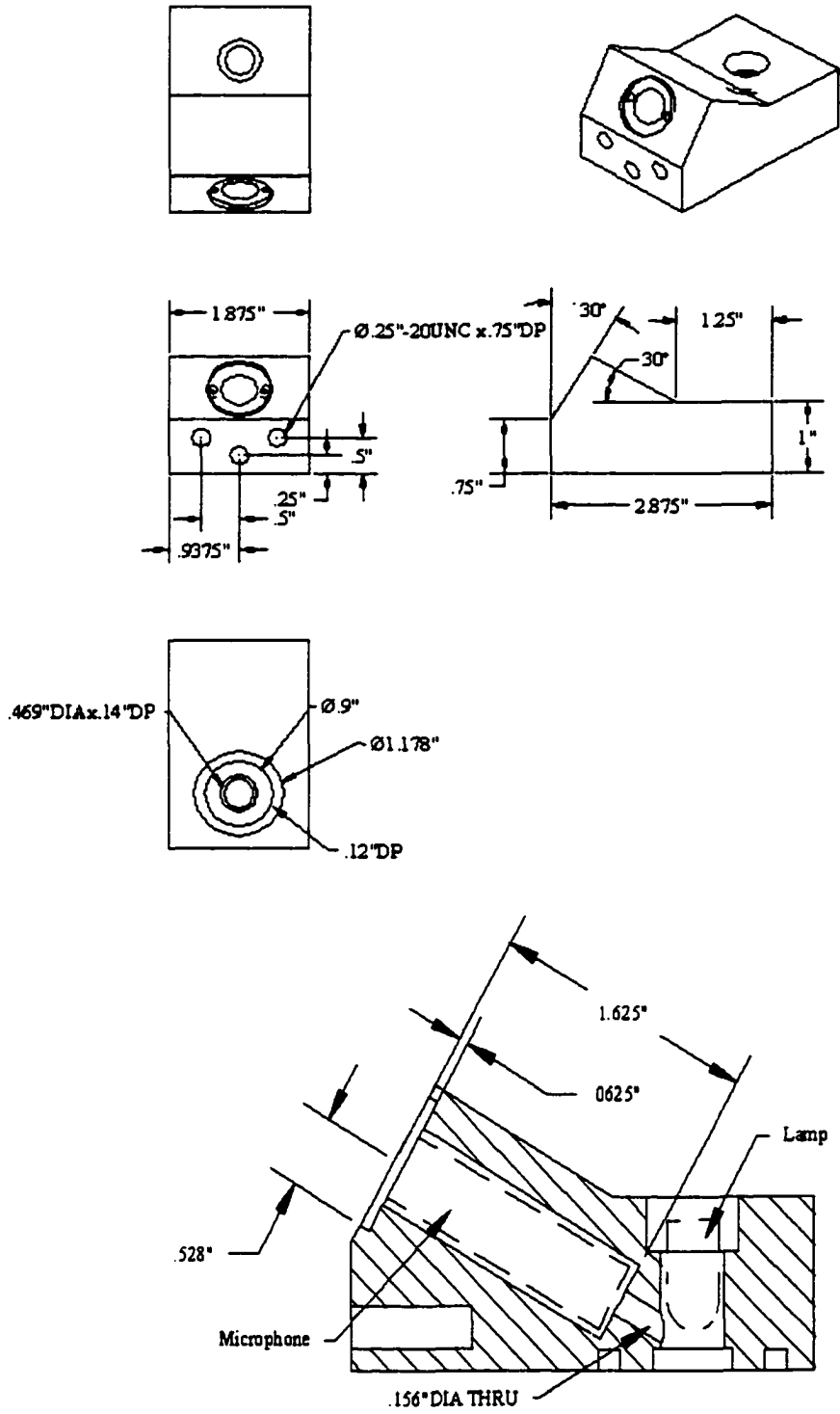


Figure 3.6. Drawing of new head

3.2.2 Design of new LED holder

The strength of the photoacoustic signal is expected to be inversely proportional to the volume of the photoacoustic chamber. The CA200 as designed by Ametek has an excessively large photoacoustic volume as a result of the manner in which radiation from an LED is coupled to the sample. As can be seen in Figure 3.5, the photoacoustic volume is a cylindrical volume formed by drilling vertically through the head of the CA200.

The visible LED is simply inserted into the top of this opening, bringing the excitation source into close proximity with the sample. However, this arrangement also leaves considerable space around the bullet-shaped bulb of the visible LED, which is anticipated to attenuate the photoacoustic signal.

Although an alternative mounting system is used for the smaller IR LED, it also presents acoustical attenuation problems. This slim, cylindrical LED is slid into a holder shown in Figure 3.7, which is fitted into the top of the head. The side of the holder contains a vertical slot, which was included as a transmission path for sound from the sample to the microphone. However, tests showed that the photoacoustic signal was independent of the angular orientation of the slot with respect to the microphone, which discounted the proposed function of the slot. Thus, the slot simply contributed to the photoacoustic volume of the chamber and should be reduced. Thus, the holder was redesigned without the slot and capped with a quartz window to minimize the photoacoustic volume. The drawing of new LED holder is shown in Figure 3.8.

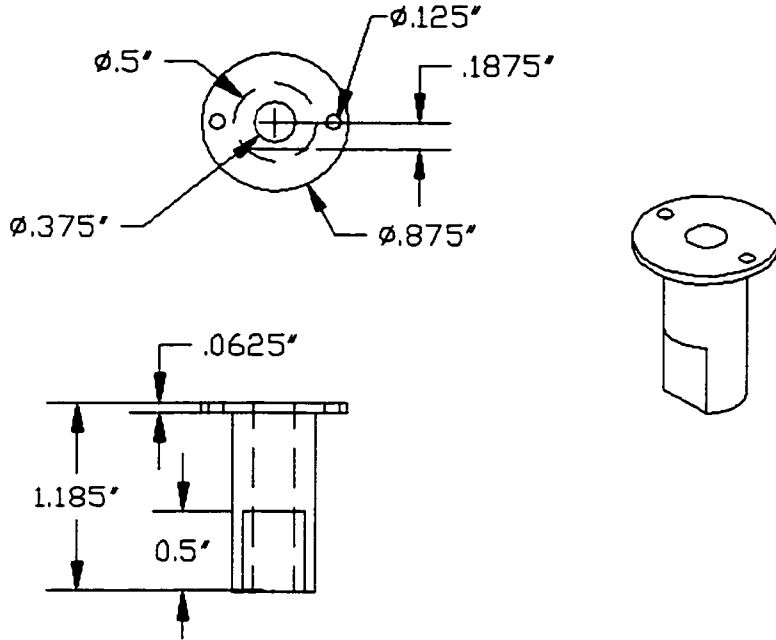


Figure 3.7. Drawing of IR LED holder designed by Ametek

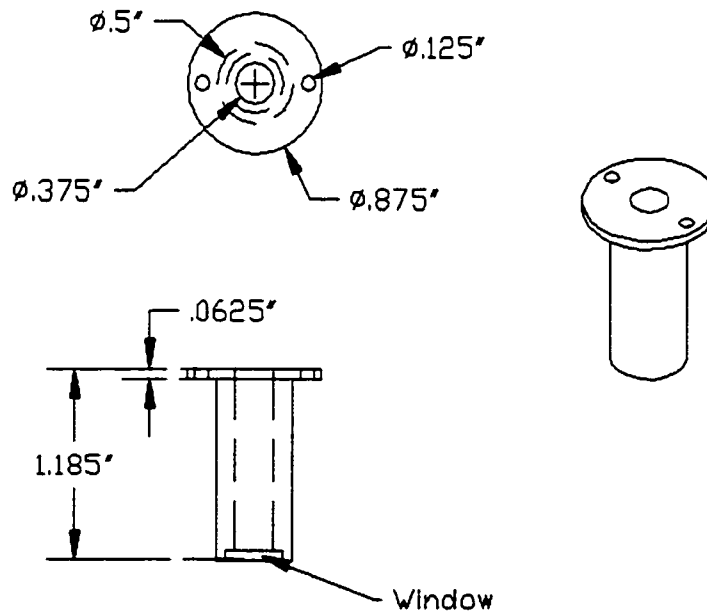


Figure 3.8. Drawing of new IR LED holder designed by ISU

3.2.3 Excitation source

The photoacoustic signal arises from absorption of the electromagnetic radiation by the sample. Three excitation sources were evaluated in this study because of their ready commercial availability: an IR laser, a visible LED and an IR LED.

The laser is a Power Technology Inc. PPMT 1.5 (1300-6) near-infrared diode laser, which was selected for its relatively low cost and power stability. The laser emits radiation at $1.315 \mu\text{m}$ (7605 cm^{-1}), features a maximum output power of 1.5 mW, and is modulated by TTL input. The laser wavelength and output power are held constant by a Peltier Junction and fan, which thermoelectrically heat or cool the laser to within $0.1 \text{ }^\circ\text{C}$. As discussed in section 2.3, the ideal wavelength for detecting carbon in fly ash is thought to be around $3.85 \mu\text{m}$, which is in the mid-IR region. Unfortunately no commercially available light sources were found at this wavelength. However, it was thought that carbon has a much stronger absorption than mineral matter in the near-IR. The diode laser is powered by an Extech model 382203 0-30 VDC analog regulated power supply adjusted with internal potentiometer.

Ametek wished to evaluate LEDs as inexpensive excitation sources, despite the absence of provisions for temperature control. An IR LED at peak wavelength of 660 nm is used in the second CA200 as an excitation source. A visible LED manufactured by Tandy Co. was evaluated in the third CA200 because of its low cost and wide availability. A Series 2000 current-regulated power controller provided by Ametek was used to modulate the output power and change power amplitude. The operation procedure of the Series 2000 current-regulated controller is described in Appendix 3.

3.2.4 Signal detection and processing

A microphone detects the photoacoustic signal. The microphone is a displacement-sensitive device, and so it is strongly sensitive to temperature-induced pressure changes in a photoacoustic chamber. If a charge is applied to the capacitor in an electrically biased microphone, capacitance modulation caused by sound-pressure produces a voltage change at the microphone output. The signal output from the microphone therefore depends on the microphone capacitance, the pressure-induced changes in capacitance, and magnitude of the applied voltage. The signal is also inversely proportional to the total capacitance of the circuit, so it is essential that the microphone capacitance, the amplifier input capacitance, and any stray capacitance be kept to a minimum.

The microphone is acoustically coupled to the photoacoustic chamber of the CA200 to detect the acoustic response of irradiated samples and send the resulting electrical signal to a lock-in amplifier for processing. The Ametek CA200 units use Panasonic omnidirectional electret condenser model WM-034B microphone cartridges. The WM-034B microphone consists of high voltage internal electrical membrane, metal electrode and a field effect transistor (FET). It does not need a high-voltage bias from the outside like ordinary condenser microphones. The microphone features highly efficient electrical specification, pressure type operating principle, low impedance ($2.2\text{ k}\Omega$), omnidirectional back directivity and a high degree of reliability under adverse shock, vibration and environmental tests. The microphone has at maximum operation voltage of 10 volts and has sensitivity of 1 V/Pa .

A lock-in amplifier is used to process the relayed signal from the microphone. The AC signal is converted to a DC signal, which is representative of the original multi-

component signal initiated in the photoacoustic chamber. Noise components at frequencies other than the specified modulation frequency are filtered out. Most experiments were performed with a Stanford Research System model SR 530 lock-in amplifier with digital signal processing. Later, a Stanford Research System model SR 830 lock-in amplifier with digital signal processing was substituted because of its superior noise rejection and sensitivity. Both lock-in amplifiers' noise filtering abilities are well beyond those of passive electronic filters. In addition, they can provide variable gain and are programmable.

The data acquisition program for the SR 530 lock in amplifier was written by Dykstra [2]. The data acquisition program for model SR 830 was written by Waller [16] with minor modifications. These menu-based programs allow real-time photoacoustic signal monitoring, data storage, and on-screen adjustment of lock-in amplifier settings.

3.3. Establishment of a Standard Sample Preparation Procedure

The photoacoustic signal from fly ash can be approximated by Equation (34) given in Section 2.2.7. This shows that the photoacoustic signal from fly ash is related to its thermal diffusion length, μ_s , and thermal conductivity, k . Both of these quantities are affected by powder density. Therefore, care must be taken to assure that bulk densities of various fly ash samples be held approximately constant if the photoacoustic signal is to be highly correlated to carbon content for different kinds of fly ash. Thus, a methodology is required to get repeatable bulk densities when samples are loaded at different times or by different operators. The easiest way to control the density of fly ash sample for testing is to with a miniature press, referred as a jig. This apparatus is illustrated in Figure 3.9. The jig compresses a standard weight of fly ash to a standard volume by adding weight to a plunger that acts on the

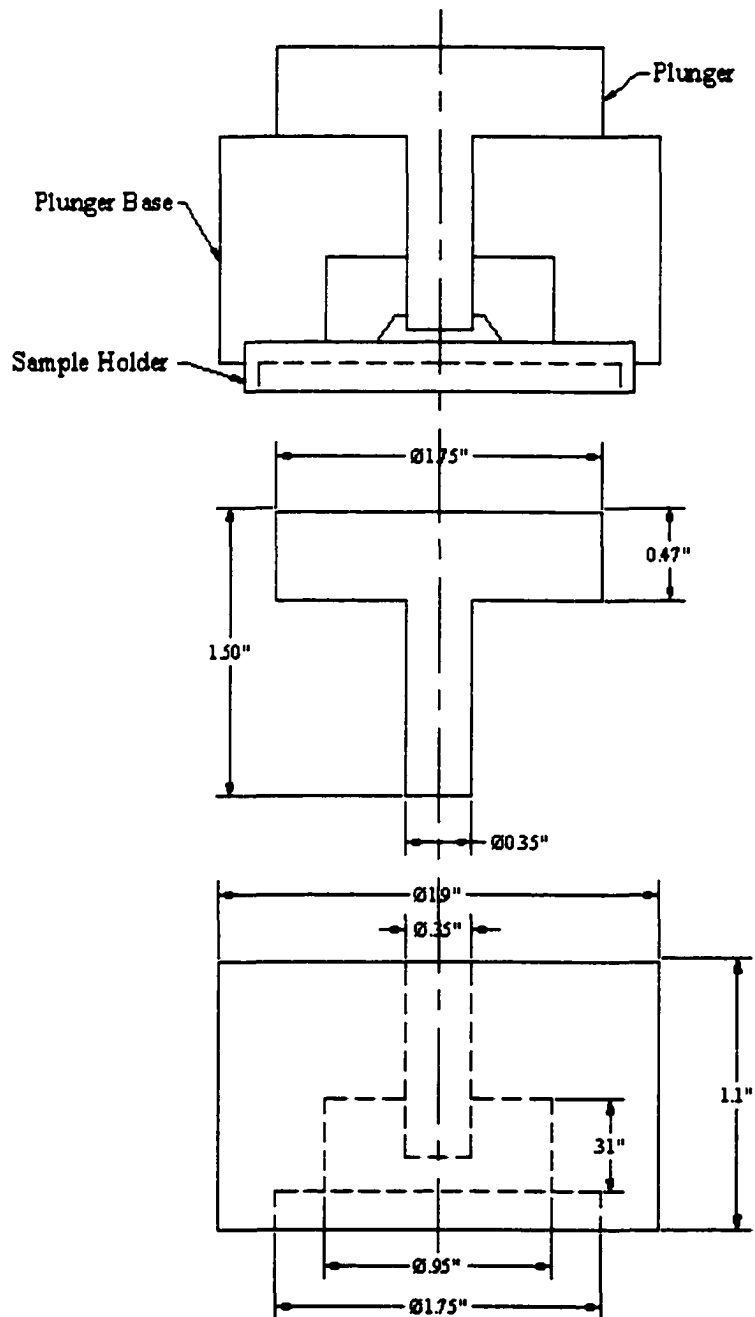


Figure 3.9. Sample preparation jig

sample. The detailed description of standardized sample preparation procedures is found in Appendix 4.

3.4 Choice of Modulation Frequency

Photoacoustic theory predicts that photoacoustic signal depends on the modulation frequency. Waller [16] successfully demonstrated that photoacoustic signal from fly ash is inversely proportional to modulation frequency. For this reason Ametek chose 1 Hz as the modulation frequency of the CA200 to get as high of signal as possible from the sample. In contrast, Waller used 100 Hz for all his photoacoustic tests to avoid ambient low frequency vibrations and to operate within the dynamic frequency range of the microphone. In fact, a number of factors that can affect the optimal modulation frequency were investigated in this study. Modulation frequency was easily varied by adjusting the function generator previously described.

3.5 Sample Homogeneity

As mentioned in section 2.2, the composition and particle size distributions of fly ashes vary considerably. Different constituents have different thermal properties. Porosity of fly ash powder also affects photoacoustic signal.

For each CA200 test, only 0.1144 ± 0.0005 g sample is placed into the sample holder. Of this amount, only 0.01 g is actually investigated by the photoacoustic process because the optical irradiation only penetrates 10 μm into the sample. Accordingly it is very important to make sure that the sample in the holder is representative of the parent fly ash.

Although the sample pan of the TGA only holds 0.030 g fly ash sample the entire is employed in the TL and TOC determination. Thus TGA measurements are inherently more accurate than CA200 measurements. Preliminary investigation results of several as-received samples are listed in Table 3.1. Table 3.1 shows that large TOC differences from triple tests of these as-received samples exist. Those differences are far beyond 0.2 –0.5% accuracy requirement for the CA200. In fact, if these large differences are not eliminated CA200 measurement, precision will become impossible because every test of parent fly ash will give a different reading. To make tested fly ash samples more homogenous, grinding is absolutely necessary.

Table 3.1 Triple TOC measurements of several as-received fly ashes

Sample	GC26	GC27	AM41	AM48	AM52	AM57
Trial 1 (%)	9.31	5.10	15.15	0.32	24.85	6.00
Trial 2 (%)	10.82	4.50	12.20	0.07	22.10	6.93
Trial 3 (%)	11.90	3.60	14.52	0.17	23.00	7.70
\bar{x} (%)	10.68	4.40	13.96	0.19	23.32	6.88
δ (%)	1.30	0.76	1.55	0.13	1.40	0.85

3.6 Photoacoustic Signal Saturation

The theory of signal saturation was described in Section 2.2.6. Waller demonstrated that noticeable reduction in photoacoustic response to unburned carbon in fly ash when carbon content of fly ash is higher than 5% [16]. Therefore, the relationship between carbon content of fly ash and photoacoustic signal is not linear in the 0-15% carbon content range of calibration for this instrument. However, Ametek used a fired fly ash and an as-received fly ash to calibrate the CA200 by drawing a line between these two data points.

Obviously, calibration equation derived in this way ignored signal saturation and consequently can not be used to calculate TOC of the other as received fly ash.

To solve this saturation problem in the calibration of the CA200, fly ash sample was diluted. Total organic carbon (TOC) of the diluted sample is lower than 5%. In this TOC region, photoacoustic signal of fly ash sample is not saturated and is linearly proportional to its carbon content. In this research different kinds of diluent were evaluated for their background signals and moisture absorbing ability. Calcium carbonate was finally chosen as the diluent of fly ash.

3.7 Precision of Carbon-in-Ash Monitor

In Ametek's evaluations of the CA200 by Ametek, precision problems with measurement were encountered. Three factors that potentially contribute to this problem were investigated in this study. First, sample heterogeneity affects on measurement precision. As-received fly ash must be ground to get representative and homogeneous sample for both TGA and CA200 tests. If the sample is not ground enough, each prepared samples of the same parent fly ash can have markedly different properties. Secondly, the compression procedure and density of fly ash samples need to be properly controlled because photoacoustic theory predicts that photoacoustic signal is affected by the thermal properties of the tested sample. Another potential source contributing to the precision problem of the CA200 is the changes in ambient temperature. A statistics program was employed to investigate the effects of ambient temperature on precision of the CA200. This program is listed in Appendix 5. Moreover, a stable temperature environment for photoacoustic

chamber of the CA200 was created by packing ice around the head of the CA200 and photoacoustic signals were recorded for comparison.

4. RESULTS AND DISCUSSIONS

4.1 Comparison of LOI and TOC As Carbon Indicators of Fly Ash

Ametek used LOI as a carbon indicator of fly ash to calibrate CA200. In this research, tests were performed to determine whether LOI was an accurate measurement of unburned carbon in fly ashes. Standard test method for fly ash in the analysis of coal and coke [1] was used to conduct LOI and TGA methodology was used to measure TL and TOC of seventy fly ash samples collected by Ametek from different countries, and the test results are listed in Table 4.1. Ametek performed LOI tests on only five samples and TOC tests on only six samples, and the results are also shown in Table 4.1.

Analysis of TGA data provided two kinds of information. First, the total loss (TL) of weight during a TGA test should correspond to LOI for the samples. Second, the weight loss upon admitting air to the heated sample represents the total organic carbon (TOC), that is, the unburned particulate char, in the fly ash sample. The relationships of LOI vs. TL and TOC of TGA tests on those seventy samples are respectively plotted in Figure 4.1 and Figure 4.2.

Figure 4.1 shows that TL and LOI are indeed equivalent measures. Total loss in Figure 4.1, in general, reads slightly higher possibly because TL of sample includes moistures absorbed during TGA sample preparation period. TGA test needs longer sample preparation time than LOI test does. The longer the dried samples are exposed to the air during sample preparation period, the more moisture is absorbed by fly ash samples especially to some extremely hygroscopic fly ashes. This correlation could be improved by including a drying period at 100 °C during the TGA tests to remove moisture.

Table 4.1. Results of “unburned carbon” determination by various measures

Sample Number	Sample Source	Ametek	ISU		
		LOI(%)	LOI(%)	TL(%)	TOC(%)
GCA4	Yaomeng/Pingdingshan, China	2.39	2.42	3.16	2.12
GCA5	Yaomeng/Pingdingshan, China	13.69	13.82	18.33	13.14
GCA13	Yaomeng/Pingdingshan, China	5.79	5.90	9.48	5.97
GCA26	Stanwell/Queensland, Australia	10.53	11.40	11.68	10.68
GCA27	Stanwell/Queensland, Australia	4.95	4.95	5.00	4.40
32AT	Scrubgrass/ Kennerdell, PA	-	10.50	11.40	9.53
AM36	Titus Station /GPU Genco, PA	-	13.70	14.36	11.99
AM37	Sikeston Power Station, MO	-	0.30	0.52	0.23
AM38	Hennepin Station, IL	-	4.70	4.74	3.15
AM39	Streeter/Cedar Falls Utilities, IA	-	3.03	3.52	2.94
AM40	Pell-Electric Dept., IA	-	8.59	9.67	2.68
AM41	Pell-Electric Dept., IA	-	8.50	9.39	2.07
AM43	Fort Drum Cogeneration	-	14.67	15.99	13.96
AM44	Fort Drum Cogeneration	-	14.54	14.82	13.80
AM45	Fort Drum Cogeneration	-	10.63	11.43	9.63
AM46	Fort Drum Cogeneration	-	2.00	2.46	1.30
AM47	Fort Drum Cogeneration	-	6.46	7.44	5.40
AM48	Wisconsin Public Service, WI	-	0.35	0.70	0.19
AM49	Unit 1/Payette Power Plant, TX	-	0.42	0.57	0.04
AM50	Unit 1 & 2/Chalk Point Units, MD	-	5.32	5.46	4.60
AM51	Texas-New Mexico Power, TX	-	1.57	1.92	0.05
AM52	Centralia Plant /PacifiCorp, WA	-	22.42	23.96	23.32
AM53	Centralia Plant/ PacifiCorp	-	0.10	0.58	0.02
AM55	Dunkirk Steam Station, NY	-	1.60	1.68	1.18
AM56	Dunkirk Steam Station, NY	-	3.76	4.58	1.93
AM57	Dunkirk Steam Station, NY	-	7.50	7.87	6.88
AM58	Four Corners/Fruitland, NM	-	1.72	1.80	1.22
AM59	Dunkirk Steam Station, NY	-	0.44	0.85	0.17
AM61	Chamois Plant, MO	-	18.02	18.62	14.38
AM62	Brandon Gen. Station, Canada	-	0.54	0.99	0.07

Table 4.1. (Cont.)

Sample Number	Sample Source	Ametek	ISU		
		LOI(%)	LOI(%)	TL(%)	TOC(%)
AM63	Muscatine Power & Water, IA	-	0.15	0.39	0.04
AM64	Elmer Smith Station, KY	-	1.05	1.47	0.81
AM65	Sundonce Plant, Canada	-	0.52	0.91	0.11
AM66	Sundonce Plant, Canada	-	0.66	0.75	0.41
AM67	Unknown	-	0.23	0.69	0.22
AM68	North Valmy Station, NV	-	1.60	2.12	0.64
AM70	UNC-CH Cogen. Facility, NC	-	3.83	4.73	1.92
AM71	UNC-CH Cogen. Facility, NC	-	13.78	13.83	12.70
AM72	J.H. Campbell Unit #2, MI	-	2.32	2.46	1.66
AM73	J.H. Campbell Unit #3, MI	-	5.68	6.15	5.66
AM75	St. Joseph Light Plant, MO	-	22.56	23.26	19.84
AM77	Lee Station/ Pelzer, SC	-	18.91	22.48	6.33
AM78	Pht. Scherer, GA	-	1.95	3.81	3.10
21839AT	Duquesne/Elrama, 4B PA	-	6.20	6.42	5.52
22001AT	Duquesne/Elrama 3B, PA	7.74	8.01	8.16	6.91
21825AT	Duquesne/Elrama 2A, PA	-	0.10	0.23	0.03
21832AT	Duquesne/Elrama 3B, PA	9.92	9.98	10.45	9.72
21837AT	Duquesne/Elrama 3B, PA	13	11.70	11.86	11.27
21846AT	Duquesne/Elrama 4B, PA	14.18	14.00	14.27	12.88
21960AT	Duquesne/Elrama 3B, PA	17.97	18.22	18.45	16.15
21964AT	Duquesne/Elrama 3B, PA	8.82	8.93	9.04	7.88
21996AT	Duquesne/Elrama 3B, PA	14.61	14.67	14.79	13.36
22368AT	Duquesne/Elrama 3B PA	-	7.01	7.90	3.84
22288AT	Duquesne/Elrama 2A, PA	-	13.67	13.89	12.82
22343AT	Duquesne/Elrama 2A, PA	-	15.00	15.20	13.86
22462AT	Duquesne/Elrama 2A, PA	-	1.83	1.93	1.03
22473AT	Duquesne/Elrama 2A, PA	-	10.50	11.93	9.46
22499AT	Duquesne/Elrama 2A, PA	-	2.10	3.09	1.92
22332AT	Duquesne/Elrama 3B, PA	-	3.01	3.59	2.44
22336AT	Duquesne/Elrama 3B, PA	-	17.00	17.41	16.23

Table 4.1. (Cont.)

Sample Number	Sample Source	Ametek	ISU		
		LOI(%)	LOI(%)	TL(%)	TOC(%)
22339AT	Duquesne/Elrama 3B, PA	-	10.70	11.2	10.03
22342AT	Duquesne/Elrama 3B, PA	-	14.70	14.90	14.49
22345AT	Duquesne/Elrama 3B, PA	-	14.4	14.7	13.00
22348AT	Duquesne/Elrama 3B, PA	-	13.50	16.51	14.14
22352AT	Duquesne/Elrama 3B, PA	-	7.10	7.42	6.04
22356AT	Duquesne/Elrama 3B, PA	-	7.20	7.90	6.54
22360AT	Duquesne/Elrama 3B, PA	-	7.30	7.50	6.44
22368AT	Duquesne/Elrama 3B, PA	-	3.63	3.83	2.74
22372AT	Duquesne/Elrama 3B, PA	-	8.02	8.10	6.26
22518AT	Duquesne/Elrama 3B, PA	-	2.60	2.71	1.33

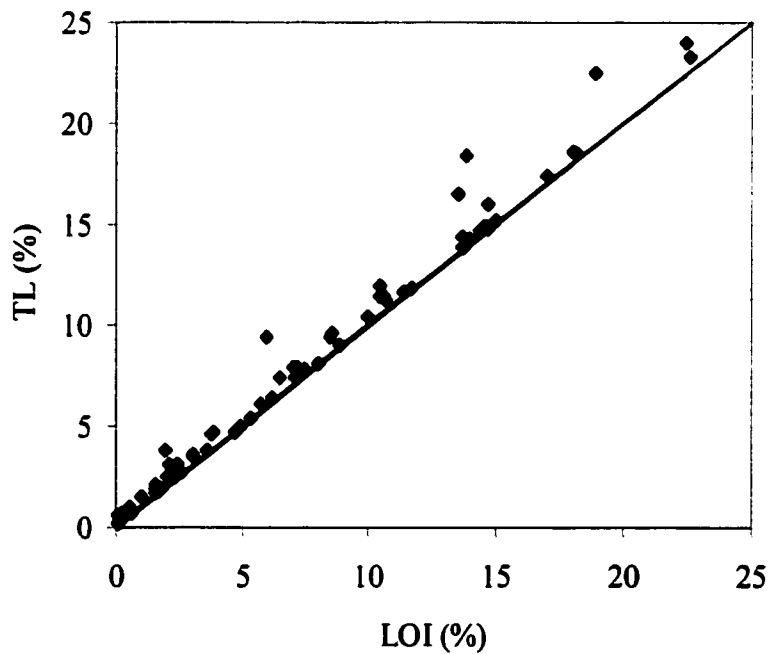


Figure 4.1. Comparison of TL based on TGA methodology and LOI based on ASTM methodology

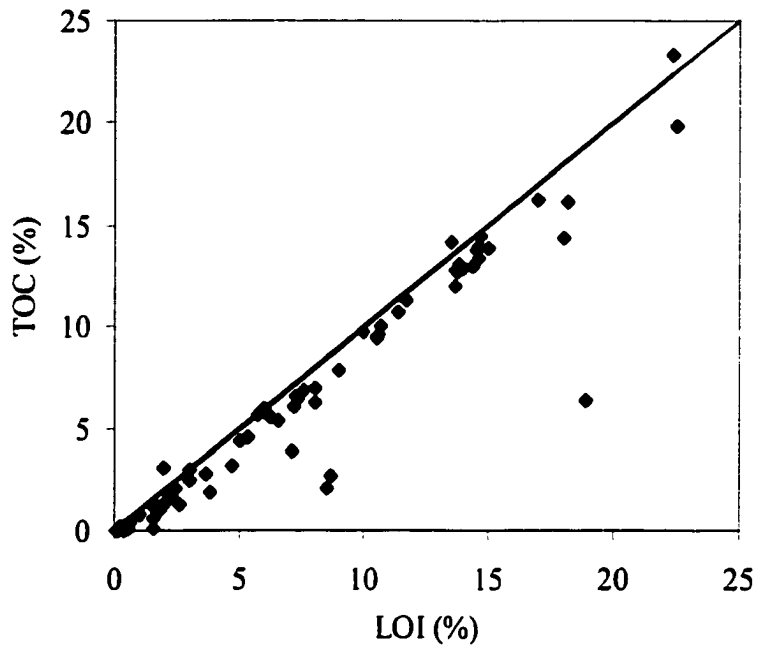


Figure 4.2. Comparison of TOC based on TGA methodology and LOI based on ASTM methodology

Figure 4.2 shows that TOC is smaller than LOI for most samples. If LOI is used as a carbon indicator of fly ash to calibrate CA200, it is obvious that CA200 accuracy will be adversely affected. The relative error of LOI as a carbon indicator can be expressed by the following relationship:

$$\frac{\text{LOI} - \text{TOC}}{\text{TOC}} \times 100\% . \quad (36)$$

Based on above formula (36), relative errors of all the samples in Table 4.1 were calculated and listed in Table 4.2. Table 4.2 shows that large relative errors exist for most samples if LOI is used as an unburned carbon indicator for fly ash. Considering the possible presence

Table 4.2 Relative errors of LOI for fly ash samples in Table 4.1

Sample	Relative Error(%)	Sample	Relative Error(%)	Sample	Relative Error(%)
GCA4	14.15	AM56	94.82	21846AT	8.70
GCA5	5.18	AM57	9.01	21960AT	12.82
GCA13	-1.17	AM58	40.98	21964AT	13.32
GCA26	6.74	AM59	158.82	21996AT	9.81
GCA27	12.50	AM61	25.31	22368AT	82.55
GCA27	10.18	AM62	671.43	22288AT	6.63
AM36	14.26	AM63	275.00	22343AT	8.23
AM37	30.43	AM64	29.63	22462AT	77.67
AM38	49.21	AM65	372.73	22473AT	10.99
AM39	3.06	AM66	60.98	22499AT	9.38
AM40	220.52	AM67	4.55	22332AT	23.36
AM41	310.63	AM68	150.00	22336AT	4.74
AM43	5.09	AM70	99.48	22339AT	6.68
AM44	5.36	AM71	8.50	22342AT	1.45
AM45	10.38	AM72	39.76	22345AT	10.77
AM46	53.85	AM73	0.35	22348AT	-4.53
AM47	19.63	AM75	13.71	22352AT	17.55
AM48	84.21	AM77	198.74	22356AT	10.09
AM49	950.00	AM78	-37.10	22360AT	13.35
AM50	15.65	21839AT	12.32	22368AT	32.48
AM51	3040.00	22001AT	15.92	22372AT	28.12
AM52	-3.86	21825AT	233.33	22518AT	95.49
AM53	400.00	21832AT	2.67		
AM55	35.59	21837AT	3.82		

of volatile materials and carbonates in the fly ash samples, it is not surprising that the correlation between LOI and TOC is not particularly strong. As expected, virtually all the LOI values are higher than the TOC values. Note that one of the largest divergences occurs for sample A41 in Table 4.2. Only 2.07% unburned carbon (TOC) is found in this sample although the LOI of 8.5% indicates that considerable volatile material exists in the ash.

The char (unburned carbon) formed in low temperature generally consists of 3~7 % fly ash, 8~12% volatile matter. The tar and light oil yield during char formation process accounts for about 6-10% of raw coal. The porosity of char in fly ash is about 40~50%, which can potentially absorb a lot of tar and oil on char's surfaces. Note that char is formed not only when air is absent but also not enough. When enough air is present, the finely divided coal entrained in air could be carbonized [50-51] to form char with volatile matters in it. Oil formed in low temperature of combustion is foul-smelling amber liquid composed mainly of mononuclear aromatic hydrocarbons such as indene, coumarone, dicyclopentadiene, benzene, toluene and xylene. The foul-smell of oil in fly ash was felt during the TGA tests.

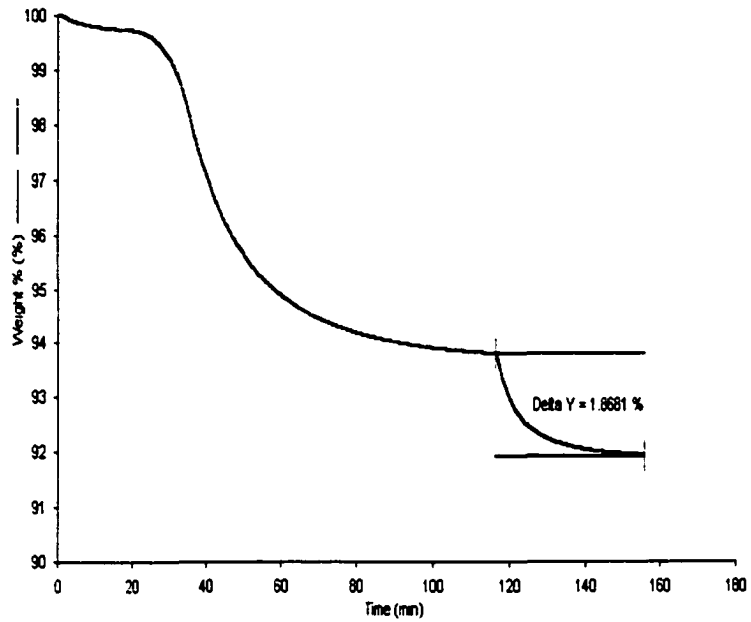
4.2 Effect of Fly Ash Sampling on Precision and Accuracy

4.2.1 Heterogeneity of as-received fly ash

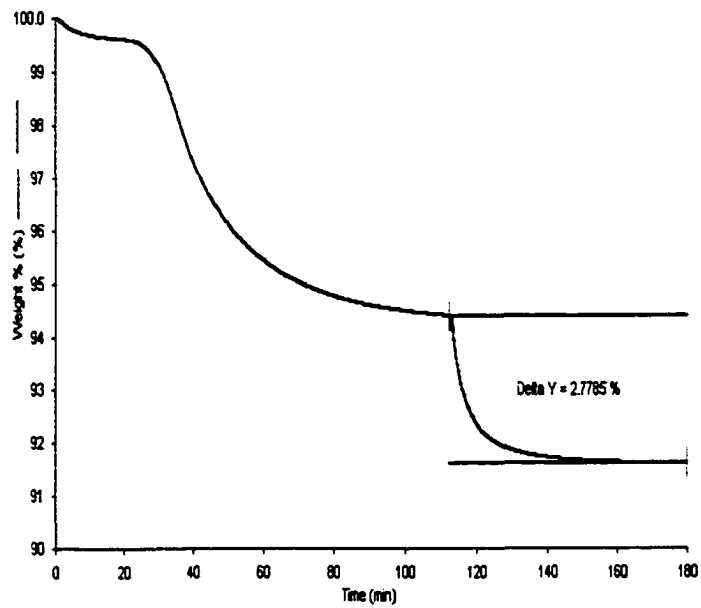
The fly ash samples used to calibrate the CA200 should be homogeneous. Tests were performed to determine whether as-received fly ashes are homogeneous enough to be used to calibrate CA200. Unground 22372AT fly ash was sampled. TGA analysis was

performed on each of these three 25 mg samples and the results are shown in Figure 4.3. The average TOC and standard deviation of three TGA trials of sample 22372AT in Figure 4.3 are 2.69% and 0.7374%, respectively. To a fly ash sample containing only 2.69% unburned carbon, clearly 0.7374% standard deviation of three trials can be considered to be very large. Therefore, as-received sample 22372AT is very heterogeneous. It is easy to image that uncertainty in sample's TOC measurement will contribute significantly to the precision problem of CA200 because TOC is used to calibrate CA200. Table 4.3 shows more triple TOC measurement results of some other as-received 2A and 3B boiler samples. Based on the standard deviation values of TOC of all those samples in Table 4.3, it is obvious that heterogeneity problem exists in every as-received fly ash sample. To further confirm the conclusion on the heterogeneity of as-received fly ashes, sample 22336AT SEM micrograph was taken and shown in Figure 4.4. In Figure 4.4, carbon, carbon-rich, as well as mineral particles of as-received sample 22336AT do not distribute uniformly in the scanned area, which again disapprove the homogeneity hypothesis of as-received fly ash sample.

CA200 signals are also very sensitive to heterogeneity of sample because only about 1.8 mg of the fly ash in the sample holder of CA200 is actually measured compared to about 25 mg of fly ash in the TGA evaluation. A non-representative sample will be obtained if fly ash sample is not highly homogeneous. To test this hypothesis, four trials with samples from a parent as-received fly ash 22473AT were performed with IR LED CA200. The average and standard deviation of these four trials were 1151.7 microvolts and 221.8 microvolts, respectively. These four trial results of sample 22473AT show that CA200 will have precision problem with the samples prepared from the same parent fly ash if the parent fly ash is not homogeneous.

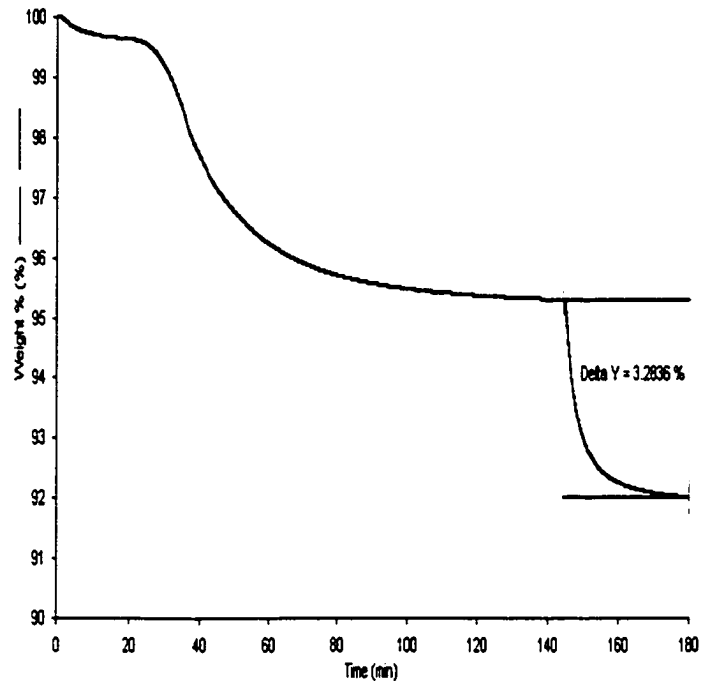


(a)



(b)

Figure 4.3. The triple TGA test results of the as-received parent fly ash 22473AT
(a) first trial (b) second trial (c) third trial



(c)

Figure 4.3. (Cont.)

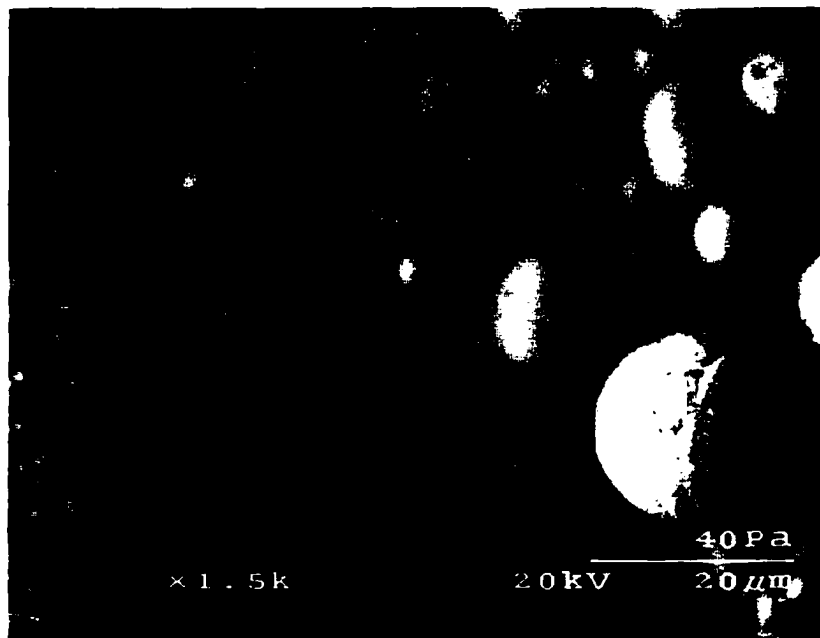


Figure 4.4. SEM micrograph of the as-received fly ash 22336AT

Table 4.3. Evaluation of heterogeneity of as-received fly ashes

Sample	22473AT	22372AT	22339AT	22288AT	22336AT	21832AT
Trail 1	8.51	2.81	9.21	11.68	15.37	9.70
Trail 2	10.40	1.90	10.9	13.89	17.00	8.91
Trail 3	8.9	3.36	9.01	12.01	15.01	10.32
\bar{x} (%)	9.27	2.69	9.71	12.53	15.79	9.64
δ (%)	0.9978	0.7374	1.0382	1.1922	1.0604	0.7067

Furthermore, the as-received 2A and 3B boiler samples were used to conduct CA200 calibration and the results were shown in Figures 4.5-4.6. The sample preparation method is referred to in Appendix 4. The reason for choosing modulation frequency 15 Hz will be explained in the later section.

Obviously, even though regression correlation coefficients are not too bad ($R_{2A}^2 = 0.9110$, $R_{3B}^2 = 0.8887$), unacceptable errors occurred for these calibration equations. In the Figures 4.5, only one point in 2A boiler calibration is close to the regression line enough to meet the accuracy standard required by Ametek; that is $\pm 0.2\%$ TOC for low carbon content fly ash and $\pm 0.5\%$ TOC for high carbon content fly ash. For 3B boiler samples in Figure 4.6 situation may get worse even though about half of 12 samples' actual CA200 readings appear to be close to regression line, which is due to the lower slope of calibration equation compared to 2A boiler samples. Clearly, grinding was needed to improve the calibrations of the both 2A and 3B as-received fly ashes. An alternative is to design a larger sample holder for the CA200 to accept more quantities of fly ash samples, which is anticipated to easily solve the precision problem using relatively relaxed sampling protocol.

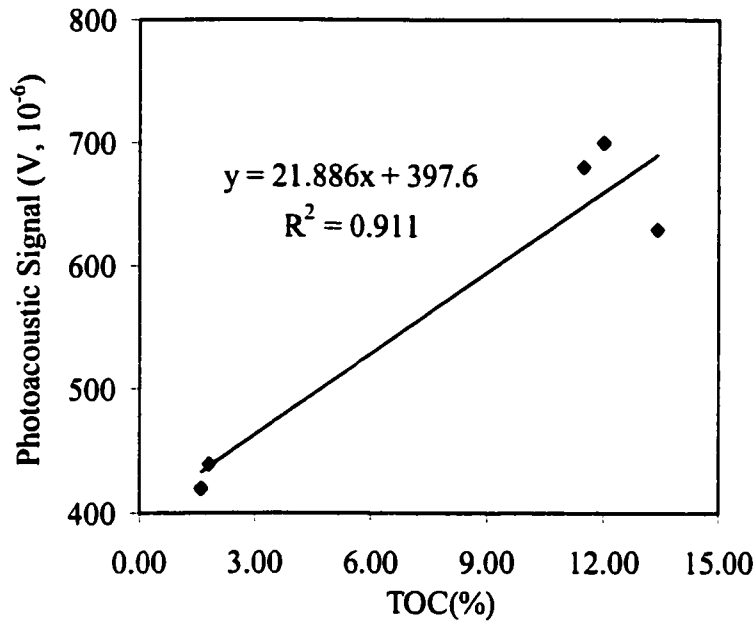


Figure 4.5. As-received 2A boiler sample calibration with IR LED excitation ($m=0.1144g$, $f=15Hz$, diluent; $CaCO_3$)

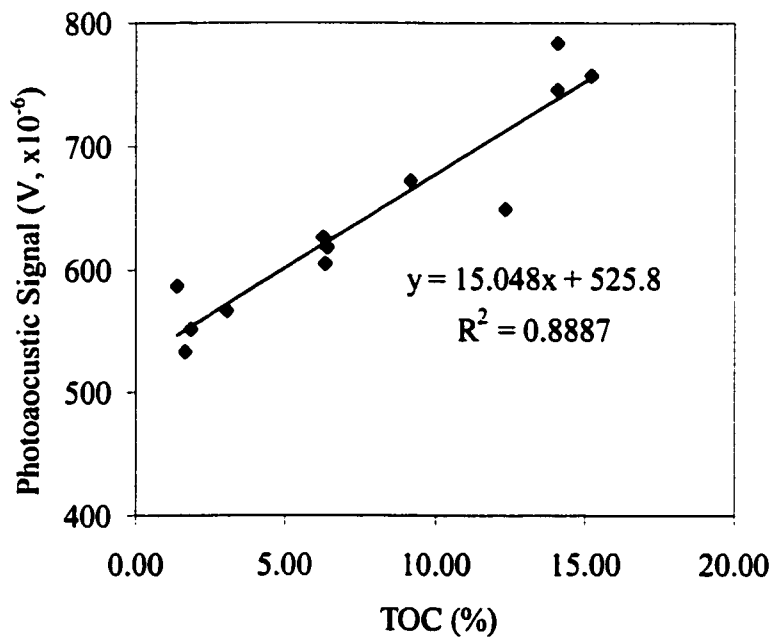


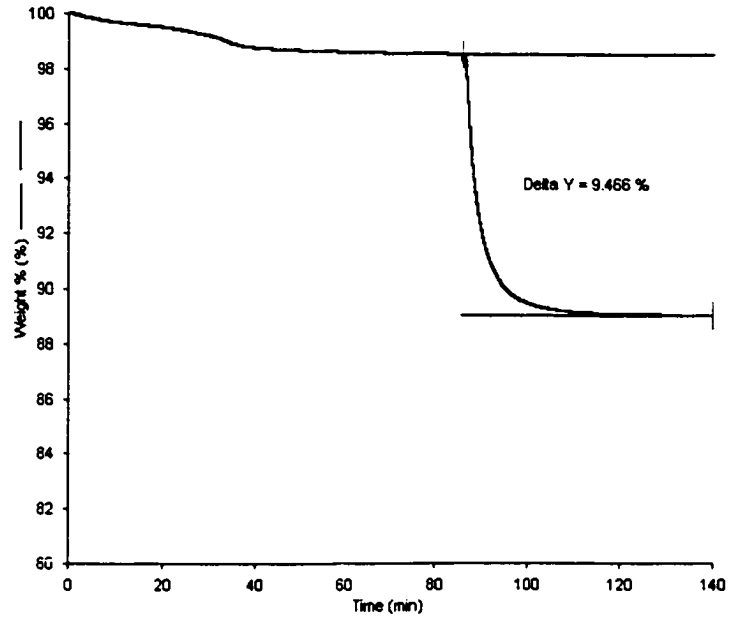
Figure 4.6. As-received 3B boiler sample calibration with IR LED excitation ($m=0.1144g$, $f=15Hz$, diluent; $CaCO_3$)

4.2.2 Effect of grinding on sample homogeneity

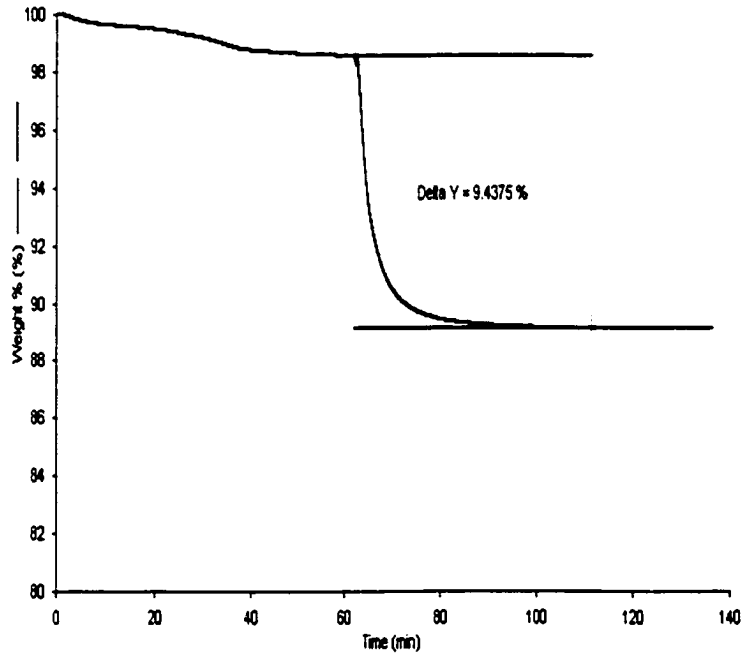
To solve the unacceptable heterogeneity problems of the as-received fly ashes found in last section, sample-grinding was tried. Both hand grinding and machine grinding are possible solution. However machine grinding is recommended to eliminate the differences of particle sizes introduced by different persons performing hand-grinding. The as-received 2A boiler samples were ground four times with a machine grinder, and tested with TGA to check each sample's homogeneity. All the 2A boiler samples were ground four times with machine grinder and TGA tests were performed on each of them. Table 4.4 lists TOC results of each trial of ground 2A boiler samples. The maximum standard deviation of triple measurements of TOC in Table 4.4 is only 0.15% and the minimum one is as low as 0.02%. These results suggest that three passes through the machine grinder were sufficient to achieve homogeneous sample for TGA analysis. As an example of 2A boiler samples, Figure 4.7 shows the TGA curves of three samples prepared from the same ground parent fly ash 22473AT. Clearly, the TOC variations among the three trials are small, compared with those of the sample 22372AT shown in Figure 4.3.

Table 4.4. TOC obtained for five fly ashes ground four times through a machine grinder

Sample		22288AT	22343AT	22462AT	22473AT	22499AT
TOC (%)	Trial 1	12.84	13.8	0.91	9.44	2.05
	Trial 2	12.85	13.9	1.2	9.47	1.89
	Trial 3	12.7	14.1	1.11	9.48	2.01
	\bar{x} (%)	12.8	13.93	1.07	9.46	1.98
	δ (%)	0.08	0.15	0.15	0.02	0.08

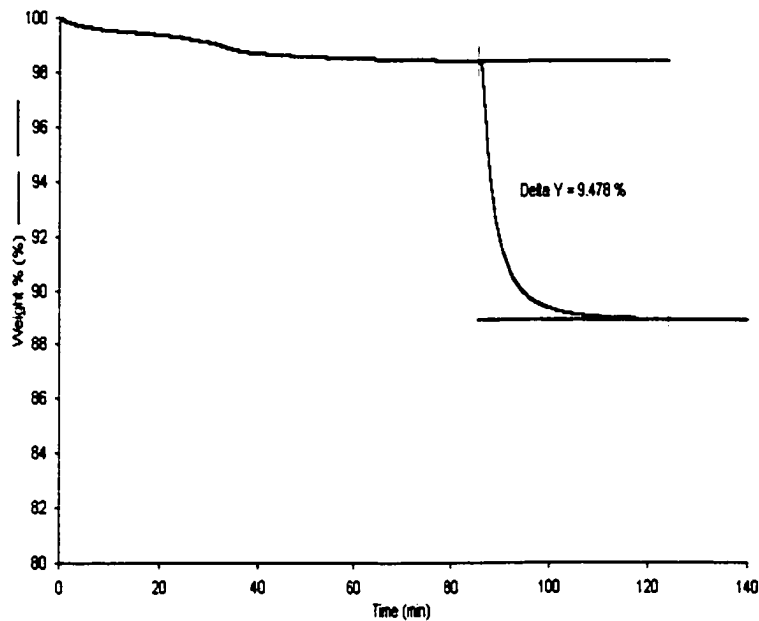


(a)



(b)

Figure 4.7. The triple TGA test results of the ground parent fly ash 22372AT
(a) first trial (b) second trial (c) third trial



(c)

Figure 4.7. (Cont.)

Improvement of sample homogeneity by grinding could also be confirmed by SEM micrograph. Figure 4.8 shows the SEM micrograph of a ground sample 22366AT. Compared with Figure 4.4, Figure 4.8 shows that particle sizes of carbons and minerals in fly ash sample 22366AT were reduced and different components of fly ash distributed more uniformly in the scanned area.

4.2.3 Evaluation of optical homogeneity of sample ground four times with a machine grinder

In the last section, 2A boiler samples were ground four times with the machine grinder before they were subjected to TGA analysis. Why were four times in stead of other times chosen when as-received sample was ground with machine grinder? First, TGA test results in Section 4.2.2 have shown that homogeneous samples were obtained after those as-

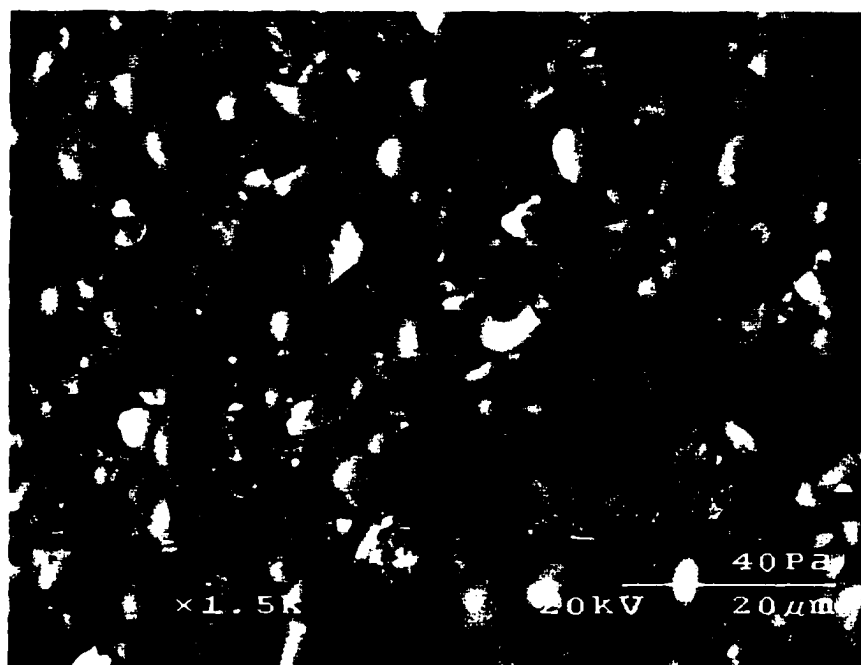


Figure 4.8. SEM micrograph of ground fly ash 22336AT

received samples were ground four times with machine-grinder. Second, it was found that photoacoustic signal of a ground sample could almost not change at all with the increase of grinding time after it was ground four times with machine grinder. The second reason is at least as important as the first one because the photoacoustic signal of a sample is not expected to vary due to the difference of grinding time. To show the relationship between photoacoustic signal and grinding time of a sample, AM36 was taken as an example and the relationship between its photoacoustic signal and its grinding time is shown in Figure 4.9. In Figure 4.9, photoacoustic signal of sample AM36 increases about 250 microvolts when it was ground with machine grinder from one to four times. When the sample was ground more times its photoacoustic signal almost stayed as a constant. Thus, sample ground four times with a machine grinder is optically homogenous.

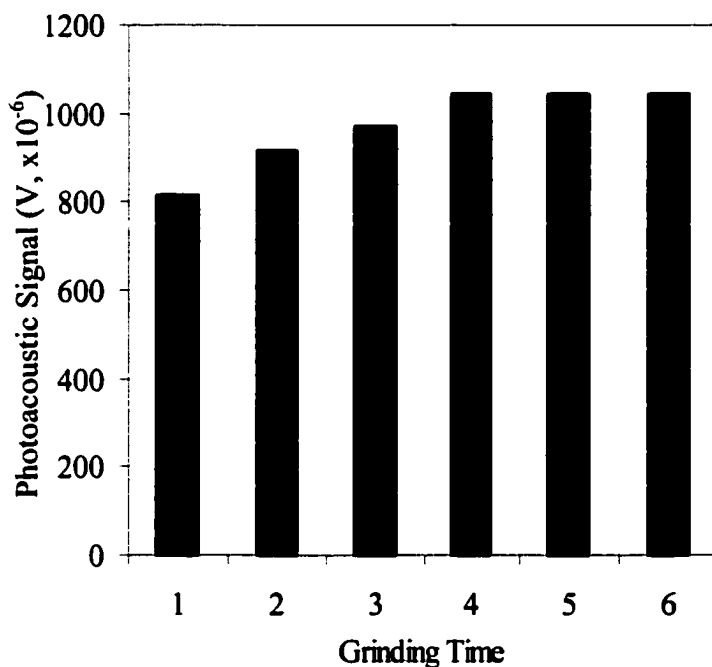


Figure 4.9. Effect of sample grinding time on photoacoustic signal for IR LED excitation source (AM36, $m=0.1144\text{g}$, $f=15\text{ Hz}$, diluent; CaCO_3)

4.2.4 Effect of sample density on photoacoustic signal

Photoacoustic theory predicts that the strength of the photoacoustic signal is related to the sample density. Jig shown in Figure 3.9 was used to control sample density by controlling both sample mass and volume while preparing samples for photoacoustic analysis. Since the length of the plunger of the height of the sample holder are set, the volume of sample set in the sample holder is a constant. The compression force applied on the plunger of jig was 5N. The only factor to affect the density of sample is mass of the sample loaded in the sample holder. To test the effect of sample density on photoacoustic signal, different densities of samples were prepared from AM36 and their photoacoustic

signals were measured. The results for laser, visible LED and IR LED excitation sources were plotted respectively in Figure 4.10-4.12.

The photoacoustic signals for all three excitation sources decrease with the increase of the sample density in the lower sample density region. Photoacoustic signals for laser and LED excitation sources start to increase after sample densities reach about 1.25 g/cm³ and 1.05 g/cm³, respectively.

In the lower density region, with the increase of sample density (ρ_s), the thermal diffusivity coefficient (α_s) of sample will increase because

$$\alpha_s \propto \rho_s^{\frac{1}{2}}. \quad (37)$$

According to Pao's photoacoustic theory [48], the thermal sampling depth (μ_s) is related to the thermal diffusivity coefficient according to:

$$\mu_s \propto \frac{1}{\alpha_s}. \quad (38)$$

Furthermore, the relationship between photoacoustic signal (q) of thermally thick (black) sample such as fly ash and μ_s can be described as [48]

$$q \propto \mu_s. \quad (39)$$

Thus, the photoacoustic signal is expected to decrease with increasing sample density, in agreement with Figure 4.9-4.11. Unfortunately, why photoacoustic signal increases with the increase of sample density can not be explained here and needs to be explored in the future studies.

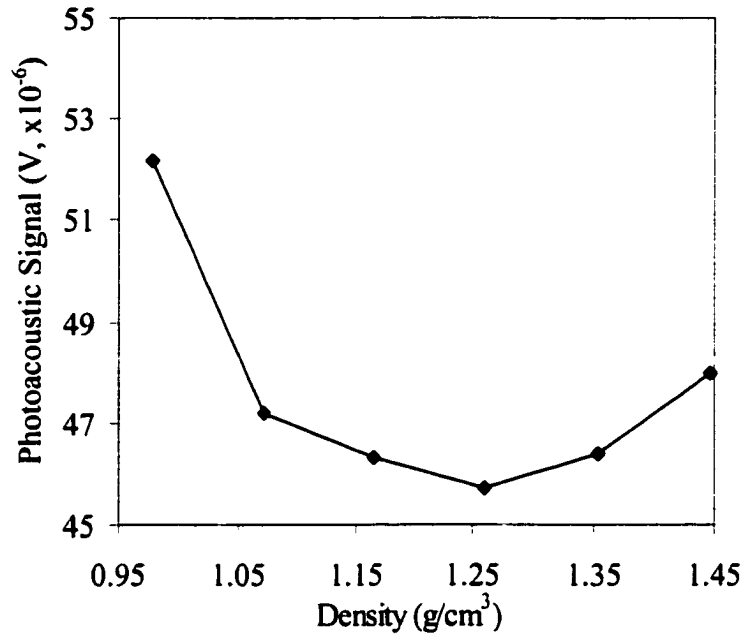


Figure 4.10. Effect of sample density on photoacoustic signal for laser excitation source (AM36, $f=15\text{Hz}$, diluent; CaCO_3)

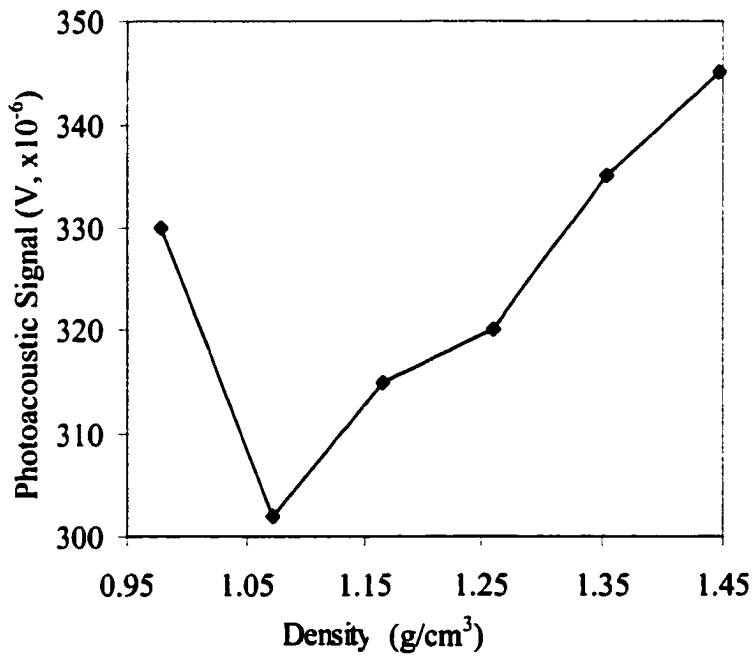


Figure 4.11. Effect of sample density on photoacoustic signal for visible LED excitation source (AM36, $f=15\text{Hz}$, diluent; CaCO_3)

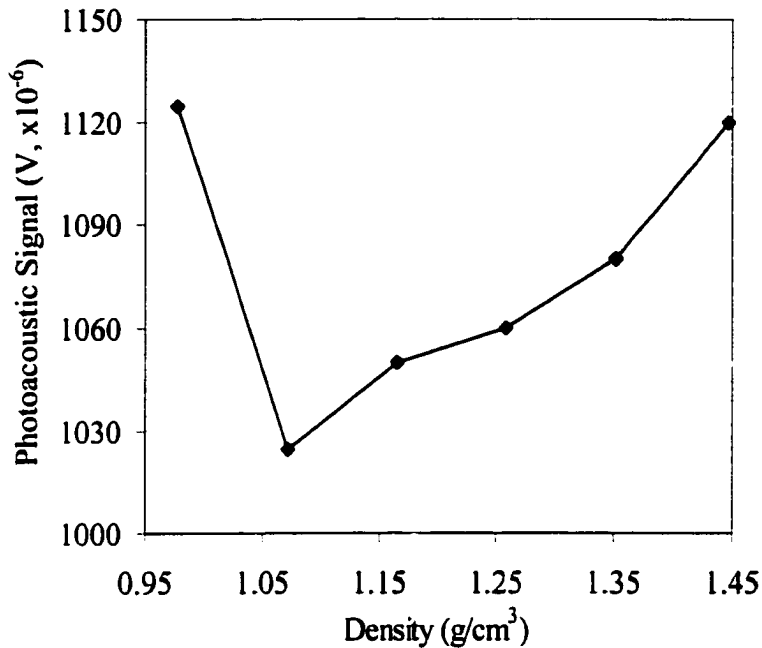
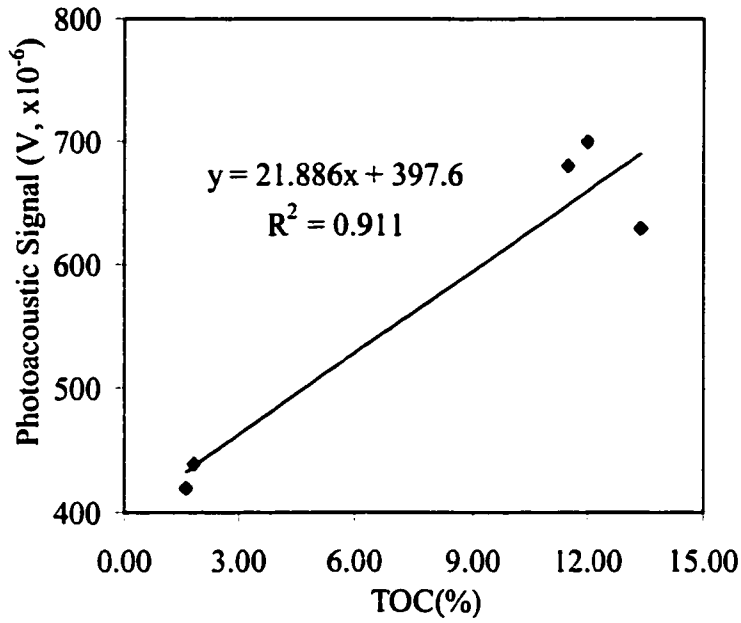


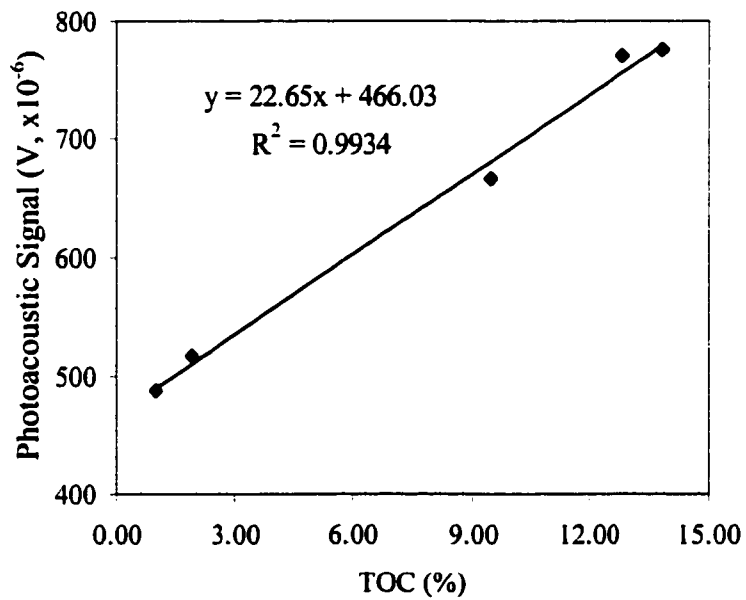
Figure 4.12. Effect of sample density on photoacoustic signal for IR LED excitation source (AM36, $f=15\text{Hz}$, diluent; CaCO_3)

4.2.5 Effect of homogeneity on the calibration of photoacoustic set-up

After the issue of sample heterogeneity was resolved, homogenous 2A and 3B boiler samples were prepared and tested for their TOC with TGA and photoacoustic signals with CA200. The test results of 2A and 3B boiler samples are plotted in Figure 4.13 and Figure 4.14, respectively. Compared with as-received 2A and 3B boiler sample calibration results in Figure 4.13 (a) and Figure 4.14 (a), Figure 4.13 (b) and Figure 4.14 (b) show improvements of ground 2A and 3B boiler sample calibrations. The absolute errors of ground 2A and 3B boiler sample calibration were calculated and listed in Table 4.5 and Table 4.6 respectively. Obviously, errors for most samples achieve the accuracy requirements specified by Ametek: 0.2 wt% TOC for fly ash with TOC less than or equal to 1% and 0.5 wt% TOC for fly ash with TOC higher than 1% TOC. However, even these excellent regression lines realized by grinding samples produced a few predictions of TOC that were outside the accuracy

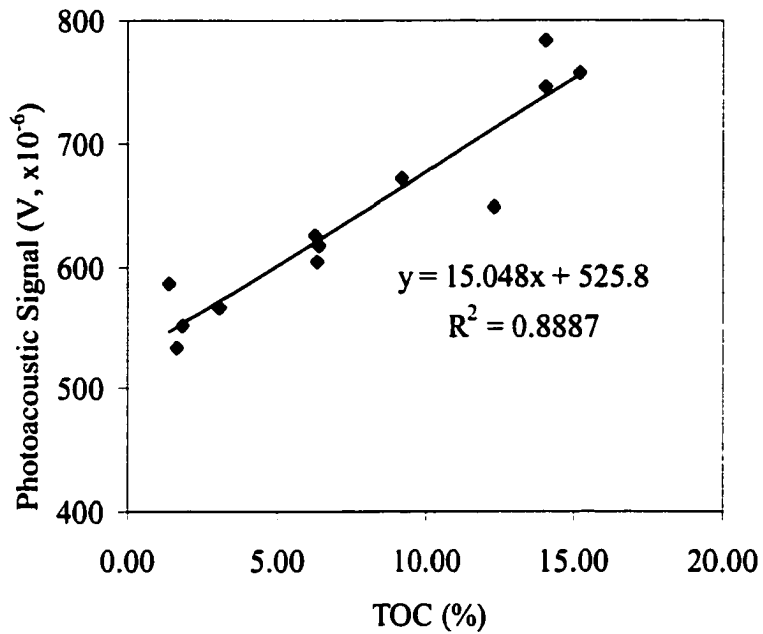


(a)

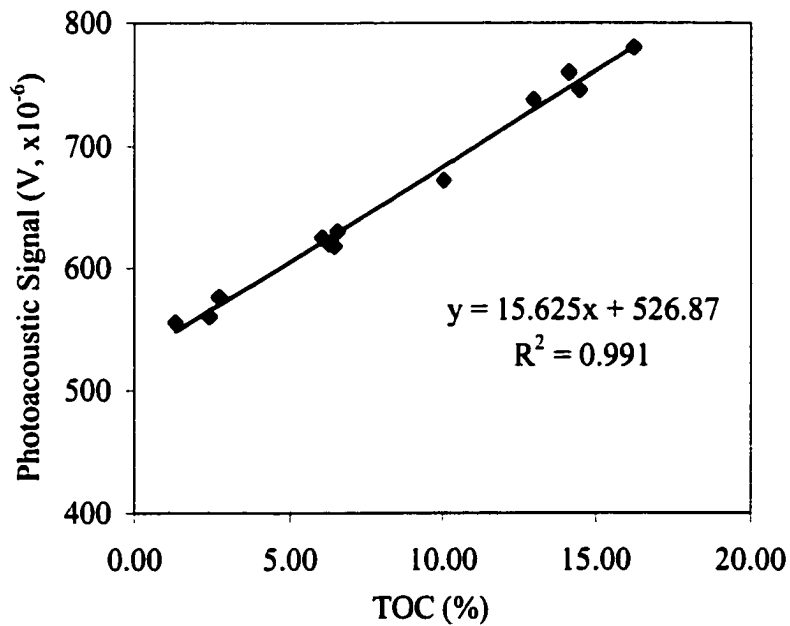


(b)

Figure 4.13. (a) As-received 2A boiler sample calibration with IR LED excitation source ($m=0.1144g$, $f=15Hz$, diluent; $CaCO_3$)
 (b) Ground 2A boiler sample calibration with IR LED excitation source ($m=0.1144g$, $f=15Hz$, diluent; $CaCO_3$)



(a)



(b)

Figure 4.14. (a) As-received 3B boiler sample calibration with IR LED excitation source ($m=0.1144\text{g}$, $f=15\text{Hz}$, diluent; CaCO_3)
(b) Ground 3B boiler sample calibration with IR LED excitation source ($m=0.1144\text{g}$, $f=15\text{Hz}$, diluent; CaCO_3)

Table 4.5. Absolute errors of ground 2A boiler sample calibration shown in Figure 4.13 (b)

Sample	TGA TOC (%)	CA200 Signal (V, $\times 10^{-6}$)	Predicted TOC (%)	Absolute Error TOC (%)
22288AT	12.82	771	13.47	0.65
22343AT	13.86	775	13.66	0.20
22462AT	1.03	487	0.93	0.10
22473AT	9.46	666	8.82	0.64
22499AT	1.92	516	2.21	0.29

Table 4.6. Absolute errors of ground 3B boiler sample calibration shown in Figure 4.14 (b)

Sample	TGA TOC (%)	CA200 Signal (V, $\times 10^{-6}$)	Predicted TOC (%)	Absolute Error TOC (%)
22332AT	2.44	560	2.056552	0.38
22336AT	16.23	780	16.09881	0.13
22339AT	10.03	672	9.205336	0.82
22342AT	14.49	746	13.92864	0.56
22345AT	13.00	738	13.41801	0.42
22348AT	14.14	760	14.82224	0.68
22352AT	6.04	625	6.2054	0.17
22356AT	6.54	630	6.524542	0.02
22360AT	6.44	618	5.758601	0.68
22368AT	2.74	576	3.077807	0.34
22372AT	6.26	620	5.886258	0.37

requirements specified by Ametek. Further investigation requires changes in instrument designs, as addressed in subsequent sections.

4.2.6 Addition of diluent to fly ash samples

It is necessary to dilute as-received fly ash samples to avoid photoacoustic saturation, which will be discussed in the later section. However the negative aspect of

sample dilution is to lead to another homogeneity problem if diluent CaCO_3 is not mixed with as-received fly ash very well during mixing process, which potentially becomes another error source. In order to investigate this potential problem, 2A boiler samples were hand ground together with CaCO_3 for 4 minutes and then photoacoustic measurements were performed with the IR LED excitation source. The results are plotted in Figure 4.15. Compared with Figure 4.13, Figure 4.15 has a better regression coefficient. The errors associated with calculation in Figure 4.15 are listed in Table 4.7. Table 4.7 shows that longer grinding time for dilution process further improves the accuracy of calibration of the CA200. Note that grinding of the dilution process was performed by hand. Machine grinding is expected to produce similar results with less manual efforts.

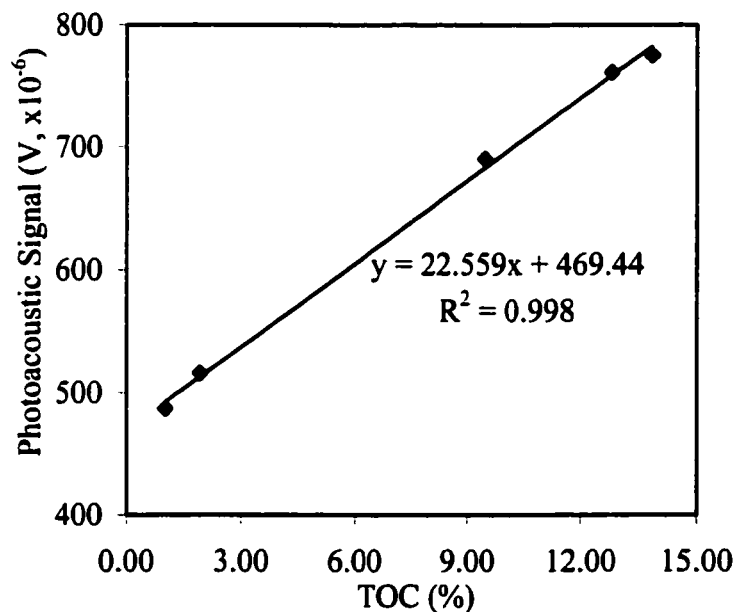


Figure 4.15. Calibration of 2A boiler samples prepared by diluting and grinding time (four minutes) for IR LED excitation source ($m=0.1144\text{g}$, $f=15\text{Hz}$, diluent; CaCO_3)

Table 4.7 Absolute errors of the 2A boiler sample calibration shown in Figure 4.15

Sample	TGA TOC (%)	CA 200 Signal (V, $\times 10^{-6}$)	Predicted TOC (%)	Absolute Error TOC (%)
22288AT	12.82	761	12.92433	0.104332
22343AT	13.86	775	13.54493	0.31507
22462AT	1.03	487	0.778403	0.2516
22473AT	9.46	690	9.777029	0.317029
22499AT	1.92	516	2.063921	0.143921

4.3 Effects of Instrument Design and Operation on Precision and Accuracy

The next area of investigation was the effect of instrument design and operation on precision and accuracy of unburned carbon measurements. These tests are detailed in the following section.

4.3.1 Investigation of modulation frequency

The modulation frequency of the excitation source affects the acoustic signal. Waller [16] found that photoacoustic signal for his system is inversely proportional to modulation frequency. Based on this result, Ametek chose 1 Hz the modulation frequency for the CA200 in an effort to maximize photoacoustic signal. However, other factors may affect this choice.

The optimum modulation frequency for the laser CA200 and the IR LED CA200 were explored for the CA200. The experimental results of photoacoustic signal vs. and modulation frequency in the range of 1-100 Hz are shown in Figures 4.16-4.17. Figure 4.16-4.17 show that strength of signal rises sharply as the modulation frequency increases at the lowest frequencies and reaches a peak value when modulation frequency is between 10-20

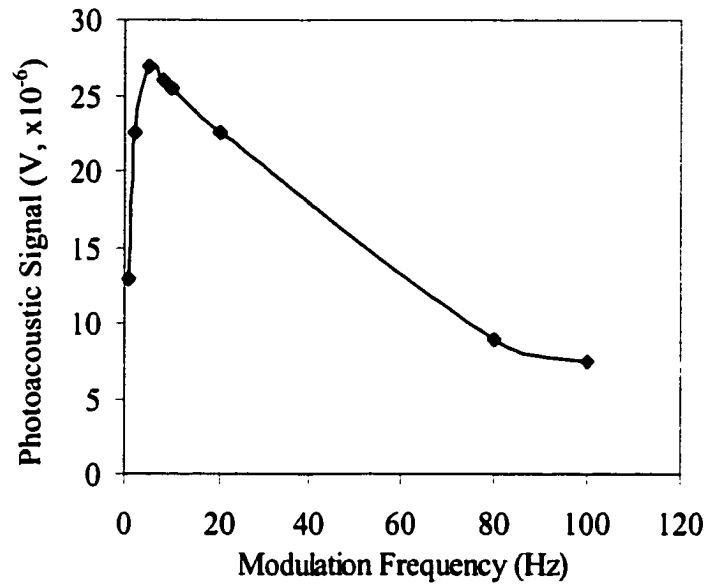


Figure 4.16 Photoacoustic signal vs. modulation frequency for laser excitation source (as-received AM36, $m=0.1144\text{g}$, diluent; CaCO_3)

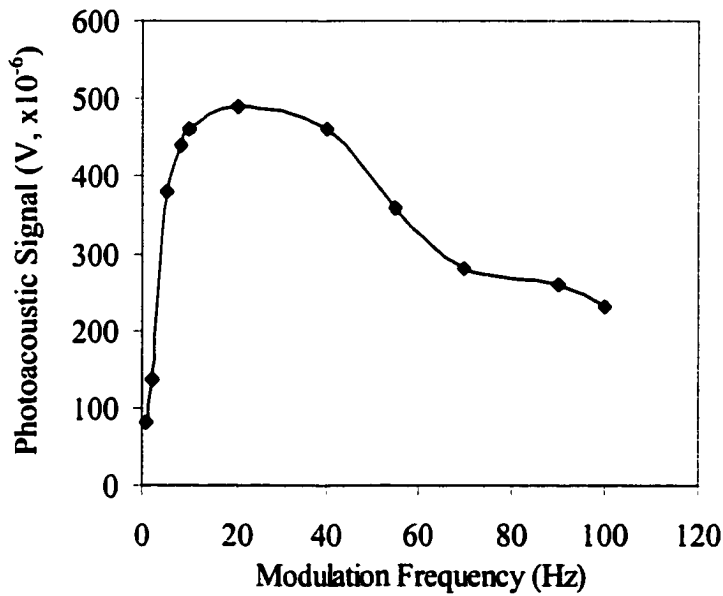


Figure 4.17 Photoacoustic signal vs. modulation frequency for IR LED excitation source (as-received AM36, $m=0.1144\text{g}$, diluent; CaCO_3)

Hz. The peaks might be the results of acoustical resonance in the photoacoustic chamber. However, a higher resonance frequency would be explored considering the small volume of the chamber. More likely, a fall off in dynamic response of the microphone at very low frequencies occurs. Clearly, the CA200 should operate at about 10-20 Hz frequency for optimum performance even though it varies a little among different excitation sources. Based on these results, 15 Hz was chosen for all the CA200 tests performed in this research.

4.3.2 Universal calibration of photocoustic instruments with various samples

Due to the differences in chemical composition of raw coal and boiler operating conditions the color of fly ash can vary considerably. Based upon visual observation of large numbers of fly ash samples, a classification scheme based on color was devised: dark green, black/gray, light brown, creme/yellow, gray/light green tint and gray/black heterogeneous. Photoacoustic measurements reveal that mineral matter can produce strong background signals for the excitation sources investigated, contrary to original expectations. The photoacoustic signals of all these different groups of fly ash were measured.

Figures 4.18-4.20 plot CA200 signal vs. TOC for six color groups of samples for the visible LED, IR LED, and IR laser, respectively. The six groups of fly ashes are chosen from available sample listed in Table 4.1. The different color classifications of fly ash are distinguished by different symbols. The scatter in the data indicates that universal calibration will not be possible with the instrument. Even the same color classes do not appear to offer prospects for generalized calibration. The result is not particularly surprising considering the relatively high background signals observed in measurements. Universal calibration will require an excitation source that does not interact with mineral matters. The current

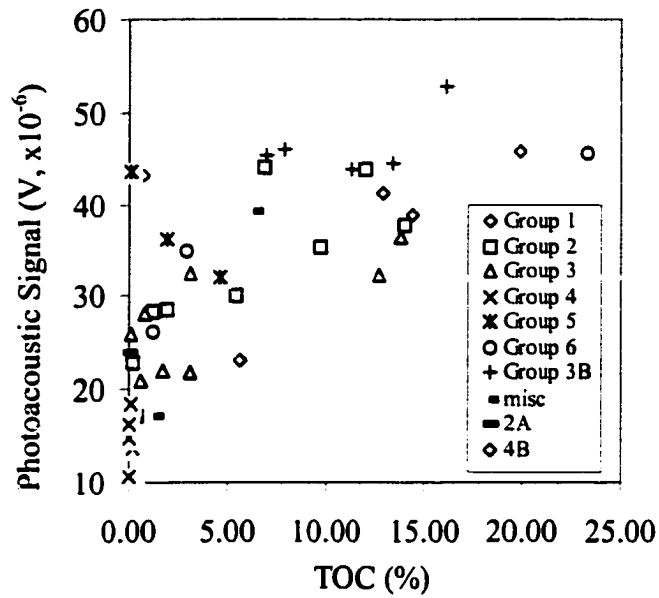


Figure 4.18. Universal calibration on various samples for laser excitation source ($m=0.1144\text{g}$, $f=15\text{Hz}$, diluent; CaCO_3)

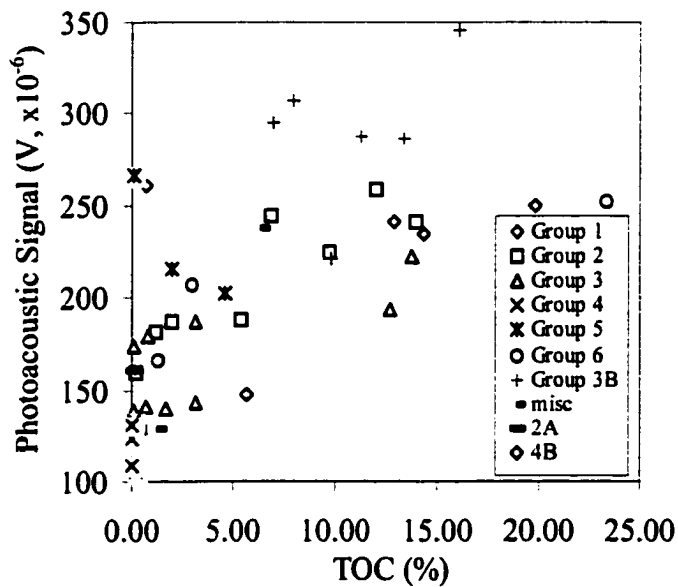


Figure 4.19. Universal calibration on various samples for visible LED excitation source ($m=0.1144\text{g}$, $f=15\text{Hz}$, diluent; CaCO_3)

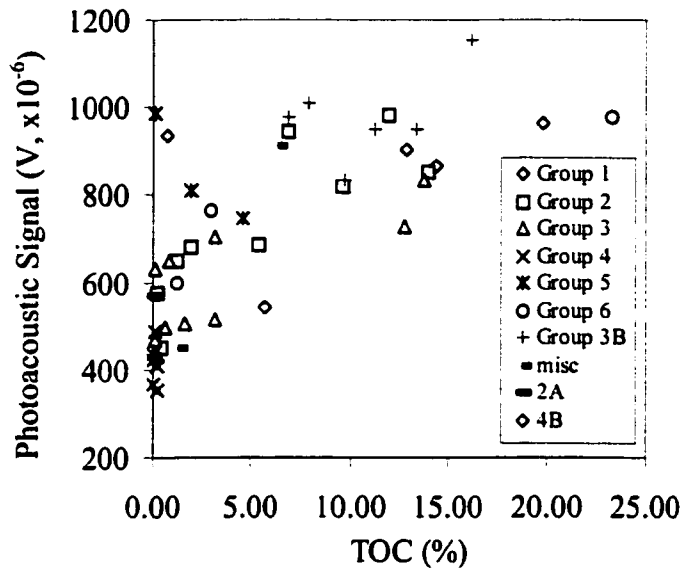


Figure 4.20. Universal calibration on various samples for IR LED excitation source ($m=0.1144\text{g}$, $f=15\text{Hz}$, diluent; CaCO_3)

excitation sources will require custom calibration to a specific boiler burning a specific fuel.

This calibration will be explored later.

4.3.3 Saturation of photoacoustic signal and dilution of fly ash

Waller [16] demonstrated photoacoustic saturation phenomena for high-carbon fly ashes. Photoacoustic signal of high-carbon fly ash does not increase proportionally or keeps as a constant with the increase of carbon in fly ash. So the calibration equation derived from the unsaturated region underestimates the carbon content of high-carbon fly ash if it is used to predict carbon content of high-carbon fly ash. Ametek tried to use fired fly ash as a diluent to calibrate CA200 to avoid this problem. It should be noticed that this method

ignores the chemical composition changes when sample is exposed to oxygen under high temperature, and thus changes its optical properties. In addition, typical fly ash contains large proportion of iron compounds and other minerals. Although relatively weak light absorber compared with carbon the predominance of mineral matter in fly ash results in a large background signal. CA200 calibrations with visible LED and IR LED excitation source for sample 21996AT with its fired ash as a diluent are shown in Figure 4.21-4.22. Efforts to fit a relationship between photoacoustic signal and TOC for this data was attempted but was unsuccessful because of saturation. Second order polynomials were used to interpolate the data in Figure 4.21 and 4.22; the results show excellent correlation, but it underestimates curvature at the higher carbon due to the saturation of photoacoustic signal.

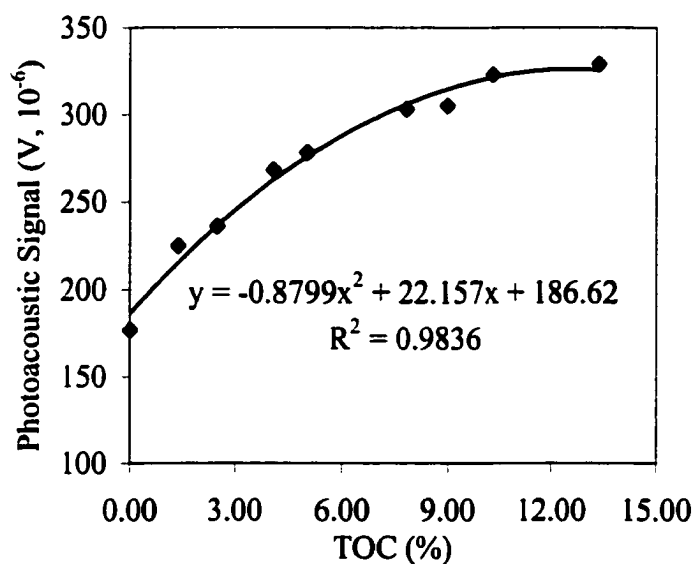


Figure 4.21. Saturation of photoacoustic signal for visible LED excitation source (21996AT, $m=0.1144\text{g}$, $f=15\text{Hz}$, diluent; fired 21996AT sample)

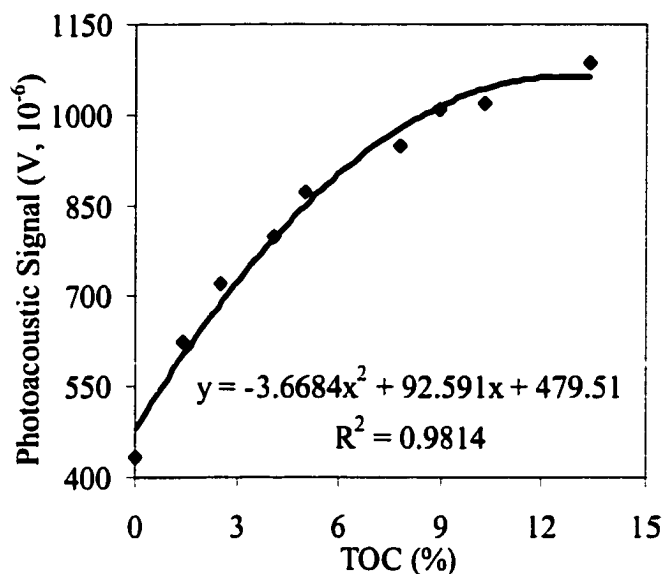


Figure 4.22. Saturation of photoacoustic signal for IR LED excitation source (21996AT, m=0.1144g, f=15Hz, diluent; fired 21996AT sample)

An important observation in Figure 4.21-4.22 is that the IR LED has the relatively greater slopes compared to the visible LED. It is suspected that this is related to the relative strength of absorption for carbon and mineral matter for the two different light sources. Iowa State University originally specified an IR wavelength in the prototype instrument to minimize absorption by mineral matter [16]. A greater slope can also be called responsivity. Responsivity is a function of excitation power, absorptivity of samples (which is a function of excitation wavelength), and chamber geometry.

To solve signal saturation problem, diluents can be used to dilute carbon in the fly ash so that CA200 only works in low carbon region. Selected diluents such as CaCO_3 and CaSO_4 were evaluated for their background photoacoustic signals and the results are listed in Table 4.8. Based on the its low cost, hygroscopic property and low IR LED CA200 signal reading, calcium carbonate was chosen as the diluent for all the tests done in this research.

Table 4.8. Photoacoustic signals of selected diluents for IR LED excitation source

Chemical Name	Chemical Formula	(V, $\times 10^{-6}$)
Oxalic Acid	$C_3H_5O_2CCO_2 C_3H_5$	5.37
CaSO ₄ Anhydrous	CaSO ₄	7
Calcium Sulfate	CaSO ₄ .2H ₂ O	6.15
Potassium Bromide	KBr	5.1
Starch Soluble	(C ₆ H ₁₀ O ₅) _n	4.79
Titanium Oxide	TiO ₂	7.78
Calcium Carbonate (99%)	CaCO ₃	6.1
Reagent CaCO ₃	CaCO ₃	5.3

4.3.4 Improvement of photoacoustic signal responsivity

As mentioned in last section, responsivity is an important characteristic of the instruments. Whether increasing responsivity could provide additional options for improving accuracy of the instrument were evaluated. The responsivity depends on several factors including modulation frequency, the wavelength of the excitation source, the power of the excitation source, the sensitivity of the microphone, and the geometry of the photoacoustic chamber and photoacoustic volume. Based on the results in Section 4.3.1, the best modulation frequency for the photoacoustic systems in this research was chosen to be 15 Hz. The sensitivity of the microphone is set by the microphone manufactures. Alternative excitation wavelengths, especially in mid-IR range are not readily available at low cost. However, there remains the possibilities that changes to the photoacoustic chamber and volume and increases in the power of the excitation source can improve measurement performance.

4.3.4.1 Effect of new head and LED holder

Inspection of the old head on the CA200 suggested geometric changes of the photoacoustic chamber needed to be made. The microphone was displaced vertically from the plane of the sample surface by about 5 mm. It was suspected that considerable damping of the photoacoustic wave occurred between the sample surface and the microphone face. It also appeared that part of the face of the microphone was covered, reducing the sensitivity of this component. A head for the CA200 was designed to more closely couple the microphone to the sample while maintaining a small air volume in the chamber. The newly designed LED holder includes a window to better define the photoacoustic chamber volume. It was found that this new head plus new holder increased photoacoustic signal by about 30% compared with original old head. Unfortunately, this increase is too modest to substantially boost the responsivity. Therefore attention was turned to increase responsivity by increasing power of the excitation sources.

4.3.4.2 Effect of the increase of the excitation power output

As a test of whether higher responsivity will improve CA200 accuracy, the current to the IR LED was varied and the slope of the calibration curve (i.e., photoacoustic signal responsivity) was evaluated, which was based on measurements on two fly ash samples diluted to the linear response range. The responsivity was proportional to power until the LED output saturated. If responsivity increase can improve the accuracy of CA200, using a higher power light source is a simple way to reduce the absolute uncertainty of measurements and improve the accuracy of the CA200.

Figure 4.23 plots responsivity estimated from two-point calibration curves obtained for sample 22462AT and 2343AT as a function of IR LED input currents. As anticipated, sensitivity increases almost linearly with the increase of the input current before signal begins to saturate, as experienced in Section 4.3.3.

Based on this result, a calibration for ground 2A boiler fly ash was conducted with IR LED current level of 80% for comparison with the result in Figure 4.24 (a). The results are shown in Figure 4.24 (b). Comparison of Figure 4.24 (a) and (b) shows that when current or power output of excitation source (IR LED) changed from 39% to 80% the slope of calibration equation almost doubled. However, the regression coefficient decreased from

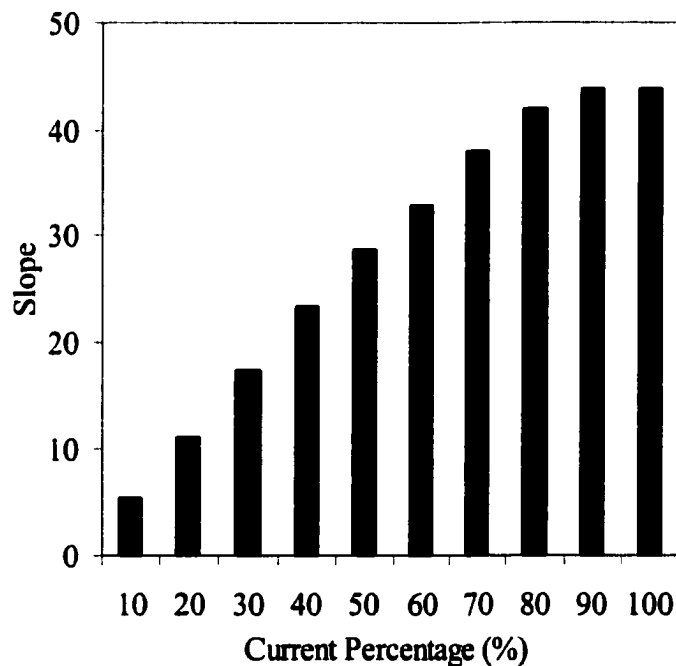
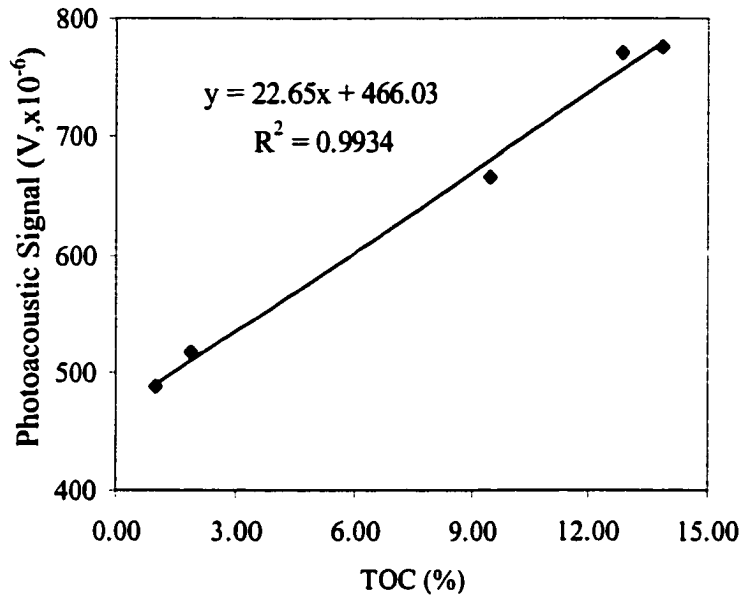
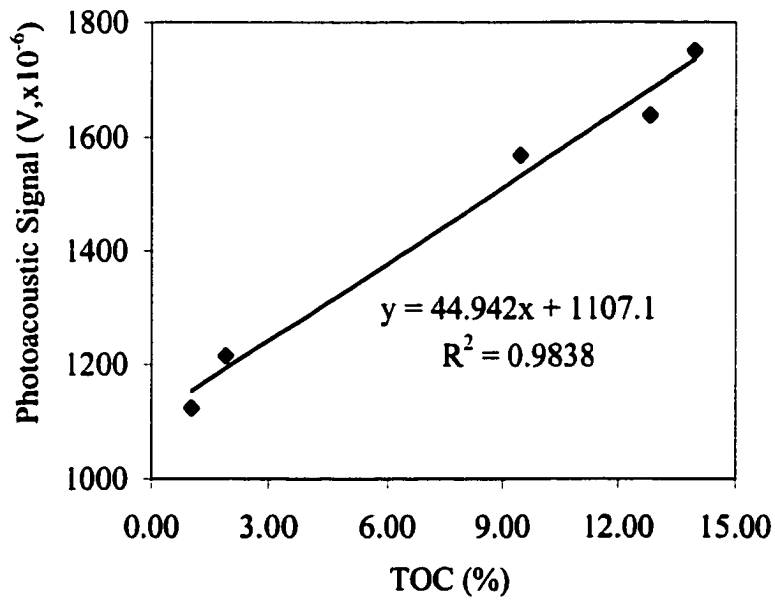


Figure 4.23. Sensitivity increase with IR LED current (sample 22462AT and 22343AT, $m=0.1144\text{g}$, $f=15\text{Hz}$, diluent; CaCO_3)



(a)



(b)

Figure 4.24. Ground 2A boiler sample calibration with IR LED excitation source (m=0.1144g, f=15Hz, diluent; CaCO₃) (a) 39% current (b) 80% current

0.9934 to 0.9838. Table 4.9 shows the absolute errors of 39% and 80% current calibration equations in Figure 4.24 (a) and Figure 4.24 (b). Comparisons of absolute errors under two different excitation outputs show that doubling of output power did not decrease absolute errors of photoacoustic measurements.

Table 4.9. Effect of IR LED output on accuracy of calibration

Sample	TOC (%)	Absolute Error (%) Current=39%	Absolute Error (%) Current=80%
22288AT	12.82	0.65	1.00
22343AT	13.96	0.20	0.35
22473AT	9.46	0.64	0.64
22499AT	1.92	0.29	0.81
22462AT	1.03	0.10	0.48

4.3.5 Effect of raw coal on instrument accuracy

Ametek hypothesized that raw coal detected in some fly ashes affected the accuracy of the CA200 calibration. The hypothesis was that points falling off the regression lines in Figure 4.24 (a) and (b) had large quantities of raw coal, which did not correlate with TOC. The test of exclusion was to measure the mass of volatiles, M_v , in a fly ash and compare it to the mass of fixed carbon (char), M_c , in the fly ash (as determined via TGA). Presence of large quantities of raw coal would be indicated by high ratios of M_v/M_c . For poor calibration curve, the fly ash with large M_v/M_c should show the largest divergences from the calibration line. Table 4.10 summarizes these divergence calculation results of 2A boiler sample calibration in Figure 4.24 (a). No correlation between raw coal content and error in

Table 4.10. Comparison of volatile content to CA200 measurements in Figure 4.25

Sample	TOC (%)	M_v/M_c	Absolute Error (%)
22288AT	12.82	0.080	0.65
22343AT	13.96	0.081	0.20
22473AT	9.46	0.099	0.64
22499AT	1.92	0.48	0.29
22462AT	1.03	0.59	0.10

M_v : The weight loss between 450 °C and 750 °C without air admission into TGA

M_c : TOC

CA200 measurements is evident. Accordingly, raw coal does not appear to be a factor contributing to the accuracy problem of the CA200.

4.3.6 Effect of ambient environment on photoacoustic signal

Standardized sampling procedures mentioned in Section 3.3 greatly improved the accuracy and precision of the CA200, as illustrated in Section 4.2. However, another accuracy problem became evident during dramatic weather change, which markedly changed the temperature and humidity in the laboratory where CA200 tests were conducted. It became evident that the photoacoustic signal could fluctuate even when a sample was retained in the instrument from one day to the next. It was suspected that temperature and humidity of laboratory might influence the photoacoustic signal. Photoacoustic signals of sample 22473AT were monitored under different laboratory temperatures and humidity for a period of seven days and the relationships between photoacoustic signal and the operation temperature and humidity of the CA200 were evaluated.

A 0.1144 g ground, undiluted sample of fly ash 22473AT was prepared according to standard sample preparation procedures and set in the sample holder to be monitored

Table 4.11. Effect of ambient temperature (°C) and humidity (%) on photoacoustic signal (microvolt), (sample 22473AT, m=0.1144g, IR LED excitation source, f=15 Hz)

T (°C)	Humidity (%)												
	32.0	34.0	35.0	36.0	38.0	51.0	53.0	55.0	55.3	56.0	59.0	62.0	64.0
20	1120	-	-	-	-	-	-	-	-	-	-	-	-
20.2	-	1135	-	-	-	-	-	-	-	-	-	-	-
20.5	-	-	-	-	1140	-	-	-	-	-	-	-	-
20.8	-	-	-	1145	-	-	-	-	-	-	-	-	-
21.2	-	1150	-	-	-	-	-	-	-	-	-	-	-
22.2	-	-	1160	-	-	1170	-	-	-	-	-	-	-
22.3	-	-	-	-	-	-	1171	1179	1180	1191	-	-	-
23	-	-	-	-	-	-	1205	-	-	-	-	-	-
23.1	-	-	-	-	-	-	-	-	-	-	-	1204	-
23.3	-	-	-	-	-	-	-	-	-	-	-	-	1215
23.5	-	-	-	-	-	-	-	-	-	-	1214	-	-
23.6	-	-	-	-	-	-	-	-	-	1215	-	-	-
24.0	-	-	-	-	-	-	-	-	-	-	1219	-	-

continuously for about one week. During the sample-monitoring process, no changes were made to the CA200 or ancillary instruments. The photoacoustic signals under different room temperatures and humidity were collected and were recorded in Table 4.11.

A regression program with the statistics analysis system (SAS) was used to investigate the relationship between photoacoustic signals and ambient temperatures and humidity of the CA200 shown in Table 4.11. The SAS program and its output are listed in Appendix 5. The linear regression model given by the SAS program shows that the

regression slopes of photoacoustic signals vs. ambient temperatures and humidity of the CA200 are $20.55 \mu\text{V}/^\circ\text{C}$ and $0.81 \mu\text{V}/^\circ\text{C}$, respectively. This indicates that ambient temperature plays a much more important role than humidity in affecting photoacoustic signals although the effect of humidity can not be ignored. The SAS program output indicated that the effect of the interaction of temperature and humidity on photoacoustic signal is not significant.

Although this test indicated that temperature affected the performance of the instrument, it was not clear which component was responsible. At first, microphone and lock-in amplifier were suspected as sources of temperature drift. However, the manufactures of microphone and lock-in amplifier manufacturers rejected these suspicions. Accordingly, attention was turned to the head of the CA200. An experiment was conducted to control the ambient temperature surrounding the CA200. The CA200 was wrapped in a plastic bag and immersed in a bucket of ice. IR LED excitation source and model SR 830 amplifier were used in this experiment. Ground sample 22343AT was prepared and its photoacoustic signal was measured and recorded in Table 4.12. Note that humidity during the experiment period did not change very much. Table 4.12 shows that the signals were very stable due to the control of ambient temperature around the CA200 head even though the room temperature fluctuated by 4°C which caused signal change more than 100 microvolts when temperature was not controlled. This result not only dismiss the lock-in amplifier as the source of temperature drift but provides strong evidence that the temperature of the sample or of the photoacoustic chamber are responsible for repeatability problem.

Table 4.12. Effect of ambient temperature control on photoacoustic signal
(sample 22343AT, $m=0.1144\text{g}$, IR LED excitation source, $f=15\text{ Hz}$)

Date	1/4/2000-1/5/2000			1/5/2000-1/6/2000		
Time	Signal (V, $\times 10^{-6}$)	Temperature ($^{\circ}\text{C}$)	Humidity (%)	Signal (V, $\times 10^{-6}$)	Temperature ($^{\circ}\text{C}$)	Humidity (%)
10:00am	1020	23.3	24	1022	23.8	22
12:00am	1020	23.4	25	1023	23.2	22
2:00pm	1024	24.0	23	1035	24.3	23
4:00pm	1023	24.1	23	1025	25.2	24
6:00pm	1023	23.9	24	1023	23.8	23
8:00pm	1021	23.5	22	1026	22.2	22
10:00pm	1020	23.4	23	1027	22.4	22
12:00pm	1023	23.8	21	1020	22.8	21
2:00am	1025	22.8	19	1026	21.0	21
\bar{x} (V, $\times 10^{-6}$)	1022.1			1025.2		
σ (V, $\times 10^{-6}$)	1.90			4.29		

5. CONCLUSIONS

The factors influencing precision and accuracy of a carbon-in-ash monitor have been identified. It is believed that a practical off-line carbon monitor instrument that meets targeted performance specifications by Ametek can be manufactured. These factors are summarized below.

5.1 Accuracy of Carbon-in-Ash Monitor

It has been determined that low accuracy resulted from both inadequate calibration procedures and sampling errors as well as environmental effects. It is believed that methodologies to avoid these accuracy-related problems have been developed.

A wide variety of fly ashes provided by Ametek were tested and it was found that large discrepancies between LOI and TOC for many of the samples exist. Accurate calibration of the CA200 is dependent on the use of TGA to measure TOC in the calibration standards.

There was no evidence that raw coal was present in large enough concentrations to affect the accuracy of carbon-in-ash monitor measurements. As described below, other sources of inaccuracy were found and successfully corrected in this research.

It was found that universal calibration of a carbon-in-ash monitor is not possible at this time. That is, calibration of the instrument using fly ash from one boiler will not necessarily provide a suitable calibration for another boiler. The reason for this is optical activity of the mineral matter in fly ash. This optical activity results in a significant background signal that adds to the signal generated by carbon in the sample. Variations in

mineralogical composition among fly ashes from different boilers appears to influence readings unless an excitation source is identified that only weakly interacts with fly ash minerals. Such an excitation source was not identified among commercially available LED. The only viable solution is to calibrate a carbon-in-ash monitor for a particular boiler.

Having established a standard sample preparation procedure and a suitable calibration procedure, the accuracy of the calibration by plotting data for several fly ashes from a particular boiler was evaluated. These evaluations were performed for the 2A and 3B boiler fly ashes. Preliminary results were not encouraging. Although all the points for a particular boiler lined up on a regression line with good regression coefficients, this was not good enough for the specified accuracy of a carbon-in-ash monitor (within 0.2 wt-% for carbon content less than or equal to 2.0 wt-% and within 0.5 wt-% for carbon content greater than 2.0 wt-%). For the current configuration of the CA200 used in this research, regression coefficients exceeding 99% would be required to meet the targeted performance specifications. Two types of errors control the accuracy of a carbon-in-ash monitor: sampling errors and instrument measurement errors. Sampling errors will be summarized below while instrument measurement errors will be summarized in the following section.

Fly ash is a heterogeneous material in its natural state, which makes representative sampling extremely difficult. Representative sampling is important in preparing samples for testing in the CA200 as well as in preparing calibration samples for TGA tests. In the case of calibration, the sample tested in the CA200 to obtain a photoacoustic signal must be identical in composition to the sample tested in the TGA to obtain a TOC value. Although this is an obvious requirement and may appear trivial to achieve, for the accuracy specifications of a carbon-in-ash monitor, it requires careful attention to sampling protocol. Regression

coefficients exceeding 99% can be achieved, as required to meet instrument accuracy specifications, by selecting samples for the CA200 and TGA measurements from the same thoroughly ground parent fly ash. Grinding has the effect of reducing all particles to roughly the same size, thus improving the homogeneity of the material. Use of sampling statistics (i.e., replications to improve representation) or loosening of accuracy requirements consistent with applications of the instrument can also help overcome this problem.

5.2 Precision of Carbon-in-Ash Monitor

At the early carbon-in-ash monitor evaluation stage, it was found that careful weighing and pressing of the sample would overcome reports of lack of precision of measurements. However, signal variations ranging between 30 and 100 μV for a nominal 1000 μV signal that could not be attributed to variations in weight and compression of samples were eventually observed. Considerable time was spent in tracking down the origins of poor precision, which appears to arise from two factors summarized below.

- **Improper modulation frequency.** Ametek originally designed the CA200 to operate at 1 Hz. Mechanical vibrations at this frequency are damped by the mass of the CA200 housing. However, It has been discovered that this frequency is outside the dynamic range of the microphone used in the CA200, which compromises the responsivity (gain) of the photoacoustic effect. The peak response of the CA200 is around 15 Hz. Substitution of a microphone that can operate efficiently at 1 Hz is possible
- **Temperature drift.** Ambient conditions of the instrument influenced the photoacoustic signals. It was found that photoacoustic signal increased with both temperature and humidity of the room, which was confirmed by the output of SAS program. Temperature

has a much bigger effect on photoacoustic signal than humidity does. Observing that humidity correlates very closely to temperature, it was concluded that photoacoustic signal fluctuation actually results from the temperature drift. A 3 to 4 °C increase in temperature resulted in a photoacoustic signal increase by more than 100 μV for a sample with a normal value of 1000 μV photoacoustic signal. Power output of excitation source and thermal properties of fly ash sample and chamber material are functions of temperature. Experiments have shown that the net result of these functions is to increase the signal when ambient temperature increases. Experiments have also shown that controlled environment of photoacoustic chamber made photoacoustic signal very stable. How to use a proper technique to control the ambient temperature of photoacoustic chamber should be the focus of future study of the carbon-in-ash monitor.

APPENDIX 1. LOSS ON IGNITION (LOI) [1]

Description: This experiment determines the amount of combustion material in the moisture-moved sample using a furnace to ignite the sample.

Warning: This experiment requires a muffle furnace at 750 °C. Use the ZETEX glove and long (1.5') tongs to place and remove the crucibles from the furnace. The oil on your fingers would affect the weighing if you touched the crucibles.

Item Needed:	Brown Vials	Long Tongs
	Reference Sample (QA)	Large Desiccator
	Small Crucibles	Analytical Balance
	Small Brass Core Sample	Large Cotton Swabs
	Holding Tray	Box of Kimwipes-wipes
	MC/LOI Data Sheet	ZETEX Glove

Procedure:

1. Turn on the muffle furnace to 750±50°C.
2. Prepare crucibles and weigh samples.
3. Place the crucibles in the furnace at 750°C for one hour.
4. Remove the samples and place them in the desiccator to cool for at least 45 min.
5. Weigh each crucible to the nearest 0.0001 grams.

Calculation:

$$LOI = \frac{W_d - W_{ig}}{W_d} * 100\%$$

W_{ig}= ignition sample weight, (g)

W_d=dry sample weight, (g)

APPENDIX 2. TGA-7 OPERATION PROCEDURE

Balance Purge Gas:

- Use only this line and clamp off the sample purge line if a single purge gas is desired
- Recommend inert gas with >99.9% purity; must be dry
- Flow rate 40-60 cc/min at 40-60 PSI (recommend about 50 PSI)

Sample Purge Gas:

- PSI less than balance purge
- Recommended 20-40 PSI, and **always** <60 PSI

Furnace Cooling/Positioning Gas:

- 25-30 PSI, and **never** exceed 40 PSI

Miscellaneous:

- Room RH <50%
- With flow restrictors on regulator, 1 PSI equals roughly 1 mL/min gas flow

Startup

- Turn on sample and balance purge gases and check for proper PSI values
- Make sure furnace cooling/positioning gas is on and set to proper PSI value
- Turn on TGA, then TAC unit (Control and/or Ready light should be lit)
- Turn on vent
- Double click on **Pyris Manager** (if needed), then click button to put TGA 7 on line

Running Samples

Conditions

- Heat rates are from 0.1 to 200°C/min (**normally 5 to 20°C/min**)
- Sample size from 1 to 500 mg (**normally 2 to 50 mg**)
- Sample gas flow rates 20 to 40 cc/min (**MUST** be less than the balance purge rate)

Procedures

- Go into Method Editor and enter all appropriate sample information, file name, location for file storage, and the thermal program
 - Do not adjust **Zero Weight** value on the **Sample Info** card
 - **Save Method** if desired (may need to use **Save As** command)
- Lower furnace tube, then put black plastic tray under sample pan such that pan is supported and pushes the pan out of the stirrup slightly
- Remove pan (using fine-tipped tweezers) and discard sample, then use can of compressed air to blow out any remaining loose sample
- Raise furnace tube and tare the pan with the **Zero Weight** button on the **Control Panel** after a steady weight has been achieved – if a zero weight of "0.0000 mg" can not be obtained, try going into **Start Pyris** and select **Close All**, then restart software
- To load samples, lower furnace tube and put black plastic tray and metal tray just under sample pan (but **not** touching the pan)
 - Make sure sample does not fall into furnace tube
 - Read weight on **Status Bar** and add desired amount of sample
 - Try to get fairly even sample distribution
- Raise furnace tube and let weight stabilize, then click **Sample Weight** button on **Control Panel** (will automatically enter sample weight on **Sample Info** card)
- Make sure the flowmeter indicating the flow of vented gases reads an appropriate value
- Start TGA run by clicking top button in the **Control Panel**
- Make sure sample pan never touches sides of furnace during the run!
- Watch for static charges which could cause sample pan to rest against side of furnace

Shutdown

- Turn off (using delivery valves) sample and balance purges
- Turn off TAC, then turn off TGA
- Turn off vent
- Make sure **Autohide** is deactivated on TGA status bar at top of screen (or screensaver will not work)

Changing Gas Cylinders

- Turn handle to delivery pressure fully counter-clockwise so that delivery pressure is at zero
- Change regulators and set proper delivery pressure
- Test for leaks by closing delivery valve on regulator, opening main cylinder valve, noting cylinder pressure, and then closing main cylinder valve
- Needles indicating cylinder pressure and delivery pressure should not move over a 5 minute period
- Correct leaks as needed

Calibration

If a high degree of accuracy is required, recalibrate temperature, weight, and furnace each time any of the following occurs:

- Temperature range of tests changes
- Type of purge gas or the purge gas flow rate changes
- New thermocouple installed or position of thermocouple changes
- Furnace height is changed
- New furnace is installed
- Hangdown wire is bent or replaced

Preliminary Procedures

- Select **Calibration** from **View** menu while in **Instrument Viewer** or **Method Editor**
- Restore default calibrations by selecting **All** from **Restore** menu (must save and apply old calibration back to a file)
- Select **Save and Apply** in **Calibration** window to send default calibration to analyzer and save current calibration file
- Select **Close** to close **Calibration** window
- Proceed with calibrations as noted below

Temperature

- Use metals with magnet to provide magnetic weight for Curie point determination
- Use fresh materials each time to avoid hysteresis and oxidation effects on Curie point
- Make sure magnet never pulls sample pan against side of furnace
- Run scan of each reference material (about 1 mm section each) under the same conditions to be used for sample testing, labeling each file as a data file for subsequent use (store in PE\Pyris\Cal folder)
- Save calibration method (as a tgm file) if desired by using the **Save As** command
- Put reference material in center of pan if possible, and run each material individually if performing multi-point calibration (will generally give highest accuracy to run individually rather than simultaneously)

- Go at least 30 degrees past transition point to get suitable base line
- Perform onset calculation at end of the Curie point transition and note onset result
 - Overlay derivative curve (using **Math** menu) and then do peak search on it to get the peak temperature
 - Enter the peak temperature from the derivative curve as the first value to be used for the onset calculation
 - Select a suitable temperature point in the baseline after the transition and enter this as the second point to be used for the onset calculation
 - Accept or alter the slopes of the lines drawn in by the computer and then select **Calculate** to obtain the Curie point (will be displayed as the onset temperature)
- Repeat previous two steps for each additional reference material to be used
- After obtaining all Curie point data, select **Calibrate** in **View** menu to get **Calibration** menu
- Select **Temperature** tab, then enter name of reference material, expected onset value, and measured onset value for each material
- Select check box in the **Use** column for each reference material to be used
- Select **Save and Apply** in Calibration window to send new calibration values to analyzer and save current calibration file
- Go to next calibration procedure by clicking on its tab or select **Close** and run samples (NOTE: furnace calibration must be performed if a temperature calibration has been performed)

Weight

- Recalibrate if:
 - Analyzer moved or relevelled
 - Hangdown wire is replaced
- Select **Weight** tab in **Calibration** menu
- Enter weight of reference material in **Reference Weight**
- Select **Begin Calibration**
- Remove any sample in pan and move away the tray, then click OK
- When zero weight is stable under **Read Zero** field, click OK
- Place reference weight (100 mg provided) in pan, move tray aside, then click OK (Perkin Elmer technical staff note that 100 mg is appropriate, even if actual sample sizes will be 10 mg or less)
- When weight is stable in **Read Value** field, click OK to complete calibration
- Select **Save and Apply**

Furnace

- Takes about 2 hours
- Furnace calibration must be performed if temperature calibration was performed, and temperature calibration must always be performed first
- Before performing furnace calibration, make sure that the new temperature calibration is saved and applied
- Make sure sample pan is in, but empty
- First make sure thermocouple working properly
 - Raise furnace and program to heat to 100°C
 - Enter 100 in the **Go To Temperature** field in **Control Panel**, then click on the **Go To Temperature** button
 - Check that the current sample temperature shown in the **Status Panel** is at or below the intended minimum calibration temp (easiest way is to click on **Go To Load** in the **Control Panel**)
- Select **Furnace** tab in **Calibration** window
- Enter **Minimum** and **Maximum** (make sure it is above the highest temperature of interest for the samples to be run) temperatures to be used for the calibration
- Difference between max and min values **MUST** be at least 100°C
- Select **Begin Calibration** (approximate calibration time remaining will be displayed)
- Select **Save and Apply** in **Calibration** window
- Close window and run samples

Misc.

Pull out old calibration file by using View/Calibrate and then opening calibration file (.tgc) in the Pyris folder. Save and Apply this.

Miscellaneous

- Use clamp if pressurizing system
- "Key" allows to run software – may have to temporarily take off while adding printer
- "H" restrictors clog over time and must be replaced
- **Autohide** in TGA status bar at top of screen must be deactivated to view icon labels and to activate screen saver

Data Display

- For overlapping plots, heaviest line is the active data set
- Use **Preferences** menu for line type, fonts, color, etc

Control Panel

- Start/Stop - Hold Temp - Sample Tare
- Go to Temp - Clean Furnace - Raise/lower furnace
- Go to Load Temp - Sample Weight - Cool Furnace

Miscellaneous

- To make desktop easier to work with, click on **Start Pyris** rectangle at top of screen with right mouse button and select **Autohide**
 - Click anywhere on desktop to hide
 - Move cursor to top of screen to bring back
- **Start** flag (used to shut down computer, find file, etc) is moved off screen, but can be brought back on by dragging right edge towards the right of the screen

Rescale Tools

- Radar window, swap Y axes, rescale axis, rescale Y axis, full scale Y axis, full scale X and Y axes), previous scaling, shift curve, change slope, text addition, switch between time and temp on X axis

Pyris Software**Installation**

- Uninstall current software
- Take out the "key"
- Install new software using Start/Run and choose Setup on the CD-ROM

Method Editor

- **Sample Info** - Enter sample ID (won't overwrite existing file with same name), sample info, sample weight, data storage location (change by selecting field and then using Browse), and filename
- **Initial State** – Set equilibration values, set up baseline subtraction, etc.
- **Program** - Enter TGA program, seconds per point or total number of points (TGA will automatically select if desired), set initial temp, etc.

Instrument Viewer

- Use to look at continuous readings from TGA (even when not in data collection mode)

- Use right mouse button to remove curve, change curve color, or change line style
- Can click and drag to draw box around area of interest, then double click in the box to blow it up

Pyris Series – TGA

View

- **Calibrate** - gets to calibration window
- **Radar** - while in Instrument Viewer only
 - Shows active curve (while in Data Analysis or Instrument Viewer) at full scale while curve is being manipulated
 - For zooming in, **MUST** take off Auto Rescale under Display menu
 - Draw box in radar window to select region for display, which will then be rescaled as needed (may need to resize box in radar window, click outside of the box, then click and drag to select region)
- **Grid** - while in Instrument Viewer only
- **Rescale Tools** - while in Instrument Viewer only
- **Tool Bar**
- **Status Panel**
- **Control Panel**
- **Thermal Program** – while in Method Editor only

Display - Select either weight or weight percent for Y axis

- Rescale axes
- Auto Rescale

Curves - Select what is to be plotted on Y axis

Tools

- **Preferences** - line style, colors, fonts, load temperature, "go to" temperature rate, purge gas and flow entries, real-time curve selection, X-axis display, graph title, autosave feature

Window - For selecting between **Method Editor** and **Instrument Viewer**

Data Analysis

- Activate by clicking on **Start Pyris** at top of screen and selecting **Data Analysis**

- Use **Calc** to calculate Delta X, Delta Y, Event Mark, Slope, Onset, Peak Area, etc.
- Use **Math** for derivative
- To edit data, go into **Data Analysis**, select **Print to File** (saves as text file), open text file and copy data, then paste data into Excel spreadsheet – plot data as scattergram

Maintenance and Troubleshooting

Use **CD-ROM** for Pyris help, maintenance instructions, part numbers, etc.

- Select **Multi Media** folder, then select either **Hardhelp** or **Pyris help**

TGA Module

- Control – if lit, power is being supplied to furnace (analyzer in control of temp)
- Ready
 - if blinking, program temp has reached load temp
 - if on, analyzer temp has reached load temp
 - if off, analyzer temp has not reached load temp
- Data – data being collected when lit
- If Heating and Cooling lights both on, cable connecting TAC to analyzer is loose or has failed, or furnace cable is broken or not connected
- If all lights on except Control, TAC not turned on or not properly connected to analyzer
- If Data blinking and Heating, Cooling, and Message are either blinking or are off, may be bad hardware component in TAC

Furnace Adjustments

- Adjust with bottom thumbscrews by trial and error
- Use bottom cylinder knob for furnace height adjustment
- Top of furnace should come to "knee" of stirrup holding sample pan

Balance

- Has counterbalance (make sure stays on) – close wire loop if necessary
- Has quartz link to keep static down
 - If pan swinging, then OK
 - If static buildup, wipe down furnace tubes with wet paper towel
- If bend hangdown wire, temp calibration affected – don't use bent wire
- Put over rest tray during balance maintenance

Cleaning

- Pans – clean by heating in air at 950C, then cool and remove residue, then carefully flame pan over Bunsen burner

- **Furnace Tube** – soak and scrub in strong detergent (e.g., Alconox), then soak in strong solvent (e.g., conc. H_2SO_4 plus K_2CrO_7), then dip in 10% HF for no more than 5 minutes, then rinse with water, then rotate over Bunsen burner (heating slowly to avoid cracking)
- **Furnace** – Can only clean with furnace tube lowered

Misc. Maintenance

- When replacing **furnace tube O-ring**, first split O-ring at right angle with razor blade
- Replace Nichrome **Hangdown** when bent and recalibrate furnace

APPENDIX 3. SERIES 2000 CONTROLLER OPERATION PROCEDURE

Plug Unit In. (120 AC)
Display Should Read:

Power Failure
Enter To Continue

Press The **Enter Key**
System Will Startup.
Display Should Read After Startup:

Set Time Of Day
Set Date

Press The **Down Arrow Key (8)** Till Display Reads:

Module Detect
System Tests Menu

Cursor Should Be Pointing To System Tests Menu.
Press The **Enter Key**

Press The **Down Arrow Key (8)** Till Display Reads:

Test Ram
Test Comb Card

Cursor Should Be Pointing To Test Comb Card.
Press The **Enter Key**

Press The **Down Arrow Key (8)** Till Display Reads &
Cursor Is Pointing To Test Comb DAC 3.

Test Comb DAC 3

Press The **Enter Key**
Enter Value "Say 39" (39 = 39% Of Full Scale Possible Current Output. [Full Scale
Approx. 260 Ma If Protection PTC Is Shorted])
Press The **Enter Key**

39% = Approx. 100 Ma,
(1 Millivolt = 1 Milliamp)

APPENDIX 4. STANDARD SAMPLE PREPARATION PROCEDURE**I. Prepare the sample**

1. Grind the sample
 - a. For each sample to be analyzed, about 10 separate 500mg aliquot of the parent fly ash were taken out and put into mortar
 - b. Use pestle to grind about 5 grams of sample in mortar for 2 minutes
 - c. Pour the ground samples onto weighing paper and clean the mortar and pestle

2. Dilute the sample with optically inactive power to a 1:4 ratio
 - a. Weigh 1 gram of ground fly ash sample and place it into the mortar
 - b. Weigh 4 grams of diluent (CaSO_4 or CaCO_3) and place it into the mortar
 - c. Mix both ground fly ash diluent and grind them together for 2 minutes
 - d. Pour out this mixed sample into a small vial and clean the mortar and pestle

3. Weigh the diluted sample
 - a. Set the mass balance and make sure all the surfaces to be contacted with the sample are clean and then zero the balance
 - b. Put a clean sample holder on balance pan
 - c. Close all windows of the balance and wait until the reading stablyzes
 - d. Zero the balance again
 - e. Carefully remove the holder from the pan and fill sample holder halfway with diluted sample and spread it evenly in the pan
 - f. Take care not to pack the sample down
 - g. Place the sample holder back onto the scale pan
 - h. Close all windows of the balance and weigh the sample mass
 - i. If sample weighs less than 0.1144 ± 0.0004 grams add small amounts until it does
 - j. Close the balance window each time when mass is checked and make sure no sample has spilled over cup to outer surface of sample holder

4. Compress the sample
 - a. Place the base of the jig on top of sample holder as shown in Figure 3.5 (a)
 - b. Insert jig plunger through the hole in the jig supporter and lower it slowly with rotation
 - c. When fully lowered rotate one complete revolution in the same direction used in the previous step
 - d. Place a standard weight (0.5 kg) on top of the plunger for 1 minute and then remove it
 - e. Remove the plunger, rotating in same direction used when lowering

- f. Carefully twist the base of the jig to take off the sample holder
- g. Check for a cleanly pressed surface and look for cracks or clumps of sample
- h. If the surface is massed, repeat compression procedure; otherwise, use a spoon and tissues to clean the lip of the cup and the outer surface of the sample holder

II. Test the sample

1. Place the sample holder into the desired CA200
2. Rotate the sample holder until the mark on the side is aligned with the mark on the shaft and raise the sample holder into the head
3. Rotate the lever on the side of the CA200 until the lip of the sample holder cup barely touches the bottom surface of the head
4. Use one hand to make sure the sample holder cup is aligned with the hole in the CA200 head
5. Use the other hand to continue raising the sample holder until the cup is inside the head
6. Use both hands now to fully rotate the levers on both sides of CA200 until the sample holder is locked into place
7. Open the data acquisition program and check for reasonable readouts
8. If the signal is unreasonably low, check the following:
 - a. Seal leakage
 - b. Light source
 - c. Power connection
 - d. Degradation
 - e. Modulation frequency
 - f. Microphone
 - g. All connections and switches
9. If signal shows no variation with time, then the sensitivity of the lock-in amplifier is wrong
 - a. Hit key F2 to change settings
 - b. Hit key F1 to change sensitivity
 - c. Hit +/- keys to adjust sensitivity desired amount
 - d. Hit key F1 to return to main menu
10. If signal remains invariant, continue adjusting sensitivity

11. Collect data

- a. Create a data file**
- b. Hit key F4 to open/create a data file**
- c. Hit key F1 to create a data file**
- d. Type name for file and hit enter**
- e. Hit key F1 to return to main menu**
- f. Hit key F3 to begin taking data**

**APPENDIX 5. SAS PROGRAM AND OUTPUT OF THE REGRESSION
MODEL FOR THE EFFECT OF TEMPERATURE AND
HUMIDITY ON PHOTOACOUSTIC SIGNAL OF CA200**

SAS Program for the Regression Model

in the following program

temt: temperature

hum: humidity

yield: signal -1170 (standardizing procedure)

q : rank for variable residual

```

data set1;
input temt  humt  yield;
cards;
    20.0  32  -50
    20.2  34  -35
    21.2  34  -20
    22.2  35  -10
    20.8  36  -25
    20.5  38  -30
    22.2  51   0
    22.3  53   1
    23.0  53  35
    22.3  55   9
    22.3  55.3 10
    22.3  56  21
    23.6  56  45
    23.5  59  44
    24.0  59  49
    23.1  62  34
    23.3  64  45
;
data set2;
set set1;
temp=temt-22.3; hum=humt-50;
th=temp*hum;
run;
proc print data=set2; run;

proc plot data=set2;
plot yield*temp='*';
plot yield*hum='*';
plot yield*th='*';

```

```

run;

proc reg data=set2;
model yield=temp hum th;
output out=set3 p=yhat r=residual; run;

proc plot data=set3;
plot residual*yhat;
run;

proc rank data=set3 normal=blom out=set3;
var residual;
ranks q;

proc plot data=set3;
plot residual*q;
run;

proc print data=set3;
run;

```

Output of Regression Model

Dependent Variable: YIELD

Analysis of Variance

Source	Sum of DF	Mean Squares	Square	F Value	Prob>F
Model	3	15778.55314	5259.51771	144.705	0.0001
Error	13	472.50569	36.34659		
C Total	16	16251.05882			
Root MSE	6.02881	R-square	0.9709		
Dep Mean	7.23529	Adj R-sq	0.9642		
C.V.	83.32506				

Parameter Estimates

Variable	DF	Parameter Estimate	Standard Error	T for H0: Parameter=0	Prob > T
INTERCEP	1	7.614333	2.23060516	3.414	0.0046
TEMP	1	20.552312	2.63880649	7.788	0.0001

HUM	1	0.807136	0.27643412	2.920	0.0119
TH	1	0.280902	0.15705674	1.789	0.0970

APPENDIX 6. DATA ACQUISITION PROGRAM

This research used two data acquisition systems. The first one employed Model SR530 lock-in amplifier and its data acquisition program was written by Jeff Dykstra (see Jeff Dykstra's thesis). The second one employed Model SR 830 lock-in amplifier and its data acquisition program was based on that written by David Waller with minor changes, which is to be shown in the following.

***** Initial Housekeeping *****

```

DECLARE SUB DISPLAYWINDOW () ' sets up program subroutines
DECLARE SUB DRAWBOX1 () ' to access a subroutine, go to
DECLARE SUB DYNRESERVE () ' View Subs in QuickBasic menu and
DECLARE SUB GRAPHBOX () ' select the subroutine of interest
DECLARE SUB GRAPHDATA ()
DECLARE SUB LOCKINREAD ()
DECLARE SUB LOCKINREAD2 ()
DECLARE SUB LOWSLOPE ()
DECLARE SUB OUTSTYLE ()
DECLARE SUB SAMPLERATE ()
DECLARE SUB SAVEDSET ()
DECLARE SUB SENSITIVITY ()
DECLARE SUB TIMECONST ()
DECLARE SUB UPDATESCREEN ()
DECLARE SUB WRITESETTINGS ()
DECLARE SUB F1 ()
DECLARE SUB F1F1 ()
DECLARE SUB F1F2 ()
DECLARE SUB F1F3 ()
DECLARE SUB F1F4 ()
DECLARE SUB F1F5 ()
DECLARE SUB F2 ()
DECLARE SUB F2F1 ()
DECLARE SUB F2F2 ()
DECLARE SUB F2F3 ()
DECLARE SUB F2F4 ()
DECLARE SUB F2F5 ()
DECLARE SUB F3 ()
DECLARE SUB F4 ()
DECLARE SUB F5 ()
DECLARE SUB F6 ()
DECLARE SUB F7 ()
DECLARE SUB F8 ()

DIM PLOTDATA(1 TO 256)
COMMON SHARED SENS$, DYNRESS$, TCONST$, UPDATES$, OUTSTYL1$, OUTSTYL2$
COMMON SHARED LSLOPES$, CH1OUT, CH2OUT, REQ, TIME, TIME0, DATAFILES$
COMMON SHARED COUNT, PLOTDATA(), SEN, INOSETS$, SNUM, STOPNUM

DEFINT I-K
SCREEN 9 ' allows graphics to be used

```

```

COLOR 7                ' assigns the correct screen color

KEY 1, CHR$(1)         ' assigns the function keys
KEY 2, CHR$(2)         ' (F1 to F9) to different
KEY 3, CHR$(3)         ' character strings
KEY 4, CHR$(4)
KEY 5, CHR$(5)
KEY 6, CHR$(6)
KEY 7, CHR$(7)
KEY 8, CHR$(8)
KEY 9, CHR$(19)
NOSETS$ = " NO CURRENTLY SAVED SETTINGS"    ' defines NOSETS$
                                           ' character string

COUNT = 1             ' sets the default number of data points
                       ' averaged for every recorded point
SNUM = 128             ' sets the default number of entries
STOPNUM = 0           ' written to the data file

OPEN "COM2:19200,N,8,2,CS,DS,CD" FOR RANDOM AS #1
'   Sets up com1 port to 19,200 baud, no parity, 8 data bits,
'   ignore CTS (clear to send), DSR (data set ready),
'   and CD (carrier detect). Com1 communicates with the Lock-In
'   through an RS232 cable.

DATAFILES$ = ""        ' sets output data filename to null

'   Communication #1 is between the Lock-In and computer
'   Communication #2 is between the output datafile and computer

***** Open communication with Lock-In and set Lock-In settings *****

PRINT #1, " "          ' clear port by sending spaces
PRINT #1, "OUTX 0"     ' direct Lock-In responses to RS232
CLS 2                  ' clears the computer screen
SOUND 200, 1
SOUND 400, 1
SOUND 600, 1
SOUND 800, 1
PRINT #1, "*RST"      ' reset Lock-In values to default
CALL SAVEDSET         ' allows user to recall saved settings

' Note: The Lock-In default values can be found on page 4-4 of the SRS
'   830 Lock-In manual. Exceptions to the default settings
'   include changes made by the user when running this program and
'   the following (stored settings will include these changes):

PRINT #1, "SYNC 1"     ' turns on synchronizer filter below 200Hz
PRINT #1, "FPOP 1,0"   ' sets CH1 output to HI display
PRINT #1, "FPOP 2,0"   ' sets CH2 output to LH2 display
PRINT #1, "SEND 0"     ' data storage stops at end of Lock-In
                       ' data buffer - alarm will sound if full

***** Call Display Menu to select user options *****

```

```

CALL DISPLAYWINDOW      ' sets up main menu and draws
CALL DRAWBOX1          ' boxes on the screen
CALL GRAPHBOX

DO
KEYS = INKEY$
IF KEYS = CHR$(1) THEN CALL F1  ' directs the program to the chosen
IF KEYS = CHR$(2) THEN CALL F2  ' subroutine based on user input
IF KEYS = CHR$(3) THEN CALL F3
IF KEYS = CHR$(4) THEN CALL F4
IF KEYS = CHR$(5) THEN CALL F5
IF KEYS = CHR$(6) THEN CALL F6
IF KEYS = CHR$(7) THEN CALL F7
IF KEYS = CHR$(8) THEN
    CLS 1: FOR i = 5 TO 255
        PLOTDATA(i) = 0: NEXT
    CALL GRAPHBOX
END IF

CALL LOCKINREAD2          ' reads Lock-In values, updates the
CALL UPDATESCREEN        ' screen, and plots photoacoustic signal
CALL GRAPHDATA           ' while waiting for menu response

LOOP UNTIL KEYS = CHR$(19)

CLOSE #1
CLOSE #2
SOUND 800, 1
SOUND 600, 1
SOUND 400, 1
SOUND 200, 1

END

SUB DISPLAYWINDOW

CLS 2

LOCATE 1, 36             ' shows main menu information
PRINT "MAIN MENU"       ' and calls appropriate subroutine
LOCATE 3, 45
PRINT "F1 LOCK-IN SETTINGS"
LOCATE 4, 45
PRINT "F2 DATA OUTPUT AND XFER SETTI
LOCATE 5, 45
PRINT "F3 OPEN OR CLOSE A DATA FILE"
LOCATE 6, 45
PRINT "F4 WRITE DATA TO THE DATA FILE"
LOCATE 7, 45
PRINT "F5 WRITE SETTINGS TO FILE"
LOCATE 8, 45
PRINT "F6 WRITE NOTES TO THE DATA FILE"
LOCATE 9, 45

```

PRINT "F7 ENGAGE LOCK-IN AUTO FUNCTIONS"

LOCATE 10, 45

PRINT "F8 CLEAR GRAPH DISPLAY"

LOCATE 11, 45

PRINT "F9 END PROGRAM"

LOCATE 14, 12

PRINT "CURRENT LOCK-IN SETTINGS:"

' prints current Lock-In settings
' to the screen

LOCATE 16, 8

PRINT "SENSITIVITY"

CALL SENSITIVITY

LOCATE 16, 32

PRINT SENS

LOCATE 17, 8

PRINT "DYNAMIC RESERVE"

CALL DYNRESERVE

LOCATE 17, 32

PRINT DYNRES\$

LOCATE 18, 8

PRINT "TIME CONSTANT"

CALL TIMECONST

LOCATE 18, 32

PRINT TCONST\$

LOCATE 19, 8

PRINT "LOW PASS FILTER SLOPE"

CALL LOWSLOPE

LOCATE 19, 32

PRINT LSLOPE\$

LOCATE 20, 8

PRINT "SAMPLING RATE"

CALL SAMPLERATE

LOCATE 20, 32

PRINT SRATES

LOCATE 21, 8

PRINT "NO. DATA FILE ENTRIES"

LOCATE 21, 31

PRINT SNUM

LOCATE 14, 50

PRINT "PHOTOACOUSTIC SIGNAL:"

CALL OUTSTYLE

LOCATE 16, 47

PRINT OUTSTYL1\$

LOCATE 17, 46

PRINT "-----"

LOCATE 16, 64

PRINT OUTSTYL2\$

LOCATE 17, 63

```

PRINT "-----"
LOCATE 20, 50
PRINT "MODULATION FREQUENCY:"
LOCATE 21, 50
PRINT "-----"
CALL DRAWBOX1
CALL GRAPHBOX

```

```
END SUB
```

```

SUB DRAWBOX1           ' draws a box around information
                      ' shown with the main menu

```

```

i = 13
J = 5
LOCATE i, J
PRINT " "
FOR k2 = 1 TO 72
LOCATE (i + k1), (J + k2)
PRINT " "
NEXT k2
LOCATE (i + k1), (J + k2)
PRINT " "

```

```

FOR k1 = 1 TO 9
LOCATE (i + k1), (J)
PRINT " "
LOCATE (i + k1), (J + k2)
PRINT " "
LOCATE (i + k1), 42
PRINT " "
NEXT k1

```

```

LOCATE (i + k1), J
PRINT " "
FOR k2 = 1 TO 72
LOCATE (i + k1), (J + k2)
PRINT " "
NEXT k2
LOCATE (i + k1), (J + k2)
PRINT " "

```

```

LOCATE i, 42
PRINT " "
LOCATE (i + k1), (42)
PRINT " "

```

```
END SUB
```

```

SUB DYNRESERVE       ' queries and returns the dynamic
                    ' reserve of the Lock-In

```

```

PRINT #1, "RMOD?"
INPUT #1, INRMOD
IF INRMOD = 0 THEN DYNRESS = "HIGH  "

```

```
IF INRMOD = 1 THEN DYNRESS = "NORMAL "
IF INRMOD = 2 THEN DYNRESS = "LOW NOISE "
```

```
END SUB
```

```
SUB F1 ' shows Lock-In settings menu and calls
       ' appropriate subroutine
```

```
CLS 2
```

```
DO
```

```
  i = 3
```

```
  J = 29
```

```
  LOCATE i, 32
```

```
  PRINT "LOCK-IN SETTINGS:"
```

```
  LOCATE i + 1, 32
```

```
  PRINT " "
```

```
  LOCATE i + 4, J
```

```
  PRINT "F1 SENSITIVITY"
```

```
  LOCATE i + 5, J
```

```
  PRINT "F2 DYNAMIC RESERVE"
```

```
  LOCATE i + 6, J
```

```
  PRINT "F3 TIME CONSTANT"
```

```
  LOCATE i + 7, J
```

```
  PRINT "F4 LOW PASS FILTER SLOPE"
```

```
  LOCATE i + 8, J
```

```
  PRINT "F5 MODULATION FREQUENCY"
```

```
keyF1$ = INKEY$
```

```
IF keyF1$ = CHR$(1) THEN CALL F1F1: keyF1$ = CHR$(19)
```

```
IF keyF1$ = CHR$(2) THEN CALL F1F2: keyF1$ = CHR$(19)
```

```
IF keyF1$ = CHR$(3) THEN CALL F1F3: keyF1$ = CHR$(19)
```

```
IF keyF1$ = CHR$(4) THEN CALL F1F4: keyF1$ = CHR$(19)
```

```
IF keyF1$ = CHR$(5) THEN CALL F1F5: keyF1$ = CHR$(19)
```

```
LOOP UNTIL keyF1$ = CHR$(19)
```

```
CLS 2
```

```
CALL DISPLAYWINDOW
```

```
END SUB
```

```
SUB F1F1 ' allows user to change the Lock-In sensitivity
```

```
CLS 2
```

```
LOCATE 3, 25
```

```
PRINT "CURRENT SENSITIVITY = "; SENS
```

```
LOCATE 5, 1
```

```
PRINT "PRESS THE KEY CORRESPONDING TO THE DESIRED SENSITIVITY"
```

```
LOCATE 6, 1
```

```
PRINT "PRESS F1 TO RETURN TO THE MAIN MENU"
```

```
LOCATE 8, 1
```

```
PRINT "A ... 2 nV
```

```
O ... 100  $\mu$ V"
```

```
PRINT "B ... 5 nV
```

```
P ... 200  $\mu$ V"
```

```

PRINT "C ... 10 nV           Q ... 500 μV"
PRINT "D ... 20 nV           R ... 1 mV"
PRINT "E ... 50 nV           S ... 2 mV"
PRINT "F ... 100 nV          T ... 5 mV"
PRINT "G ... 200 nV          U ... 10 mV"
PRINT "H ... 500 nV          V ... 20 mV"
PRINT "I ... 1 μV            W ...50 mV"
PRINT "J ... 2 μV            X ... 100 mV"
PRINT "K ... 5 μV            Y ... 200 mV"
PRINT "L ... 10 μV           Z ... 500 mV"
PRINT "M ... 20 μV           * ... 1 V"
PRINT "N ... 50 μV"

```

DO

KEYF1F2\$ = INKEY\$

```

IF KEYF1F2$ = "A" OR KEYF1F2$ = "a" THEN PRINT #1, "SENS 0"
IF KEYF1F2$ = "B" OR KEYF1F2$ = "b" THEN PRINT #1, "SENS 1"
IF KEYF1F2$ = "C" OR KEYF1F2$ = "c" THEN PRINT #1, "SENS 2"
IF KEYF1F2$ = "D" OR KEYF1F2$ = "d" THEN PRINT #1, "SENS 3"
IF KEYF1F2$ = "E" OR KEYF1F2$ = "e" THEN PRINT #1, "SENS 4"
IF KEYF1F2$ = "F" OR KEYF1F2$ = "f" THEN PRINT #1, "SENS 5"
IF KEYF1F2$ = "G" OR KEYF1F2$ = "g" THEN PRINT #1, "SENS 6"
IF KEYF1F2$ = "H" OR KEYF1F2$ = "h" THEN PRINT #1, "SENS 7"
IF KEYF1F2$ = "I" OR KEYF1F2$ = "i" THEN PRINT #1, "SENS 8"
IF KEYF1F2$ = "J" OR KEYF1F2$ = "j" THEN PRINT #1, "SENS 9"
IF KEYF1F2$ = "K" OR KEYF1F2$ = "k" THEN PRINT #1, "SENS 10"
IF KEYF1F2$ = "L" OR KEYF1F2$ = "l" THEN PRINT #1, "SENS 11"
IF KEYF1F2$ = "M" OR KEYF1F2$ = "m" THEN PRINT #1, "SENS 12"
IF KEYF1F2$ = "N" OR KEYF1F2$ = "n" THEN PRINT #1, "SENS 13"
IF KEYF1F2$ = "O" OR KEYF1F2$ = "o" THEN PRINT #1, "SENS 14"
IF KEYF1F2$ = "P" OR KEYF1F2$ = "p" THEN PRINT #1, "SENS 15"
IF KEYF1F2$ = "Q" OR KEYF1F2$ = "q" THEN PRINT #1, "SENS 16"
IF KEYF1F2$ = "R" OR KEYF1F2$ = "r" THEN PRINT #1, "SENS 17"
IF KEYF1F2$ = "S" OR KEYF1F2$ = "s" THEN PRINT #1, "SENS 18"
IF KEYF1F2$ = "T" OR KEYF1F2$ = "t" THEN PRINT #1, "SENS 19"
IF KEYF1F2$ = "U" OR KEYF1F2$ = "u" THEN PRINT #1, "SENS 20"
IF KEYF1F2$ = "V" OR KEYF1F2$ = "v" THEN PRINT #1, "SENS 21"
IF KEYF1F2$ = "W" OR KEYF1F2$ = "w" THEN PRINT #1, "SENS 22"
IF KEYF1F2$ = "X" OR KEYF1F2$ = "x" THEN PRINT #1, "SENS 23"
IF KEYF1F2$ = "Y" OR KEYF1F2$ = "y" THEN PRINT #1, "SENS 24"
IF KEYF1F2$ = "Z" OR KEYF1F2$ = "z" THEN PRINT #1, "SENS 25"
IF KEYF1F2$ = "*" THEN PRINT #1, "SENS 26"

```

CALL SENSITIVITY

LOCATE 23, 1

PRINT "NEW SENSITIVITY = "; SENS

LOOP UNTIL KEYF1F2\$ = CHR\$(1)

END SUB

SUB F1F2

' allows user to change the Lock-In dynamic reserve

CLS 2

```

LOCATE 3, 18
PRINT "CURRENT DYNAMIC RESERVE = "; DYNRESS
LOCATE 6, 5
PRINT "F1 DYNAMIC RESERVE 'HIGH'"
LOCATE 7, 5
PRINT "F2 DYNAMIC RESERVE 'NORMAL'"
LOCATE 8, 5
PRINT "F3 DYNAMIC RESERVE 'LOW NOISE'"
LOCATE 9, 5
PRINT "F4 RETURN TO MAIN MENU"

```

```

DO
KEYF1F2$ = INKEY$
IF KEYF1F2$ = CHR$(1) THEN PRINT #1, "RMOD 0"
IF KEYF1F2$ = CHR$(2) THEN PRINT #1, "RMOD 1"
IF KEYF1F2$ = CHR$(3) THEN PRINT #1, "RMOD 2"

```

```

CALL DYNRESERVE
LOCATE 12, 18
PRINT "NEW DYNAMIC RESERVE = "; DYNRESS

```

```

LOOP UNTIL KEYF1F2$ = CHR$(4)

```

```

END SUB

```

```

SUB F1F3 ' allows user to change the Lock-In time constant
CLS 2

```

```

LOCATE 3, 14
PRINT "CURRENT TIME CONSTANT = "; TCONST$
LOCATE 5, 1
PRINT "PRESS THE KEY CORRESPONDING TO THE DESIRED TIME CONSTANT"
LOCATE 6, 1
PRINT "PRESS F1 TO RETURN TO THE MAIN MENU"

```

```

LOCATE 9, 1
PRINT "A ...10 µs           K ... 1 ε"
PRINT "B ...30 µs           L ... 3 s"
PRINT "C ...100 µs           M ...10 s"
PRINT "D ...300 µs           N ... 30 s"
PRINT "E ...1 ms              O ...100 s"
PRINT "F ... 3 ms             P ... 300 s"
PRINT "G ...10 ms            Q ... 1 ks"
PRINT "H ...30 ms            R ... 3 ks"
PRINT "I ... 100 ms          S ... 10 ks"
PRINT "J ... 300 ms          T ... 30 ks"

```

```

DO
KEYF1F3$ = INKEY$
IF KEYF1F3$ = "A" OR KEYF1F3$ = "a" THEN PRINT #1, "OFLT 0"
IF KEYF1F3$ = "B" OR KEYF1F3$ = "b" THEN PRINT #1, "OFLT 1"
IF KEYF1F3$ = "C" OR KEYF1F3$ = "c" THEN PRINT #1, "OFLT 2"
IF KEYF1F3$ = "D" OR KEYF1F3$ = "d" THEN PRINT #1, "OFLT 3"

```

```

IF KEYF1F3$ = "E" OR KEYF1F3$ = "e" THEN PRINT #1, "OFLT 4"
IF KEYF1F3$ = "F" OR KEYF1F3$ = "f" THEN PRINT #1, "OFLT 5"
IF KEYF1F3$ = "G" OR KEYF1F3$ = "g" THEN PRINT #1, "OFLT 6"
IF KEYF1F3$ = "H" OR KEYF1F3$ = "h" THEN PRINT #1, "OFLT 7"
IF KEYF1F3$ = "I" OR KEYF1F3$ = "i" THEN PRINT #1, "OFLT 8"
IF KEYF1F3$ = "J" OR KEYF1F3$ = "j" THEN PRINT #1, "OFLT 9"
IF KEYF1F3$ = "K" OR KEYF1F3$ = "k" THEN PRINT #1, "OFLT 10"
IF KEYF1F3$ = "L" OR KEYF1F3$ = "l" THEN PRINT #1, "OFLT 11"
IF KEYF1F3$ = "M" OR KEYF1F3$ = "m" THEN PRINT #1, "OFLT 12"
IF KEYF1F3$ = "N" OR KEYF1F3$ = "n" THEN PRINT #1, "OFLT 13"
IF KEYF1F3$ = "O" OR KEYF1F3$ = "o" THEN PRINT #1, "OFLT 14"
IF KEYF1F3$ = "P" OR KEYF1F3$ = "p" THEN PRINT #1, "OFLT 15"
IF KEYF1F3$ = "Q" OR KEYF1F3$ = "q" THEN PRINT #1, "OFLT 16"
IF KEYF1F3$ = "R" OR KEYF1F3$ = "r" THEN PRINT #1, "OFLT 17"
IF KEYF1F3$ = "S" OR KEYF1F3$ = "s" THEN PRINT #1, "OFLT 18"
IF KEYF1F3$ = "T" OR KEYF1F3$ = "t" THEN PRINT #1, "OFLT 19"

```

```

CALL TIMECONST
LOCATE 21, 14
PRINT "NEW TIME CONSTANT = "; TCONST$

```

```

LOOP UNTIL KEYF1F3$ = CHR$(1)

```

```

END SUB

```

```

SUB F1F4          ' allows user to change the Lock-In low pass filter slope
CLS 2

```

```

LOCATE 3, 15
PRINT "CURRENT LOW PASS FILTER SLOPE = "; LSLOPES$
LOCATE 6, 1
PRINT "F1 LOW PASS FILTER SLOPE OF '6 dB/oct'"
LOCATE 7, 1
PRINT "F2 LOW PASS FILTER SLOPE OF '12 dB/oct'"
LOCATE 8, 1
PRINT "F3 LOW PASS FILTER SLOPE OF '18 dB/oct'"
LOCATE 9, 1
PRINT "F4 LOW PASS FILTER SLOPE OF '24 dB/oct'"
LOCATE 10, 1
PRINT "F5 RETURN TO MAIN MENU"

```

```

DO
KEYF1F4$ = INKEY$
IF KEYF1F4$ = CHR$(1) THEN PRINT #1, "OFSL 0"
IF KEYF1F4$ = CHR$(2) THEN PRINT #1, "OFSL 1"
IF KEYF1F4$ = CHR$(3) THEN PRINT #1, "OFSL 2"
IF KEYF1F4$ = CHR$(4) THEN PRINT #1, "OFSL 3"

```

```

CALL LOWSLOPE
LOCATE 13, 15
PRINT "NEW LOW PASS FILTER SLOPE = "; LSLOPES$

```

```

LOOP UNTIL KEYF1F4$ = CHR$(5)

```

END SUB

SUB F1F5 ' allows user to change the Lock-In modulation frequency
CLS 2

```
PRINT #1, "FREQ?"
INPUT #1, MODFREQ!
LOCATE 3, 15
PRINT "CURRENT MODULATION FREQUENCY = "; MODFREQ!
LOCATE 6, 1
PRINT "ENTER THE KEY CORRESPONDING TO THE DESIRED MODULATION FREQUENCY"
LOCATE 7, 1
PRINT "OR MAKE OTHER CHANGES MANUALLY USING THE LOCK-IN KNOB"
LOCATE 8, 1
PRINT "PRESS F1 TO RETURN TO THE MAIN MENU"
```

```
LOCATE 10, 1
PRINT "A ... 100 Hz"
PRINT "B ... 1.4 kHz"
```

```
DO
KEYF1F5$ = INKEY$
IF KEYF1F5$ = "A" OR KEYF1F5$ = "a" THEN PRINT #1, "FREQ 100"
IF KEYF1F5$ = "B" OR KEYF1F5$ = "b" THEN PRINT #1, "FREQ 1400"
```

```
PRINT #1, "FREQ?"
INPUT #1, NEWFREQ!
LOCATE 14, 15
PRINT "THE NEW MODULATION FREQUENCY IS "; NEWFREQ!
```

```
LOOP UNTIL KEYF1F5$ = CHR$(1)
```

END SUB

SUB F2 ' shows Lock-In data outp nsfer
 ' settings and calls appropriate subroutine

CLS 2

```
i = 3
J = 15
LOCATE i, 25
PRINT "DATA OUTPUT AND TRANSFER SETTINGS:"
LOCATE i + 1, 25
PRINT "
LOCATE i + 4, J
PRINT "F1 SAMPLING RATE"
LOCATE i + 5, J
PRINT "F2 CHANNEL 1 DISPLAY"
LOCATE i + 6, J
PRINT "F3 CHANNEL 2 DISPLAY"
LOCATE i + 7, J
PRINT "F4 NUMBER OF DATA POINTS AVERAGED PER RECORDED POINT"
LOCATE i + 8, J
PRINT "F5 NUMBER OF DATA FILE ENTRIES"
```

```

DO
keyF2$ = INKEY$
IF keyF2$ = CHR$(1) THEN CALL F2F1: keyF2$ = CHR$(19)
IF keyF2$ = CHR$(2) THEN CALL F2F2: keyF2$ = CHR$(19)
IF keyF2$ = CHR$(3) THEN CALL F2F3: keyF2$ = CHR$(19)
IF keyF2$ = CHR$(4) THEN CALL F2F4: keyF2$ = CHR$(19)
IF keyF2$ = CHR$(5) THEN CALL F2F5: keyF2$ = CHR$(19)
LOOP UNTIL keyF2$ = CHR$(19)

```

```

CLS 2
CALL DISPLAYWINDOW

```

```

END SUB

```

```

SUB F2F1          ' allows user to change Lock-In sampling rate
CLS 2

```

```

LOCATE 2, 20
PRINT "CURRENT SAMPLE RATE = ", SRATES$
LOCATE 5, 1
PRINT "ENTER THE KEY CORRESPONDING TO THE DESIRED SAMPLE RATE"
LOCATE 6, 1
PRINT "ENTER F1 TO RETURN TO MAIN MENU"

```

```

LOCATE 8, 1
PRINT "A ...  SAMPLE RATE OF 62.5 mHz"
PRINT "B ...  SAMPLE RATE OF 125 mHz"
PRINT "C ...  SAMPLE RATE OF 250 mHz"
PRINT "D ...  SAMPLE RATE OF 500 mHz"
PRINT "E ...  SAMPLE RATE OF 1 Hz"
PRINT "F ...  SAMPLE RATE OF 2 Hz"
PRINT "G ...  SAMPLE RATE OF 4 Hz"
PRINT "H ...  SAMPLE RATE OF 8 Hz"
PRINT "I ...  SAMPLE RATE OF 16 Hz"
PRINT "J ...  SAMPLE RATE OF 32 Hz"
PRINT "K ...  SAMPLE RATE OF 64 Hz"
PRINT "L ...  SAMPLE RATE OF 128 Hz"
PRINT "M ...  SAMPLE RATE OF 256 Hz"
PRINT "N ...  SAMPLE RATE OF 512 Hz"
PRINT "O TRIGGER"

```

```

DO
KEYF2F1$ = INKEY$
IF KEYF2F1$ = "A" OR KEYF2F1$ = "a" THEN PRINT #1, "SRAT 0"
IF KEYF2F1$ = "B" OR KEYF2F1$ = "b" THEN PRINT #1, "SRAT 1"
IF KEYF2F1$ = "C" OR KEYF2F1$ = "c" THEN PRINT #1, "SRAT 2"
IF KEYF2F1$ = "D" OR KEYF2F1$ = "d" THEN PRINT #1, "SRAT 3"
IF KEYF2F1$ = "E" OR KEYF2F1$ = "e" THEN PRINT #1, "SRAT 4"
IF KEYF2F1$ = "F" OR KEYF2F1$ = "f" THEN PRINT #1, "SRAT 5"
IF KEYF2F1$ = "G" OR KEYF2F1$ = "g" THEN PRINT #1, "SRAT 6"
IF KEYF2F1$ = "H" OR KEYF2F1$ = "h" THEN PRINT #1, "SRAT 7"
IF KEYF2F1$ = "I" OR KEYF2F1$ = "i" THEN PRINT #1, "SRAT 8"
IF KEYF2F1$ = "J" OR KEYF2F1$ = "j" THEN PRINT #1, "SRAT 9"

```

```

IF KEYF2F1$ = "K" OR KEYF2F1$ = "k" THEN PRINT #1, "SRAT 10"
IF KEYF2F1$ = "L" OR KEYF2F1$ = "l" THEN PRINT #1, "SRAT 11"
IF KEYF2F1$ = "M" OR KEYF2F1$ = "m" THEN PRINT #1, "SRAT 12"
IF KEYF2F1$ = "N" OR KEYF2F1$ = "n" THEN PRINT #1, "SRAT 13"
IF KEYF2F1$ = "O" OR KEYF2F1$ = "o" THEN PRINT #1, "SRAT 14"

```

```

CALL SAMPLERATE
LOCATE 23, 20
PRINT "NEW SAMPLE RATE = "; SRATES$

```

```

LOOP UNTIL KEYF2F1$ = CHR$(1)

```

```

END SUB

```

```

SUB F2F2          ' allows user to change Lock-In channel 1 output format
CLS 2

```

```

LOCATE 3, 15
PRINT "CURRENT CHANNEL 1 OUTPUT IS "; OUTSTYL1$
LOCATE 5, 1
PRINT "ENTER THE LETTER CORRESPONDING TO THE DESIRED CH1 OUTPUT"
LOCATE 6, 1
PRINT "ENTER F1 TO RETURN TO THE MAIN MENU"
LOCATE 8, 1
PRINT "A ...   X VOLTS"
PRINT "B ...   X VOLTS/AUX1"
PRINT "C ...   X VOLTS/AUX2"
PRINT "D ...   R VOLTS"
PRINT "E ...   R VOLTS/AUX1"
PRINT "F ...   R VOLTS/AUX2"
PRINT "G ...   X NOISE"
PRINT "H ...   X NOISE/AUX1"
PRINT "I ...   X NOISE/AUX2"
PRINT "J ...   AUX1"
PRINT "K ...   AUX1/AUX1"
PRINT "L ...   AUX1/AUX2"
PRINT "M ...   AUX2"
PRINT "N ...   AUX2/AUX1"
PRINT "O ...   AUX2/AUX2"

```

```

DO

```

```

KEYF2F2$ = INKEY$

```

```

IF KEYF2F2$ = "A" OR KEYF2F2$ = "a" THEN PRINT #1, "DDEF 1,0,0"
IF KEYF2F2$ = "B" OR KEYF2F2$ = "b" THEN PRINT #1, "DDEF 1,0,1"
IF KEYF2F2$ = "C" OR KEYF2F2$ = "c" THEN PRINT #1, "DDEF 1,0,2"
IF KEYF2F2$ = "D" OR KEYF2F2$ = "d" THEN PRINT #1, "DDEF 1,1,0"
IF KEYF2F2$ = "E" OR KEYF2F2$ = "e" THEN PRINT #1, "DDEF 1,1,1"
IF KEYF2F2$ = "F" OR KEYF2F2$ = "f" THEN PRINT #1, "DDEF 1,1,2"
IF KEYF2F2$ = "G" OR KEYF2F2$ = "g" THEN PRINT #1, "DDEF 1,2,0"
IF KEYF2F2$ = "H" OR KEYF2F2$ = "h" THEN PRINT #1, "DDEF 1,2,1"
IF KEYF2F2$ = "I" OR KEYF2F2$ = "i" THEN PRINT #1, "DDEF 1,2,2"
IF KEYF2F2$ = "J" OR KEYF2F2$ = "j" THEN PRINT #1, "DDEF 1,3,0"
IF KEYF2F2$ = "K" OR KEYF2F2$ = "k" THEN PRINT #1, "DDEF 1,3,1"
IF KEYF2F2$ = "L" OR KEYF2F2$ = "l" THEN PRINT #1, "DDEF 1,3,2"

```

```

IF KEYF2F2$ = "M" OR KEYF2F2$ = "m" THEN PRINT #1, "DDEF 1,4,0"
IF KEYF2F2$ = "N" OR KEYF2F2$ = "n" THEN PRINT #1, "DDEF 1,4,1"
IF KEYF2F2$ = "O" OR KEYF2F2$ = "o" THEN PRINT #1, "DDEF 1,4,2"

```

```

CALL OUTSTYLE
LOCATE 23, 15
PRINT "NEW CHANNEL 1 OUTPUT IS "; OUTSTYL1$

```

```

LOOP UNTIL KEYF2F2$ = CHR$(1)

```

```

END SUB

```

```

SUB F2F3          ' allows user to change Lock-In channel 2 output format
CLS 2

```

```

LOCATE 3, 15
PRINT "CURRENT CHANNEL 2 OUTPUT IS "; OUTSTYL2$
LOCATE 5, 1
PRINT "ENTER THE LETTER CORRESPONDING TO THE DESIRED CH2 OUTPUT"
LOCATE 6, 1
PRINT "ENTER F1 TO RETURN TO THE MAIN MENU"
LOCATE 8, 1
PRINT "A ...   Y VOLTS"
PRINT "B ...   Y VOLTS/AUX3"
PRINT "C ...   Y VOLTS/AUX4"
PRINT "D ...   θ DEGREES"
PRINT "E ...   θ DEGREES/AUX3"
PRINT "F ...   θ DEGREES/AUX4"
PRINT "G ...   Y NOISE"
PRINT "H ...   Y NOISE/AUX1"
PRINT "I ...   Y NOISE/AUX2"
PRINT "J ...   AUX3"
PRINT "K ...   AUX3/AUX4"
PRINT "L ...   AUX3/AUX4"
PRINT "M ...   AUX4"
PRINT "N ...   AUX4/AUX3"
PRINT "O ...   AUX4/AUX4"

```

```

DO

```

```

KEYF2F3$ = INKEY$
IF KEYF2F3$ = "A" OR KEYF2F3$ = "a" THEN PRINT #1, "DDEF 2,0,0"
IF KEYF2F3$ = "B" OR KEYF2F3$ = "b" THEN PRINT #1, "DDEF 2,0,1"
IF KEYF2F3$ = "C" OR KEYF2F3$ = "c" THEN PRINT #1, "DDEF 2,0,2"
IF KEYF2F3$ = "D" OR KEYF2F3$ = "d" THEN PRINT #1, "DDEF 2,1,0"
IF KEYF2F3$ = "E" OR KEYF2F3$ = "e" THEN PRINT #1, "DDEF 2,1,1"
IF KEYF2F3$ = "F" OR KEYF2F3$ = "f" THEN PRINT #1, "DDEF 2,1,2"
IF KEYF2F3$ = "G" OR KEYF2F3$ = "g" THEN PRINT #1, "DDEF 2,2,0"
IF KEYF2F3$ = "H" OR KEYF2F3$ = "h" THEN PRINT #1, "DDEF 2,2,1"
IF KEYF2F3$ = "I" OR KEYF2F3$ = "i" THEN PRINT #1, "DDEF 2,2,2"
IF KEYF2F3$ = "J" OR KEYF2F3$ = "j" THEN PRINT #1, "DDEF 2,3,0"
IF KEYF2F3$ = "K" OR KEYF2F3$ = "k" THEN PRINT #1, "DDEF 2,3,1"
IF KEYF2F3$ = "L" OR KEYF2F3$ = "l" THEN PRINT #1, "DDEF 2,3,2"
IF KEYF2F3$ = "M" OR KEYF2F3$ = "m" THEN PRINT #1, "DDEF 2,4,0"
IF KEYF2F3$ = "N" OR KEYF2F3$ = "n" THEN PRINT #1, "DDEF 2,4,1"

```

```
IF KEYF2F3$ = "O" OR KEYF2F3$ = "o" THEN PRINT #1, "DDEF 2,4,2"
```

```
CALL OUTSTYLE
```

```
LOCATE 23, 15
```

```
PRINT "NEW CHANNEL 2 OUTPUT IS "; OUTSTYL2$
```

```
LOOP UNTIL KEYF2F3$ = CHR$(1)
```

```
END SUB
```

```
SUB F2F4          ' allows user to change the number of data
```

```
                  ' points averaged per every data point
```

```
                  ' written to the output file
```

```
CLS 2
```

```
LOCATE 3, 10
```

```
PRINT "CURRENT NUMBER OF AVERAGED DATA POINTS = "; COUNT
```

```
LOCATE 5, 1
```

```
PRINT "ENTER THE NUMBER OF DATA POINTS TO AVERAGE PER RECORDED POINT"
```

```
LOCATE 6, 1
```

```
PRINT "PRESS <RETURN> TO ENTER"
```

```
LOCATE 9, 5
```

```
PRINT "*** BE AWARE! INCREASING THIS NUMBER CAUSES THIS SYSTEM   ***"
```

```
LOCATE 10, 5
```

```
PRINT "*** TO RESPOND VERY SLOWLY! A GOOD IDEA IS 1 DATA POINT. ***"
```

```
INPUT COUNT
```

```
LOCATE 13, 10
```

```
PRINT "NEW NUMBER OF AVERAGED DATA I    S = "; COUNT
```

```
SLEEP (2)
```

```
CALL DISPLAYWINDOW
```

```
END SUB
```

```
SUB F2F5          ' allows user to change the number of data
```

```
                  ' entries written to the output file
```

```
CLS 2
```

```
LOCATE 3, 10
```

```
PRINT "CURRENT NUMBER OF ENTRIES = "; SNUM
```

```
LOCATE 5, 1
```

```
PRINT "ENTER THE NEW NUMBER OF ENTRIES WRITTEN TO THE DATA FILE"
```

```
LOCATE 6, 1
```

```
PRINT "THE DEFAULT IS 128 ENTRIES"
```

```
LOCATE 7, 1
```

```
PRINT "PRESS <RETURN> TO ENTER"
```

```
INPUT SNUM
```

```
LOCATE 13, 10
```

```
PRINT "THE NEW NUMBER OF ENTRIES WRITTEN TO THE DATA FILE IS = "; SNUM
```

```
SLEEP (2)
```

```
CALL DISPLAYWINDOW
```



```

        LOCATE 14, 25
        PRINT DATAFILES; " HAS BEEN CLOSED"
        DATAFILES$ = ""
        LOCATE 16, 25
        PRINT "PRESS ANY KEY TO CONTINUE"
        DO
        LOOP UNTIL INKEY$ <> ""
    END IF
END IF
CLS 2
END IF

LOOP UNTIL KEYF3$ = CHR$(3)
CLS 2

CALL DISPLAYWINDOW

END SUB

SUB F4                ' writes data to the output file

IF DATAFILES$ = "" THEN
    CLS 2
    LOCATE 7, 26
    PRINT "NO DATA FILE HAS BEEN OPENED"
    LOCATE 14, 23
    PRINT "HIT ANY KEY TO RETURN TO MAIN MENU"
    DO
    LOOP UNTIL INKEY$ <> ""
    GOTO 400
END IF

MARKS$ = "MARK @ TIME = "
COLOR 15

LOCATE 2, 40
PRINT "WRITING TO DATA FILE "; DATAFILES
LOCATE 12, 35
PRINT "PRESS 'M' TO MARK AN EVENT IN THE DATA FILE"
LOCATE 13, 35
PRINT "HIT 'S' TO STOP WRITING DATA TO THE FILE"
IF TIME0 < 0 THEN
    TIME0 = TIMER
    T$ = "TIME"
    F$ = "FREQ"
    T2$ = "TIMER"
    O1$ = RTRIMS$(OUTSTYL1$)
    O2$ = RTRIMS$(OUTSTYL2$)
    PRINT #2, T$, TAB(15); O1$, TAB(30); O2$, TAB(45); F$, TAB(60); T2$
        ' prints headings to the data file
END IF

COLOR 7

```

```

DO
CALL LOCKINREAD           ' updates screen as
CALL UPDATESCREEN       ' data is written to file
CALL GRAPHDATA
PRINT #2, TIME - TIME0; TAB(15); CH1OUT; TAB(30); CH2OUT; TAB(45);
FREQ; TAB(60); TIME
' prints data to the data file

```

```

KEYF4$ = INKEY$
IF KEYF4$ = "M" OR KEYF4$ = "m" THEN PRINT #2, MARK$; TIMER - TIME0
IF STOPNUM = SNUM THEN           ' stops writing to data
    STOPNUM = 0                  ' file when number of
    KEYF4$ = "S"                 ' preset entries is reached
END IF
LOOP UNTIL KEYF4$ = "S" OR KEYF4$ = "s"
400
SOUND 800, 1

```

```
CALL DISPLAYWINDOW
```

```
END SUB
```

```
SUB F5                          ' writes current Lock-In settings
                                ' to the data file

```

```
CLS 2
```

```
IF DATAFILES$ = "" THEN
    CLS 2
    LOCATE 7, 26
    PRINT "NO DATA FILE HAS BEEN OPENED"
    LOCATE 14, 23
    PRINT "HIT ANY KEY TO RETURN TO THE MAIN MENU"
    DO
    LOOP UNTIL INKEY$ <> ""
    GOTO 500

```

```
END IF
LOCATE 3, 23
PRINT "WRITING SETTINGS TO THE DATA FILE"
LOCATE 4, 23
PRINT "
CALL WRITESETTINGS
LOCATE 17, 23
PRINT "HIT ANY KEY TO RETURN TO MAIN MENU"

```

```
DO
LOOP UNTIL INKEY$ <> ""

```

```
500
CALL DISPLAYWINDOW
```

```
END SUB
```

```
SUB F6                          ' writes user-written notes to the data file
CLS 2

```

```

IF DATAFILES$ = "" THEN
  CLS 2
  LOCATE 7, 26
  PRINT "NO DATA FILE HAS BEEN OPENED"
  LOCATE 14, 23
  PRINT "HIT ANY KEY TO RETURN TO MAIN MENU"
  DO
  LOOP UNTIL INKEY$ <> ""
  GOTO 600
END IF
LOCATE 7, 10
PRINT "TO WRITE NOTES TO THE DATA FILE TYPE THE NOTE AND PRESS <RETURN>"
INPUT NOTES
PRINT #2, " "
PRINT #2, NOTES
PRINT #2, " "
LOCATE 10, 10
PRINT """, NOTES; "" HAS BEEN ADDED TO THI      A FILE"
LOCATE 17, 15
PRINT "HIT ANY KEY TO RETURN TO THE MAIN MENU"
DO
LOOP UNTIL INKEY$ <> ""

600
CALL DISPLAYWINDOW

END SUB

SUB F7          ' allows user to implement Lock-In auto-functions
CLS 2

70
LOCATE 3, 15
PRINT "PRESS THE KEY CORRESPONDING TO THE AUTO FUNCTION DESIRED"
LOCATE 6, 25
PRINT "F1 AUTO GAIN"
LOCATE 7, 25
PRINT "F2 AUTO RESERVE"
LOCATE 8, 25
PRINT "F3 AUTO PHASE"
LOCATE 9, 25
PRINT "F4 AUTO OFFSET X"
LOCATE 10, 25
PRINT "F5 AUTO OFFSET Y"
LOCATE 11, 25
PRINT "F6 AUTO OFFSET R"
LOCATE 12, 25
PRINT "F7 STORE LOCK-IN SETTINGS"
LOCATE 13, 25
PRINT "F8 RETURN TO MAIN MENU"

DO
KEYF7$ = INKEY$
IF KEYF7$ = CHR$(1) THEN PRINT #1, "AGAN"

```

```

IF KEYF7$ = CHR$(2) THEN PRINT #1, "ARSV"
IF KEYF7$ = CHR$(3) THEN PRINT #1, "APHS"
IF KEYF7$ = CHR$(4) THEN PRINT #1, "AOFF 1"
IF KEYF7$ = CHR$(5) THEN PRINT #1, "AOFF 2"
IF KEYF7$ = CHR$(6) THEN PRINT #1, "AOFF 3"
IF KEYF7$ = CHR$(7) THEN
  CLS 2
  LOCATE 3, 10
  PRINT "ENTER THE KEY CORRESPONDING TO THE DESIRED SETTING NUMBER"
  LOCATE 4, 10
  PRINT "ENTER <M> TO RETURN TO THE PREVIOUS MENU"
  LOCATE 6, 1
  PRINT "A SETTING 1", " SETTINGS GROUP #1 - 22 SEPT 1994"
  PRINT "B SETTING 2", " SETTINGS GROUP #2 - 15 NOV 1994"
  PRINT "C SETTING 3", NOSETS$
  PRINT "D SETTING 4", NOSETS$
  PRINT "E SETTING 5", NOSETS$
  PRINT "F SETTING 6", NOSETS$
  PRINT "G SETTING 7", NOSETS$
  PRINT "H SETTING 8", NOSETS$
  PRINT "I SETTING 9", NOSETS$

  DO
  KEYF7A$ = INKEY$
  IF KEYF7A$ = "A" OR KEYF7A$ = "a" THEN PRINT #1, "SSET 1": GOTO 77
  IF KEYF7A$ = "B" OR KEYF7A$ = "b" THEN PRINT #1, "SSET 2": GOTO 77
  IF KEYF7A$ = "C" OR KEYF7A$ = "c" THEN PRINT #1, "SSET 3": GOTO 77
  IF KEYF7A$ = "D" OR KEYF7A$ = "d" THEN PRINT #1, "SSET 4": GOTO 77
  IF KEYF7A$ = "E" OR KEYF7A$ = "e" THEN PRINT #1, "SSET 5": GOTO 77
  IF KEYF7A$ = "F" OR KEYF7A$ = "f" THEN PRINT #1, "SSET 6": GOTO 77
  IF KEYF7A$ = "G" OR KEYF7A$ = "g" THEN PRINT #1, "SSET 7": GOTO 77
  IF KEYF7A$ = "H" OR KEYF7A$ = "h" THEN PRINT #1, "SSET 8": GOTO 77
  IF KEYF7A$ = "I" OR KEYF7A$ = "i" THEN PRINT #1, "SSET 9": GOTO 77
  LOOP UNTIL KEYF7A$ = "M" OR KEYF7A$ = "m"

77
  CLS 2
  GOTO 70
END IF

LOOP UNTIL KEYF7$ = CHR$(8)
CALL DISPLAYWINDOW

END SUB

SUB GRAPHBOX          ' draws a box around the data plot

VIEW (27, 30)-(282, 150)
WINDOW (0, 0)-(255, 130)
i = 5
J = 2

LOCATE i, J          ' prints photoacoustic signal axis title
PRINT "V"
LOCATE i + 1, J

```

```

PRINT "O"
LOCATE i + 2, J
PRINT "L"
LOCATE i + 3, J
PRINT "T"
LOCATE i + 4, J
PRINT "S"
LOCATE 12, 9
PRINT "TIME / 250 DATA POINTS"      ' prints horizontal axis title
LOCATE 2, 2
PRINT SENS                            ' prints full scale sensitivity above the plot

LINE (5, 5)-(255, 5)
LINE (255, 5)-(255, 130)
LINE (255, 130)-(5, 130)
LINE (5, 130)-(5, 5)
LINE (5, 5)-(5, 0)
LINE (55, 5)-(55, 0)
LINE (105, 5)-(105, 0)
LINE (155, 5)-(155, 0)
LINE (205, 5)-(205, 0)
LINE (255, 5)-(255, 0)
LINE (5, 5)-(0, 5)
LINE (5, 30)-(0, 30)
LINE (5, 55)-(0, 55)
LINE (5, 80)-(0, 80)
LINE (5, 105)-(0, 105)
LINE (5, 130)-(0, 130)

END SUB

SUB GRAPHDATA                          ' plots photoacoustic data real-time
                                      ' on the computer screen

FOR i = 7 TO 240
PLOTDATA(i - 1) = PLOTDATA(i)
NEXT i

'IF INT(PLOTDATA(239) * 125 / SEN + 5) > 5 THEN
'  IF INT(PLOTDATA(239) * 125 / SEN + 5) < 130 THEN
'    PRESET (240, PLOTDATA(239) * 125 / SEN + 5)
'    END IF
'END IF
PRESET (240, PLOTDATA(239) * 125 / SEN + 5)
PLOTDATA(240) = CH1OUT
PSET (240, PLOTDATA(240) * 125 / SEN + 5)

FOR i = 239 TO 7 STEP -1
'IF INT(PLOTDATA(i - 1) * 125 / SEN + 5) > 5 THEN
'  IF INT(PLOTDATA(i - 1) * 125 / SEN + 5) < 130 THEN
'    PRESET (i, PLOTDATA(i - 1) * 125 / SEN + 5)
'    END IF
'END IF
PRESET (i, PLOTDATA(i - 1) * 125 / SEN + 5)
PSET (i, PLOTDATA(i) * 125 / SEN + 5)

```

```
NEXT i
CALL GRAPHBOX
```

```
END SUB
```

```
SUB LOCKINREAD          ' reads Lock-In values (CH1 and CH2)
                        ' averages this data over the specified
                        ' number of data points (=count)
```

```
J = 0
```

```
CH1OUTJ = 0
```

```
CH2OUTJ = 0
```

```
CH1TOT = 0
```

```
CH2TOT = 0
```

```
PRINT #1, "STRT"      ' "strt" tells the Lock-In to start taking
FOR J = 1 TO COUNT:   ' data into its output buffer
```

```
    PRINT #1, "OUTR? 1"
```

```
    INPUT #1, CH1OUTJ
```

```
    PRINT #1, "OUTR? 2"
```

```
    INPUT #1, CH2OUTJ
```

```
    CH1TOT = CH1TOT + CH1OUTJ    ' code for averaging multiple
```

```
    CH2TOT = CH2TOT + CH2OUTJ    ' data points and writing to data
```

```
                                ' file as a single entry
```

```
NEXT J
```

```
CH1OUT = CH1TOT / COUNT
```

```
CH2OUT = CH2TOT / COUNT
```

```
STOPNUM = STOPNUM + 1    ' increments the number of written entries
```

```
PRINT #1, "REST"      ' "rest" tells the Lock-In to stop taking
```

```
TIME = TIMER          ' data and to reset its output buffer
```

```
PRINT #1, "FREQ?"
```

```
INPUT #1, FREQ
```

```
END SUB
```

```
SUB LOCKINREAD2        ' reads Lock-In values (CH1 and CH2)
                        ' without averaging. This information
                        ' is used to update the screen without
                        ' having to wait for averaging
```

```
PRINT #1, "STRT"
```

```
PRINT #1, "OUTR? 1"
```

```
INPUT #1, CH1OUT
```

```
PRINT #1, "OUTR? 2"
```

```
INPUT #1, CH2OUT
```

```
PRINT #1, "REST"
```

```
TIME = TIMER
```

```
PRINT #1, "FREQ?"
```

```
INPUT #1, FREQ
```

```
END SUB
```

```
SUB LOWSLOPE          ' queries and returns the Lock-In
                        ' low-pass filter slope value
```

```
PRINT #1, "OFSL?"
```

```
INPUT #1, INSLOPE
```

```
IF INSLOPE = 0 THEN LSLOPE$ = "6 dB/oct "
```

```
IF INSLOPE = 1 THEN LSLOPE$ = "12 dB/oct"
```

```
IF INSLOPE = 2 THEN LSLOPE$ = "18 dB/oct"
```

```
IF INSLOPE = 3 THEN LSLOPE$ = "24 dB/oct"
```

```
END SUB
```

```
SUB OUTSTYLE                                     ' queries and returns the Lock-In
                                                ' CH1 and CH2 output format
```

```
PRINT #1, "DDEF? 1"
INPUT #1, S1A$, S1B$
PRINT #1, "DDEF? 2"
INPUT #1, S2A$, S2B$
```

```
IF S1A$ = "0" AND S1B$ = "0" THEN OUTSTYL1$ = " X VOLTS   "
IF S1A$ = "0" AND S1B$ = "1" THEN OUTSTYL1$ = " X VOLTS/AUX 1"
IF S1A$ = "0" AND S1B$ = "2" THEN OUTSTYL1$ = " X VOLTS/AUX 2"
IF S1A$ = "1" AND S1B$ = "0" THEN OUTSTYL1$ = " R VOLTS   "
IF S1A$ = "1" AND S1B$ = "1" THEN OUTSTYL1$ = " R VOLTS/AUX 1"
IF S1A$ = "1" AND S1B$ = "2" THEN OUTSTYL1$ = " R VOLTS/AUX 2"
IF S1A$ = "2" AND S1B$ = "0" THEN OUTSTYL1$ = " X NOISE   "
IF S1A$ = "2" AND S1B$ = "1" THEN OUTSTYL1$ = " X NOISE/AUX 1"
IF S1A$ = "2" AND S1B$ = "2" THEN OUTSTYL1$ = " X NOISE/AUX 2"
IF S1A$ = "3" AND S1B$ = "0" THEN OUTSTYL1$ = " AUX 1     "
IF S1A$ = "3" AND S1B$ = "1" THEN OUTSTYL1$ = " AUX 1/AUX 1 "
IF S1A$ = "3" AND S1B$ = "2" THEN OUTSTYL1$ = " AUX 1/AUX 2 "
IF S1A$ = "4" AND S1B$ = "0" THEN OUTSTYL1$ = " AUX 2     "
IF S1A$ = "4" AND S1B$ = "1" THEN OUTSTYL1$ = " AUX 2/AUX 1 "
IF S1A$ = "4" AND S1B$ = "2" THEN OUTSTYL1$ = " AUX 2/AUX 2"
```

```
IF S2A$ = "0" AND S2B$ = "0" THEN OUTSTYL2$ = " Y VOLTS   "
IF S2A$ = "0" AND S2B$ = "1" THEN OUTSTYL2$ = " Y VOLTS/AUX 3"
IF S2A$ = "0" AND S2B$ = "2" THEN OUTSTYL2$ = " Y VOLTS/AUX 4"
IF S2A$ = "1" AND S2B$ = "0" THEN OUTSTYL2$ = " é DEG     "
IF S2A$ = "1" AND S2B$ = "1" THEN OUTSTYL2$ = " é DEG/AUX 3 "
IF S2A$ = "1" AND S2B$ = "2" THEN OUTSTYL2$ = " é DEG/AUX 4 "
IF S2A$ = "2" AND S2B$ = "0" THEN OUTSTYL2$ = " Y NOISE   "
IF S2A$ = "2" AND S2B$ = "1" THEN OUTSTYL2$ = " Y NOISE/AUX 3"
IF S2A$ = "2" AND S2B$ = "2" THEN OUTSTYL2$ = " Y NOISE/AUX 4"
IF S2A$ = "3" AND S2B$ = "0" THEN OUTSTYL2$ = " AUX 3     "
IF S2A$ = "3" AND S2B$ = "1" THEN OUTSTYL2$ = " AUX 3/AUX 3 "
IF S2A$ = "3" AND S2B$ = "2" THEN OUTSTYL2$ = " AUX 3/AUX 4 "
IF S2A$ = "4" AND S2B$ = "0" THEN OUTSTYL2$ = " AUX 4     "
IF S2A$ = "4" AND S2B$ = "1" THEN OUTSTYL2$ = " AUX 4/AUX 3 "
IF S2A$ = "4" AND S2B$ = "2" THEN OUTSTYL2$ = " AUX 4/AUX 4 "
```

```
END SUB
```

```
SUB SAMPLERATE                                 ' queries and returns the Lock-In sample rate
```

```
PRINT #1, "SRAT?"
INPUT #1, INSRAT
```

```
IF INSRAT = 0 THEN SRATES = "62.5 mHz "
IF INSRAT = 1 THEN SRATES = "125 mHz  "
IF INSRAT = 2 THEN SRATES = "250 mHz  "
IF INSRAT = 3 THEN SRATES = "500 mHz  "
```

```

IF INSRAT = 4 THEN SRATES$ = "1 Hz  "
IF INSRAT = 5 THEN SRATES$ = "2 Hz  "
IF INSRAT = 6 THEN SRATES$ = "4 Hz  "
IF INSRAT = 7 THEN SRATES$ = "8 Hz  "
IF INSRAT = 8 THEN SRATES$ = "16 Hz "
IF INSRAT = 9 THEN SRATES$ = "32 Hz "
IF INSRAT = 10 THEN SRATES$ = "64 Hz "
IF INSRAT = 11 THEN SRATES$ = "128 Hz "
IF INSRAT = 12 THEN SRATES$ = "256 Hz "
IF INSRAT = 13 THEN SRATES$ = "512 Hz "
IF INSRAT = 14 THEN SRATES$ = "Trigger "

```

```
END SUB
```

```
SUB SAVEDSET
CLS 2
```

```

LOCATE 3, 5
PRINT " WELCOME TO THE PHOTOACOUSTIC CARBON MONITOR PROGRAM!"
LOCATE 5, 5
PRINT " ENTER THE FUNCTION KEY CORRESPONDING TO STORED SETTINGS"
LOCATE 6, 5
PRINT " ENTER <D> TO REVERT TO PROGRAM (DEFAULT) SETTINGS"
LOCATE 8, 1
PRINT "F1 SETTING 1", " SETTINGS GROUP #1 - 22 SEPT 1994"
PRINT "F2 SETTING 2", " SETTINGS GROUP #2 - 15 NOV 1994"
PRINT "F3 SETTING 3", NOSETS$
PRINT "F4 SETTING 4", NOSETS$
PRINT "F5 SETTING 5", NOSETS$
PRINT "F6 SETTING 6", NOSETS$
PRINT "F7 SETTING 7", NOSETS$
PRINT "F8 SETTING 8", NOSETS$
PRINT "F9 SETTING 9", NOSETS$

```

```
SETS$ = "DEFAULT"
```

```
DO
```

```
KEYSETS$ = INKEY$
```

```

IF KEYSETS$ = CHR$(1) THEN PRINT #1, "RSET 1": SETS$ = " 1": GOTO 150
IF KEYSETS$ = CHR$(2) THEN PRINT #1, "RSET 2": SETS$ = " 2": GOTO 150
IF KEYSETS$ = CHR$(3) THEN PRINT #1, "RSET 3": SETS$ = " 3": GOTO 150
IF KEYSETS$ = CHR$(4) THEN PRINT #1, "RSET 4": SETS$ = " 4": GOTO 150
IF KEYSETS$ = CHR$(5) THEN PRINT #1, "RSET 5": SETS$ = " 5": GOTO 150
IF KEYSETS$ = CHR$(6) THEN PRINT #1, "RSET 6": SETS$ = " 6": GOTO 150
IF KEYSETS$ = CHR$(7) THEN PRINT #1, "RSET 7": SETS$ = " 7": GOTO 150
IF KEYSETS$ = CHR$(8) THEN PRINT #1, "RSET 8": SETS$ = " 8": GOTO 150
IF KEYSETS$ = CHR$(9) THEN PRINT #1, "RSET 9": SETS$ = " 9": GOTO 150

```

```
LOOP UNTIL KEYSETS$ = "D" OR KEYSETS$ = "d"
```

```
150
```

```
LOCATE 18, 5
```

```
PRINT "THE SETTING SELECTED IS ", SETS$
```

```
SLEEP (2)
```

```
CLS 2
```

```
END SUB
```

SUB SENSITIVITY ' queries and returns the Lock-In sensitivity

PRINT #1, "SENS?"
INPUT #1, INSEN

```

IF INSEN = 0 THEN SENS$ = "2 nV ": SEN = .00000002#
IF INSEN = 1 THEN SENS$ = "5 nV ": SEN = .00000005#
IF INSEN = 2 THEN SENS$ = "10 nV ": SEN = .0000001#
IF INSEN = 3 THEN SENS$ = "20 nV ": SEN = .0000002#
IF INSEN = 4 THEN SENS$ = "50 nV ": SEN = .0000005#
IF INSEN = 5 THEN SENS$ = "100 nV ": SEN = .000001#
IF INSEN = 6 THEN SENS$ = "200 nV ": SEN = .000002#
IF INSEN = 7 THEN SENS$ = "500 nV ": SEN = .000005#
IF INSEN = 8 THEN SENS$ = "1 μV ": SEN = .00001#
IF INSEN = 9 THEN SENS$ = "2 μV ": SEN = .00002#
IF INSEN = 10 THEN SENS$ = "5 μV ": SEN = .00005#
IF INSEN = 11 THEN SENS$ = "10 μV ": SEN = .0001#
IF INSEN = 12 THEN SENS$ = "20 μV ": SEN = .0002#
IF INSEN = 13 THEN SENS$ = "50 μV ": SEN = .0005#
IF INSEN = 14 THEN SENS$ = "100 μV": SEN = .001#
IF INSEN = 15 THEN SENS$ = "200 μV": SEN = .002#
IF INSEN = 16 THEN SENS$ = "500 μV": SEN = .005#
IF INSEN = 17 THEN SENS$ = "1 mV ": SEN = .001#
IF INSEN = 18 THEN SENS$ = "2 mV ": SEN = .002#
IF INSEN = 19 THEN SENS$ = "5 mV ": SEN = .005#
IF INSEN = 20 THEN SENS$ = "10 mV ": SEN = .01#
IF INSEN = 21 THEN SENS$ = "20 mV ": SEN = .02#
IF INSEN = 22 THEN SENS$ = "50 mV ": SEN = .05#
IF INSEN = 23 THEN SENS$ = "100 mV": SEN = .1#
IF INSEN = 24 THEN SENS$ = "200 mV": SEN = .2#
IF INSEN = 25 THEN SENS$ = "500 mV": SEN = .5#
IF INSEN = 26 THEN SENS$ = "1 V ": SEN = 1#

```

END SUB

SUB TIMECONST ' queries and returns the Lock-In time constant

PRINT #1, "OFLT?"
INPUT #1, INTIME

```

IF INTIME = 0 THEN TCONST$ = "10 μs "
IF INTIME = 1 THEN TCONST$ = "30 μs "
IF INTIME = 2 THEN TCONST$ = "100 μs "
IF INTIME = 3 THEN TCONST$ = "300 μs "
IF INTIME = 4 THEN TCONST$ = "1 ms "
IF INTIME = 5 THEN TCONST$ = "3 ms "
IF INTIME = 6 THEN TCONST$ = "10 ms "
IF INTIME = 7 THEN TCONST$ = "30 ms "
IF INTIME = 8 THEN TCONST$ = "100 ms "
IF INTIME = 9 THEN TCONST$ = "300 ms "
IF INTIME = 10 THEN TCONST$ = "1 s "
IF INTIME = 11 THEN TCONST$ = "3 s "

```

```

IF INTIME = 12 THEN TCONST$ = "10 s "
IF INTIME = 13 THEN TCONST$ = "30 s "
IF INTIME = 14 THEN TCONST$ = "100 s "
IF INTIME = 15 THEN TCONST$ = "300 s "
IF INTIME = 16 THEN TCONST$ = "1 ks "
IF INTIME = 17 THEN TCONST$ = "3 ks "
IF INTIME = 18 THEN TCONST$ = "10 ks "
IF INTIME = 19 THEN TCONST$ = "30 ks "

```

END SUB

```

SUB UPDATESCREEN          ' updates the CH1 and CH2 output and the
                          ' modulation frequency

```

```

COLOR 15
LOCATE 18, 47
PRINT USING "+#.###^"; CH1OUT
LOCATE 18, 64
PRINT USING "+#.###^"; CH2OUT
LOCATE 22, 58
PRINT USING "##### Hz "; FREQ
COLOR 7

```

END SUB

```

SUB WRITSETTINGS          ' writes settings to the output file

```

```

PRINT #2, " "
PRINT #2, "LOCK-IN SETTINGS:"
PRINT #2, " "
PRINT #2, TIMES$, DATES$
PRINT #1, "*IDN?"
INPUT #1, IDN1$, IDN2$, IDN3$, IDN4$
PRINT #2, "LOCK-IN: "; IDN1$; IDN2$; IDN3$; IDN4$
PRINT #2, "SENSITIVITY: "; SENS$
PRINT #2, "DYNAMIC RESERVE: "; DYNRESS$
PRINT #2, "TIME CONSTANT: "; TCONST$
PRINT #2, "LOW PASS FILTER: "; LSLOPES$
PRINT #2, "SAMPLING RATE: "; SRATES$
PRINT #2, "NUMBER OF AVGERAGED POINTS PER RECORDED POINT: "; COUNT$
PRINT #2, "NUMBER OF WRITTEN ENTRIES TO THE DATA FILE: "; SNUM$
PRINT #2, " "

```

END SUB

REFERENCES

- [1] 'Standard Test Method for Ash in the Analysis of Coal and Coke.' ASTM Standard No.d3174-82, Annual Book of ASTM Standards, Part 26, ASTM, Philadelphia, 1982.
- [2] Dykstra J. Carbon in fly ash analysis using photoacoustic spectroscopy, Ph.D. Thesis, Iowa State University, Ames, IA, 1993.
- [3] Rosencraig, A. Photoacoustics and Photoacoustic Spectroscopy, Wiley and Sons, New York, 8, 1980
- [4] Rosencwaig, A. and Gersho, A. "Theory of the photoacoustic effect with solids." J. Appl. Phys., 47(1), 64, 1976.
- [5] Rosencwaig, A. "Solid state photoacoustic spectroscopy." In Optoacoustic Spectroscopy and Detection, Pao, Y. H., Academic Press, New York, 1977.
- [6] Wendlandt, W. W., and Hecht, H. G. Reflectance Spectroscopy, Wiley, New York, 1966.
- [7] Wilks, P. A. Jr., and Hirschfeld, T. "Internal reflection spectroscopy." Appl. Spectrosc. Rev. 1, 99, 1967.
- [8] Wright, G. B. (Ed.), Light scattering of solids, Springer-Verlag, Berlin and New York, 1969.
- [9] McClelland, J. F., Jones, R. W., Luo., S., and Seaverson, L. M. "A practical guide to FT-IR photoacoustic spectroscopy." In Practical Sampling Techniques for Infrared Analysis, Coleman, P. B., ed. CRC Press, Boca Raton, Florida, 1993.
- [10] McClelland, J. F. "Photoacoustic spectroscopy." Anal. Chem., 55(1), 89a, 1983.
- [11] Petzold, A. and Niessner, R. "Photoacoustic soot sensor for in-situ black carbon monitoring." Applied physics, B, Lasers and Optics, 63(2), 191,1996.
- [12] Havaux, M and Malkin, S., "Studies on photoacoustic uptake signals in tobacco leaves under high carbon dioxide levels." Photosynthesis research, 158(3), 293, 1998.
- [13] Schneider, D. and Schwarz, T., "Photoacoustic method for characterizing thin films." Surface & Coatings Technology, 91(1-2), 136-146, 1997.

- [14] Schlageter, B., Porting, S., Strassburger, J., Moreno-Bondi, M. C., Braslavsky, S. E., Oliveros, E. and Braun, A. M., "Development of an optoacoustic sensor module for pH and/or CO₂ determination in aqueous solutions." *Sensors and Actuators, B: Chemical Poster Sessions, Proceedings of the 1996 3rd European Conference on Optical Chemical Sensors and Biosensors, EUROPT(R)ODE III. Part 2 (of 2) Mar 31-Apr 3 1996 v B39 n 1-3 pt 2 Mar-Apr 1997 Zurich, Switz, Elsevier Science S.A. Lausanne Switzerland p 443-447.*
- [15] Larsen, R. M. and Thorsen, K. A., "Equilibrium and kinetics of gas-metal reactions during sintering of austenitic stainless steel." *Powder Metallurgy* 37(1), 61-66, 1994.
- [16] Waller, D. J. "Measurement of unburned carbon in fly ash using infrared photoacoustics." *Master Degree Thesis, Iowa State University, Ames, IA, 1995.*
- [17] Waller, D. J. and Brown, R. C. "Photoacoustic response of unburnt carbon in fly ash to infrared radiation." *Fuel*, 75(13), 1996.
- [18] Sahu, R. and Flagan, R. C. "Particle measurements in coal char combustion." *Combustion Measurements*, Chigie, N., ed. Hemisphere Publishing, New York, 1991.
- [19] Lowry, H. H. *Chemistry of Coal Utilization*, John Wiley & Sons, New York, 1062.
- [20] Robert B. Finkelman ... [et al.]. *The U.S. Geological survey coal quality data base, [Microform]*, Geological Survey (U.S.) Publication, 1994.
- [21] *The U. S. Geological Survey Coal Quality Data Base by U. S. Geological Survey, [Computer file]*, Geological Survey (U. S.) Publication, 1994.
- [22] Hecht, N. L. and Duvalé D. S. "Characterization and utilization of municipal and Utility sludge and ashes." *Utility Coal Ash*, University of Dahton, Environmental Protection Agency, 2(5), 66, 1975.
- [23] Plumley, A. L. "Fossil fuel and the environmental-present systems and their emissions", *Combustion*, 42(10). 1971.
- [24] Hemmings, R. T., Berry, E. E., Cornelius, B. J. and Scheetz, B. E. "Fly ash and coal conversion by-product." *Characterization, Utilization and Disposal III*, edited by Mccarthy, G. J., Glasser, F. P. and Roy, D. M., *Res. Soc. Symp. Proc. Vol. 86, 81*, Materials Research Society, Pittsburgh, 1987.
- [25] Hemmings, R. T. and Berry, E. E. "Evaluation of plastic filler applications for leached fly ash." *EPRI Report CS-4765/RP2422-11*, Sept. 1986.

- [26] Chu, T. Y. J., Krenkel, P. A. and Ruane, R. J. "Reuse of ash sluicing water in coal-fired power plants." Tennessee Valley Authority, Chattanooga, Tennessee, Prepared for the Third National Conference on Complete Water Reuse, Cincinnati, Ohio, June 27-30, 6, 1976.
- [27] Mather, B. "Nature and distribution of particles of various sizes in fly ash." Corps of Engineers, Vicksburg, Mississippi, Technical Report, No.6-583,1963.
- [28] Moulton, L. K. "Bottom ash and boiler slag." West Virginia University, Presented at Third International Ash Utilization Symposium, Pittsburgh, Pa, March 13-14, 22, 1973.
- [29] Magee, E. M, Hall, H. J. and Varga, G. M. "Potential pollutants in fossil fuels." Esso Research and Engineering Company, Linden, New Jersey, Publication Number: PB-225039, Environmental Protection Agency, 151, June 1973.
- [30] Lowry, H. H. Chemistry of Coal Utilization, John Wiley & Sons, New York, 226, 1962.
- [31] Cotton, F. A., Advanced Inorganic Chemistry, John Wiley & Sons, New York, appendix for periodic table for the element, 1988.
- [32] McCarthy, G. J. and Lauf, R. J. Fly Ash and Coal Conversion By-Product: Characterization, and Disposal I, Materials Research Society, Pittsburgh, PA, Vol. 43, 135, 1985.
- [33] McCarthy, G. J. and Lauf, R. J. Fly Ash and Coal Conversion By-Product: Characterization, and Disposal IV, Materials Research Society, Pittsburgh, PA, Vol. 113, 56, 1988.
- [34] McCarthy, G. J. and Lauf, R. J. Fly Ash and Coal Conversion By-Product: Characterization, and Disposal I, Materials Research Society, Pittsburgh, PA, Vol. 86, 172, 1987.
- [35] Bell, A. G. "On the production and reproduction of sound by light." Am. J. Sci. 20, 305, 1880.
- [36] Rontgen, W. C. "On tones produced by the intermittent irradiation of a gas." Philos. Mag., 11, 308, 1881.
- [37] Tyndall, J. "Action of an international beam of radiant heat upon gaseous matter." Proc. Roy. Soc. London, 31, 301, 1881.
- [38] Elving, P. J and Winefordner, J. D. Photoacoustics and Photoacoustic Spectroscopy." John Wiley & Sons, New York, 60, 1980.

- [39] Holman, J. P. *Experimental Methods for Engineers*, McGraw-Hill, Inc., 567, 1994.
- [40] Pao Y. H. *Optoacoustic Spectroscopy and Detection*, Academic Press, Inc., New York, 9, 1977.
- [41] Pao Y. H. *Optoacoustic Spectroscopy and Detection*, Academic Press, Inc., New York, 52, 1977.
- [42] Kreuzer, L. B., Kenyon, N. D., and Patel, C. K. N. "Air pollution: science detection of ten pollutant gases by carbon monoxide and carbon dioxide lasers." *Science* 177, 347, 1972.
- [43] Patel, C. K. N. *Coherence and Quantum Optics* (Mandel, L and Wolf, E. eds.), Plenum Press, New York, 567, 1973.
- [44] Patel, C. K. N, Burkhardt, E. G. and Lamber, C. A., *Science* 184, 1173, 1974.
- [45] Dewey, C. F., Kamm, R. D and Hackett, C. E. *Appl. Phys. Lett.* 26, 300, 1973.
- [46] Pao Y. H. *Optoacoustic Spectroscopy and Detection*, Academic Press, Inc., New York, 63, 1977.
- [47] Rosencwaig, A. *Photoacoustics and Photoacoustic Spectroscopy*, John Wiley & Sons, New York, 21, 1980.
- [48] Pao Y. H. *Optoacoustic Spectroscopy and Detection*, Academic Press, Inc., New York, 198-207, 1977.
- [49] Lin, J. W. and Dudek, L. P. "Signal saturation effect and analytical techniques in photoacoustic spectroscopy of solids." *Anal. Chem.*, 51, 1627, 1979.
- [50] Parry, V. F. "Low-temperature carbonation of coal and lignite for industrial uses." *U. S. Bur. Mines, Rept. Invest. No. 5123*, 27, 1955.
- [51] Anon. "Coal gets a double lift." *Chem. and Eng. News*, 34, 1318-20, 1397, 1956.